**Macrophage CXCR7: A Potential New Target for Atherosclerosis**

by

Wanshu Ma

A dissertation submitted to the Graduate Faculty of
Auburn University
in partial fulfillment of the
requirements for the Degree of
Doctor of Philosophy

Auburn, Alabama
August 3, 2013

Keywords: SDF-1; CXCR7; atherosclerosis; macrophage; cell signaling



Approved by

Jianzhong Shen, Chair, Assistant Professor of Pharmacal Sciences
Vishnu Suppiramaniam, Associate Professor of Pharmacal Sciences
Murali Dhanasekaran, Associate Professor of Pharmacal Sciences
Peter Panizzi, Assistant Professor of Pharmacal Sciences
Rajesh Amin, Assistant Professor of Pharmacal Sciences
Juming Zhong, Associate Professor of Veterinary Histology

Abstract

**Objective**—The discovery of CXCR7 as a new receptor for SDF-1 places many previously described SDF-1 functions attributed to CXCR4 in question, though whether CXCR7 acts as a signaling or "decoy" receptor has been in debate. It is known that CXCR7 is not expressed in normal blood leukocytes; however, the potential role of leukocyte CXCR7 in disease states has not been addressed. The aim of this study was to determine the expression and function of macrophage CXCR7 linked to atherosclerosis.

**Methods and Results**— Here we show for the first time that CXCR7 was detected in macrophage-positive area of aortic atheroma of *ApoE*-null mice, but not in healthy aorta. During monocyte-to-macrophage differentiation, CXCR7 was up-regulated at mRNA and protein levels, with more expression in M1 than in M2 phenotype. In addition, CXCR7 induction was associated with a SDF-1 signaling switch from pro-survival ERK and AKT pathways in monocytes to pro-inflammatory JNK and p38 pathways in macrophages. The latter effect was mimicked by CXCR7-selective agonist TC14012, and abolished by siRNA knockdown of CXCR7. Moreover, CXCR7 activation increased macrophage phagocytic activity, which was suppressed by CXCR7 siRNA silencing or by inhibiting either the JNK or p38 pathways, but was not affected by blocking CXCR4. Activation of CXCR7 by I-TAC showed a similar signaling and phagocytic activity in macrophages with no

detectable CXCR3. Our results also suggest that CXCR7 activation potentially prompted macrophage migration and adhesion, and also modulated some candidate genes expression related to atherosclerosis and inflammation. Finally, we found that the induced CXCR7 expression during monocyte-to-macrophage differentiation was diminished by atorvastatin treatment.

**Conclusions**—CXCR7 is induced during monocyte-to-macrophage differentiation, which is required for SDF-1 and I-TAC signaling to JNK and p38 pathways, leading to enhanced macrophage phagocytosis, thus possibly contributing to atherogenesis. In addition, atorvastatin inhibits CXCR7 induction on macrophages, suggesting a new CXCR7-dependent mechanism to benefit atherosclerosis treatment independent of lipid lowering effect.

Acknowledgments

My thesis work would not have been possible without the guidance of my committee members, help from my workmates, support from my family, and numerous friends, to only some of whom it is possible to give particular mention here.

Above all, I would like to express my deepest and sincerest gratitude to my advisor, Dr. Jianzhong Shen, for his inspiring guidance, endless patience, attentive supports, and the excellent atmosphere for research, which has been invaluable and gone beyond academic level.

I would like to thank all my committee members, Dr. Vishnu Suppiramaniam, Dr. Murali Dhanasekaran, Dr. Peter Panizzi, and Dr. Rajesh Amin, for their encouraging comments, thoughtful criticism, as well as their time and efforts. My thanks also go to Dr. Juming Zhong for acceptance to be my committee as an official reviewer. I would also like to thank Dr. David Riese for providing the proposal-writing course.

I also would like to thank the postdoctoral Dr. Ling Ding, Ms. Yiwei Liu, Ms. Lingxin Zhang, Dr. Manuj Ahuja, and Ms. Gayani Nanayakarra as supportive, cheerful and generous friends. I have and will always cherish the friendships and wonderful memories with them.

I would like to acknowledge the financial, academic, and technical support of the School of Pharmacy, Auburn University, and our staffs that provided the indispensable supports for my life here.

There were numerous people that helped me during my study in Auburn. Ms. Marianna Jungnickel, and Ms. Zhiping Chen, Dr. Shen`s wife, took care of me and gave me tremendous help when I was sick the first semester. Junyi Li has been a friend with unique personality, strong mind, and contiguous fun. Patrick Walters has been an invaluable help over my English and a lot more.

Finally, I would like to thank my parents for their unconditional love, selfless sacrifice to support my dream, and much more for which my mere expression of thanks likewise does not suffice. I hope what I did make them proud.

Table of Contents

List of Tables

List of Figures

List of Abbreviations

Cardiovascular diseases (CVDs)
World Health Organization (WHO)

Low-density lipoproteins (LDL)

Oxidized low-density lipoprotein (ox-LDL)

Reactive oxygen species (ROS)

Vascular adhesion molecule-1 (VCAM-1)

Intercellular adhesion molecule-1 (ICAM-1)

Very late antigen-4 (VLA-4)

Lymphocyte function associated antigen-1 (LFA-1)

Scavenger receptor-A (SR-A)

Monocyte attractant protein-1 (MCP-1) or Chemokine (C-C motif) ligand 2 (CCL2)

Macrophage inflammatory protein-1α (MIP-1α)

Cluster of differentiation 36 (CD36)

ATP binding cassette transporter A1 (ABCA1)

ATP binding cassette transporter G1 (ABCG1)

Interleukin-1β (IL-1β)

Tumor necrosis factor-α (TNF-α)

Smooth muscle cell (SMC)

Platelet derived growth factor (PDGF)

Matrix metalloproteinase (MMP)

Nitric oxide (NO)

3-hydroxy-3-methylglutaryl coenzyme A (HMG-CoA)

Farnesyl pyrophosphate (FPP)

Geranylgeranyl pyrophosphate (GGPP)

Macrophage-colony stimulating factor (M-CSF)

Granulocyte-macrophage colony-stimulating factor (GM-CSF)

Apolipoprotein E (Apo E)

Stromal cell-derived factor-1 (SDF-1) or chemokine (C-X-C motif) ligand 12 (CXCL12)

Chemokine (C-X-C motif) receptor 7(CXCR7) or Chemokine Orphan Receptor 1 (RDC1)

Chemokine (C-X-C motif) receptor 4 (CXCR4)

Regulated on activation, normal T cell expressed and secreted (RANTES) or Chemokine (C-C motif) ligand 5 (CCL5)

Dipeptidyl peptidase 4 (DPP4) or CD26

Macrophage migration inhibitory factor (MIF)

Trefoil factor-2 (TFF2)

Hypoxia-inducible factor-1 (HIF-1)

Vascular endothelial growth factor (VEGF)

Nuclear factor kappa B (NF-κB)

AMD3100 (Plerixafor)

Interferon-inducible T cell chemoattractant (I-TAC) or Chemokine (C-C motif) ligand 11 (CXCL11)

Vasoactive intestinal peptide hormone (VIP)

Extracellular signal-regulated kinase 1/2 (ERK)

Protein kinase B (AKT)

P38 mitogen-activated protein kinase (p38)

c-Jun N-terminal kinase (JNK)

Small interfering RNA (siRNA)

Phorbol-12-myristate-13-acetate (PMA)

Interferon-γ (IFN-γ)

Lipopolysaccharide (LPS)

Human peripheral blood mononuclear cells (PBMCs)

Reverse transcription polymerase chain reaction (RT-PCR)

Glyceraldehyde 3-phosphate dehydrogenase (GAPDH)

Fluorescein isothiocyanate (FITC)

Immunoglobulin G (Ig G)

Phosphate buffered saline (PBS)

Optimal cutting temperature (OCT)

Hematoxylin and eosin stain (H&E stain)

EGF-like module-containing mucin-like hormone receptor-like 1 (F4/80)

Acetylated-LDL (Ac-LDL)

Geranylgeranyltransferase I inhibitor-298 (GGTI-298)

Farnesyltransferase inhibitor-276 (FTI-276)

# Chapter 1. Introduction

## 1.1. Atherosclerosis

The term atherosclerosis derives from the Greek words with “athero” meaning paste and “sclerosis” meaning hardness. Atherosclerosis is a pathological condition in which the artery wall thickens mainly due to the accumulation of lipids such as cholesterol and triglyceride. Complications of atherosclerosis constitute the crucial contributor of cardiovascular diseases (CVDs), the number one cause of death worldwide (Libby, 2002; Lusis, 2000; Ross, 1999; Swirski and Nahrendorf, 2013; Weber and Noels, 2011). The complications of atherosclerosis are usually associated with chronic stenotic occlusion or nonstenotic occlusion. (Figure 1.1.) Typically, stenotic lesions show a narrow lumen and less compensatory enlargement of the arteries. The stenotic fibrous lesions without thrombotic risks have inadequate blood flow to the perfused organs thus evoke symptoms such as stable angina and could be detected by perfusion scans. Treatment of stenotic lesion generally requires combined medical therapy and surgical revascularization. On the other hand, nonstenotic lesions are more common than stenotic plaques. They usually have larger lipid cores, thin fibrous caps, and do not cause perfusion defects on nuclear scans. The weakened fibrous caps made them susceptible to rupture and thrombosis. Nonstenotic plaques may be asymptomatic for many years. Upon disruptive influences, the exposure of the thrombogenic materials in the lesion may suddenly result in the formation of a blood clot and provoke acute coronary events such as unstable angina, myocardial infarctions, stroke, and peripheral vascular disease, thus are more fatal

(Libby, 2001; Virmani *et al.*, 2002). If a prompt treatment is unavailable, the distal tissues will be irreversibly damaged. Clinically, the lesions may lie between these two extremes or coexist and produce mixed manifestations. Until the late 1980s, studies revealed that most of the acute myocardial infarctions result from non-occlusive atherosclerotic lesions. Later studies identified plaque disruption and succeeding thrombosis rather than stenosis as the final pathologic steps that cause acute clinical events.

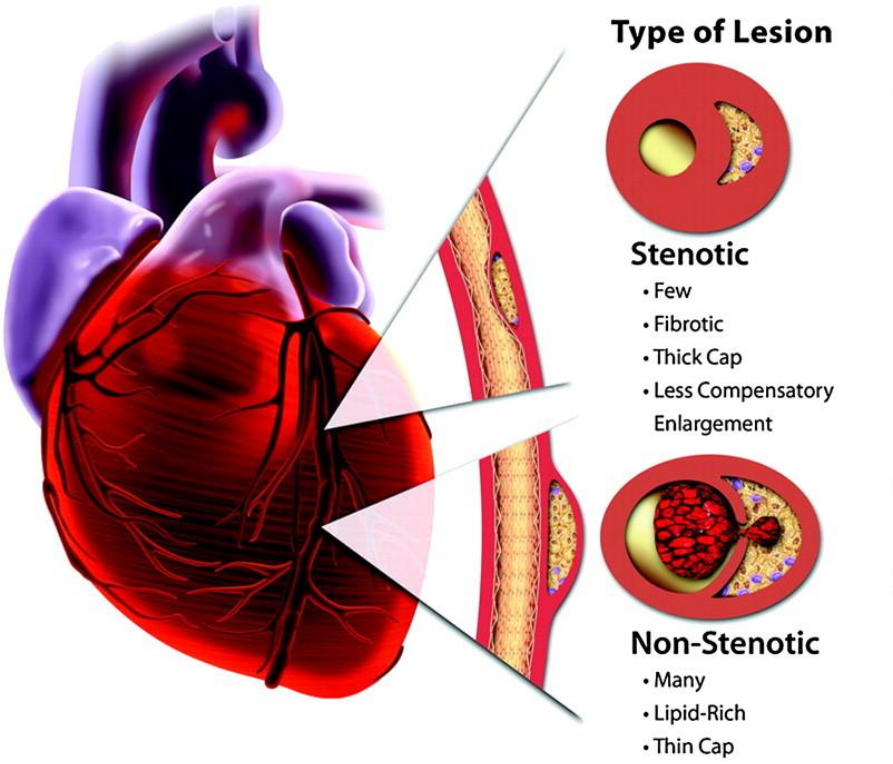


**Figure 1.1. Scheme of atherosclerosis lesion types.**

Adapt from Libby P and Theroux P. *Circulation.* 2005.

According to the latest statistic from the World Health Organization (WHO), CVDs are the leading cause of death over any other ailments globally (Swirski and Nahrendorf, 2013). In 2008, it is estimated that 17.3 million people died from CVDs, representing 30% of all global deaths. Of these, an estimated 7.3 million were due to coronary heart disease and 6.2 million

were due to stroke. Based on these figures, the WHO estimates, almost 25 million people will die from CVDs by 2030. The total economic burden of CVDs cost an estimated $863 billion in 2010, and is projected to increase to $1,044 billion by 2030 (Swirski and Nahrendorf, 2013). Owing to both the rapid prevalence and global incidence of risk factors, such as obesity, sedentary lifestyle, hypertension, and diabetes, CVDs will continue to be the single leading cause of death. Despite its unfavorable consequences, the pathological mechanisms underlying the disease remain incompletely understood. Thus, these facts emphasize the importance of continued scientific research into CVDs and preventive therapeutic targets against CVDs.

### 1.2. Pathology of Atherosclerosis

Previous researches have led to many hypotheses about the pathophysiology of atherosclerotic lesion formation. For a long time, atherosclerosis has been viewed as a passive deposition of lipids in the sub-endothelial space. In the last few decades, experimental and clinical evidence has confirmed that inflammation drives the progression of atherosclerosis and suggested inflammatory targets for possible future therapy (De Meyer *et al.*, 2012; Hansson *et al.*, 2006; Swirski and Nahrendorf, 2013; Weber and Noels, 2011).

The exact cause of atherosclerosis is unclear. However, it is well accepted that atherosclerosis is initiated by endothelium dysfunction (Moore and Tabas, 2011; Ross, 1999). The endothelial cells normally resist leukocyte attachment. A variety of risk factors such as hypertension,

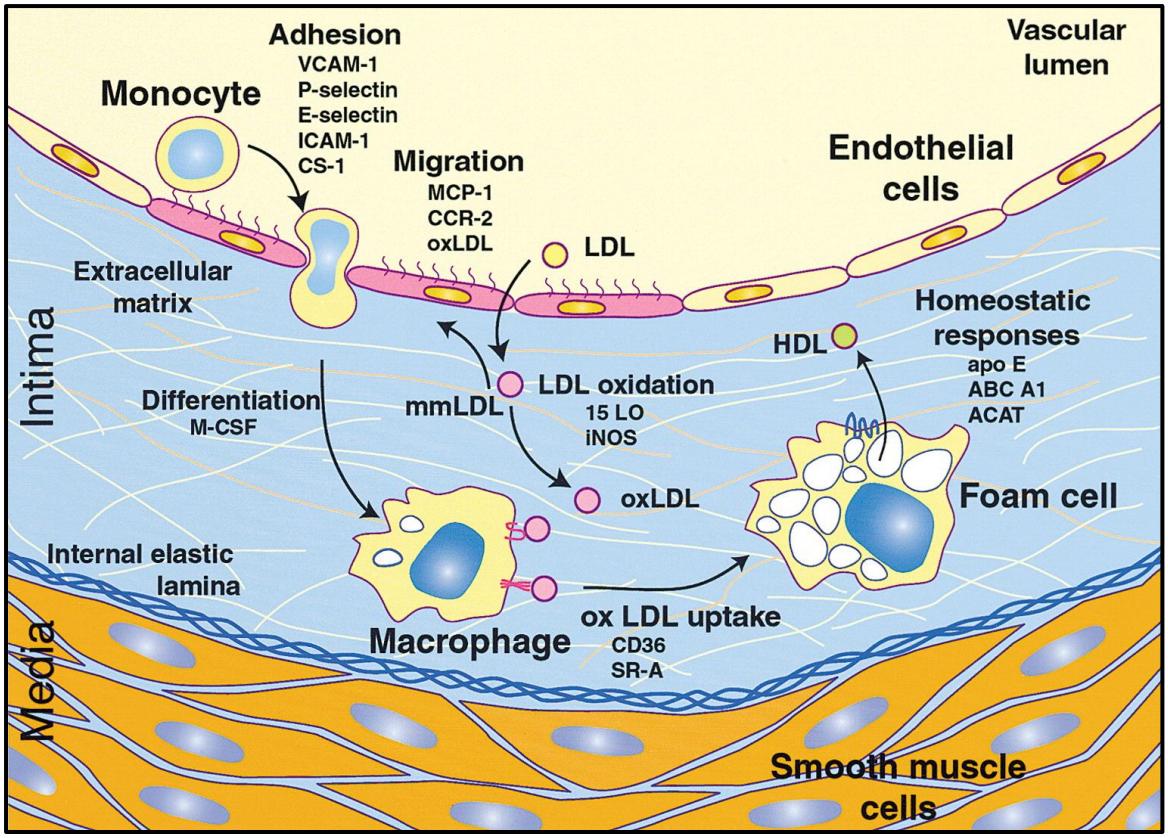


**Figure 1.2. Macrophage recruitment and foam cell formation in atherosclerosis.**

Adapt from Glass CK and Witztum JL. *Cell.* 2001.

diabetes, hyperlipidemia, smoking, obesity, and high level of homocystine can cause endothelium dysfunction and expression adhesion molecules that retain leukocytes. Among them, elevated blood cholesterol level itself is sufficient to drive the progression of atherosclerosis in humans and experimental animals. The majority of cholesterol is carried by low-density lipoproteins (LDL) particles in humans. In atherosclerosis, the ApoB-100 containing LDL is accumulated in the sub-endothelial area and undergoes various modifications. The most atherogenic form of LDL is oxidized low-density lipoprotein (ox-LDL), which are modified by reactive oxygen species (ROS), lipoxygenase, cyclooxygenase, phospholipase A2, and myeloperoxidase. Ox-LDLs incite an inflammatory response such as chemokine secretion and cause the malfunction of endothelium. The

malfunctioned endothelium is pro-inflammatory and expresses a variety of adhesion molecules such as P-selectin, E-selectin, vascular adhesion molecule 1 (VCAM-1), and intercellular adhesion molecule 1 (ICAM-1). The E- and P-selectins facilitate the initial rolling of monocytes, whereas VCAM-1 and ICAM-1 are involved in leukocyte tether and adhesion by selectively binding to the integrin on leucocytes, such as very late antigen-4 (VLA-4) and lymphocyte function associated antigen-1 (LFA-1) (Galkina and Ley, 2007). Once bound, the adherent leukocytes are recruited to the intima in response to chemotactic molecules, such as monocyte chemoattractant protein-1 (MCP-1) and macrophage inflammatory protein-1α (MIP-1α) (De Meyer *et al.*, 2012; Glass and Witztum, 2001; Moore and Tabas, 2011). The majority of infiltrated leukocytes are monocytes that could further differentiate into macrophages or dendritic cells depending on the growth factors and cytokine in the microenvironment. The inflammatory process accelerates the internalization of ox-LDL primarily via scavenger receptors A (SR-A) and the class B scavenger receptor family member, Cluster of Differentiation 36 (CD36) and CD68. However, ox-LDL cannot be efficiently eliminated due to the dysfunction of cholesterol efflux caused by dysfunctioned ATP-binding cassette cholesterol transporters, such as ABCA1 and ABCG1 and *ApoE* (De Meyer *et al.*, 2012). (Figure 1.2.) Thus, the uptaken cholesterol accumulates as cytosolic droplets of cholesterol esters and forms foam cells. Foam cells further amplify lipoprotein modifications and retention. Persistent lipid accumulation causes pro-inflammatory cytokines secretion, including interleukin-1β (IL-1β) and tumor necrosis factor-α (TNF-α). These mediators activate cells within the lesion, thereby accelerating the inflammatory process.

Accumulation of leukocytes and LDL in the intima constitutes the earliest visible form of atherosclerosis, fatty streak. As the atherosclerotic lesion expands, smooth muscle cells (SMC)

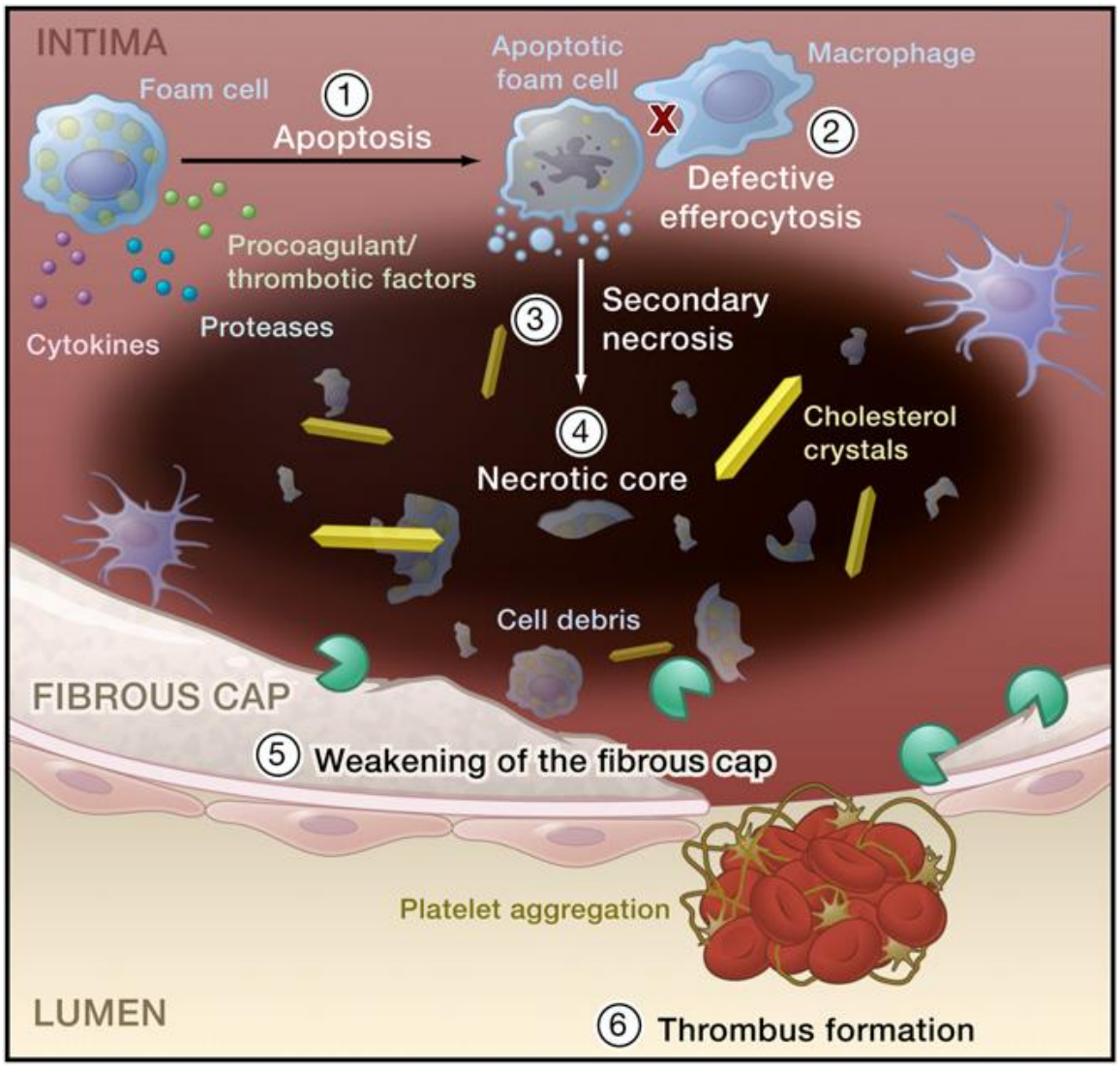


**Figure 1.3. Macrophages in advanced atherosclerotic lesions.**

Adapt from Moore KJ, *et al*. *Cell.* 2011.

migrate into the lesion in response to platelet derived growth factor (PDGF) and other chemoattractants, forming a fibrous cap by synthesis of extracellular matrix proteins. The thickness of fibrous cap positively correlates with the stability of the plaque and segregates the thrombogenic lipid core from the blood. If the inflammation remains unabated, the lesions begin to affect the media and adventitia thus causing the remodeling of the vascular wall.

Atherosclerotic macrophages release matrix metalloproteinases (MMPs) to degrade the extracellular matrix and the increased oxidative stress burden prompts the macrophage foam cells and SMC undergo apoptosis (Moore and Tabas, 2011). The accumulation of apoptotic cells exceeds the phagocytic capacity of macrophages thus result in defective efferocytosis as well as secondary necrosis. Together, these leads to the formation of a necrotic core (Becker *et al.*, 2010; Moore and Tabas, 2011). (Figure 1.3.) The death of SMC and the degradation of the extracellular matrix caused by the protease released by macrophages thins the fibrous cap, thus make it prone to rupture. Upon interruption, the exposure of thrombogenic material, such as tissue factor, in the lesion causes platelet aggregation and thrombus formation.

### 1.3. Treatment of Atherosclerosis: Pleiotropic Effects of Statins

Treatment of atherosclerosis includes medications that relieve symptoms such as anti-thrombosis drug aspirin; reduce risk factors such as thrombosis, hypertension, hyperlipidemia; surgical operations that widen or bypass occluded arteries, and lifestyle modifications. In the past, it was believed that the progressively occlusion of an artery causes acute coronary events, thus strategies were focused on the reduction of severity of stenosis. It is now recognized that the nonstenotic, yet vulnerable lesions virtually cause the most acute coronary syndromes than severely stenosis lesions (Libby, 2001). Thus, the new therapeutic goal is to stabilize the rupture-prone lesions rather than revascularization.

The most widely used and effective way to prevent or treat atherosclerosis is the lipid lowering medication referred to as statins. Statins are a potent class of medicines that inhibit 3-hydroxy-

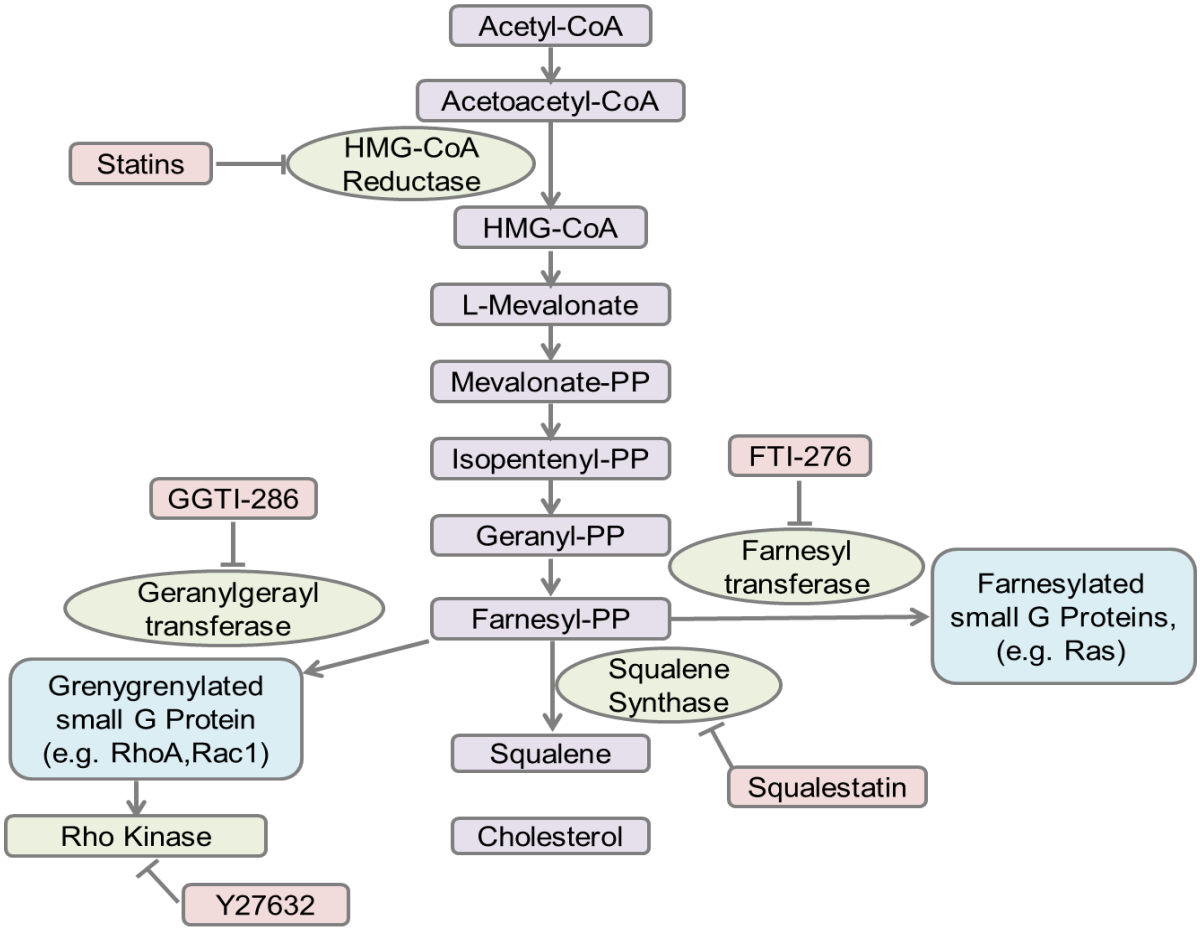


**Figure 1.4. Diagram of the mevalonate pathway.**

Based on Senokuchi *et al. The Journal of biological chemistry* 2005.

3-methylglutaryl coenzyme A (HMG-CoA) reductase, a rate-limiting enzyme for the endogenous cholesterol biosynthesis in humans, thus blocking the conversion of acetoacetyl-CoA and acetyl-CoA to mevalonate leading to less cholesterol synthesis. The hepatic cholesterol lowering effect leads to a compensatory increase in hepatic LDL receptors therefore decreasing systemic cholesterol (Ii and Losordo, 2007; Massy and Guijarro, 2001). (Figure 1.4.)

Statins have gained great success by reducing the incidence of acute coronary syndromes in patients with high cholesterol. Interestingly, statins even benefit the patients at increased risks for cardiovascular events independent of their cholesterol levels (Arnaud *et al.*, 2005; Zhou and Liao, 2009). Studies have shown that statins attenuate cell-adhesion-molecule expression by leukocytes and endothelial cells, resulting in reduced adhesion and transvascular migration. Moreover, statins inhibit chemokines and MMPs secretion, which further interferes with leukocyte migration. In addition, statins modulate the signaling pathways and transcriptional factors involved in oxidative stress and inflammation (Ii and Losordo, 2007; Liao and Laufs, 2005; Libby and Aikawa, 2003). On the other hand, DNA array of laser microdissection of the macrophage-rich shoulder areas from human lesions shows HMG-CoA reductase overexpression, which accompanied by increased integrin expression and inflammation, suggesting a potential beneficial mechanism of statins on atherosclerotic macrophages (Tuomisto, 2003). By inhibiting the earliest step in cholesterol synthesis, statins not only reduce the cellular production of cholesterol, but also prevents the biosynthesis of several intermediates of the mevalonate pathway such as farnesyl pyrophosphate (FPP) and geranylgeranyl pyrophosphate (GGPP) also decreased (Liao and Laufs, 2005). (Figure 1.4.) These isoprenoids are essential for protein prenylation, which is a post translational modification by addition of isoprene units to several proteins involved in important intracellular signaling pathways such as the small GTP-binding proteins Ras and Rho.

Notably, squalene synthase is the first step committed toward cholesterol synthesis but not affect the isoprenoids. Because the mevalonate pathway is not only active on the hepatic cell but also in vascular cells, such as endothelial cells, SMCs and others, this partially explains the

beneficial pleiotropic effects on the cardiovascular system independent of their lipid lowering activity. (Figure 1.5.)

However, statins remain ineffective for two thirds of patients (De Meyer *et al.*, 2012; Glass and Witztum, 2001; Sever *et al.*, 2003). Despite changes in lifestyle and the use of pharmacologic approaches, overall morbidity and mortality from cardiovascular disease continues to be the principal cause of death on this planet. Thus more robust treatment strategies against this disease are needed, and the better understanding of atherosclerosis will hopefully enable additional pharmacological targets and improvement of the clinical intervention of atherosclerosis.

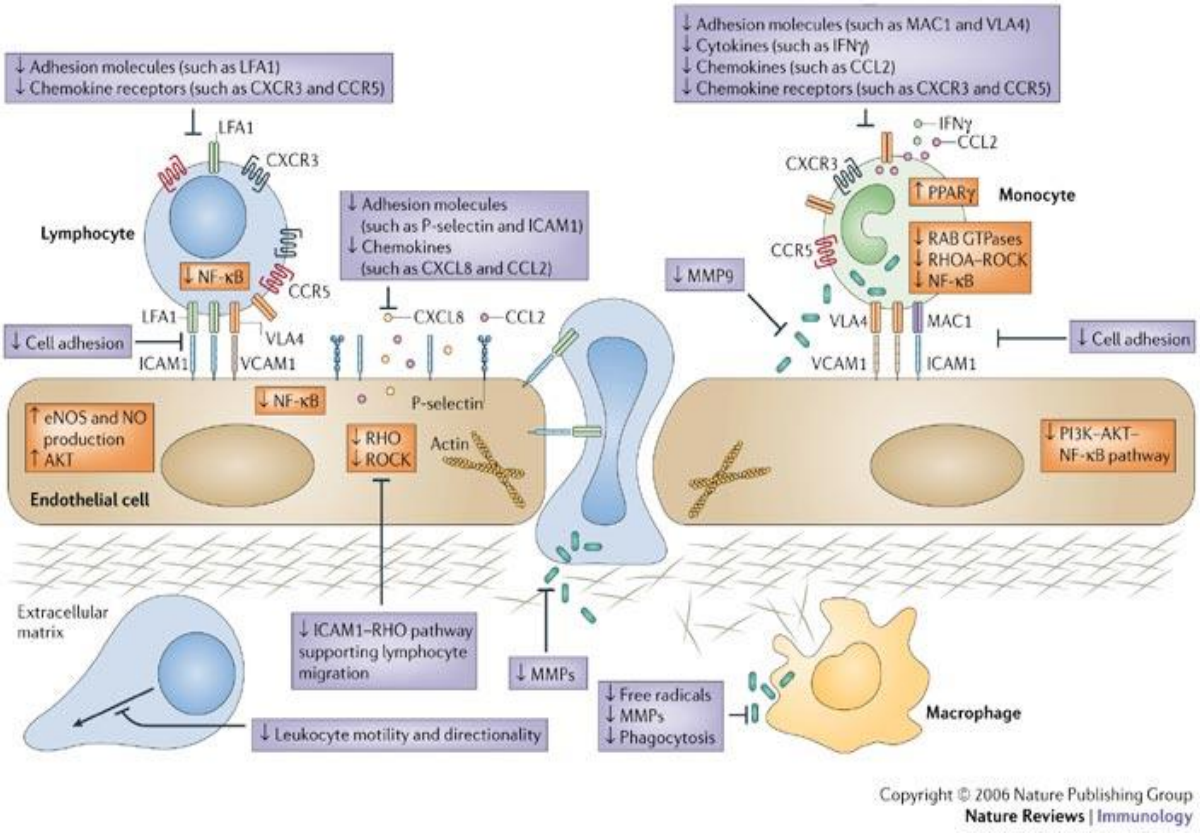


**Figure 1.5. Effect of statins on monocytes and macrophages.**

Adapt from Greenwood J, Steinman L, and Zamvil SS. *Nature Reviews Immunology.* 2006.

### 1.4. Monocytes and Macrophages in Atherosclerosis

Monocytes are the dominant leukocyte in the plaque. Their accumulation drives disease progression and is in proportional to atherosclerotic mass (Woollard and Geissmann, 2010). Monocytes are a type of white blood cell that originates from hematopoietic stem cell precursors in the bone marrow and carry out surveillance in blood circulation. In general half of them are circulating in the peripheral bloodstream for about 1~3 days and then enter tissues to replenish the tissue macrophages, while the others are stored in the spleen. Several well-characterized subsets with differential expression of surface markers, chemokine receptors and a variety of genes were highlighted on human and mice (Gordon and Taylor, 2005; Woollard and Geissmann, 2010). In addition, their ability to enter into tissues and provoke inflammation responses varies. In the mouse, two major subsets have been characterized; the classic, pro-inflammatory $Ly6C^{high}CCR2^{+}CX3CR1^{low}$ and alternative, anti-inflammatory $Ly6C^{low}CCR2^{-}CX3CR1^{high}$. $Ly6C^{high}$ population are elevated in atherosclerotic mice, and are the main monocyte subpopulation infiltrated in early atherosclerotic plaques (Swirski *et al.*, 2007). In human, the $CD14^{high}CD16^{-}CCR2^{high}$ population has been proposed to be the counterpart of mice $Ly6C^{high}$ subset and is predominant. On the other hand, the human $CD14^{low}CD16^{+}CCR2^{low}$ population resemble the mouse $Ly6C^{low}$ monocytes and is less abundant.

During atherogenesis, circulating monocytes are recruited into intima and differentiate into macrophages or dendritic cells under the stimuli of chemokines mainly macrophage-colony stimulating factor (M-CSF) or granulocyte-macrophage colony-stimulating factor (GM-CSF).

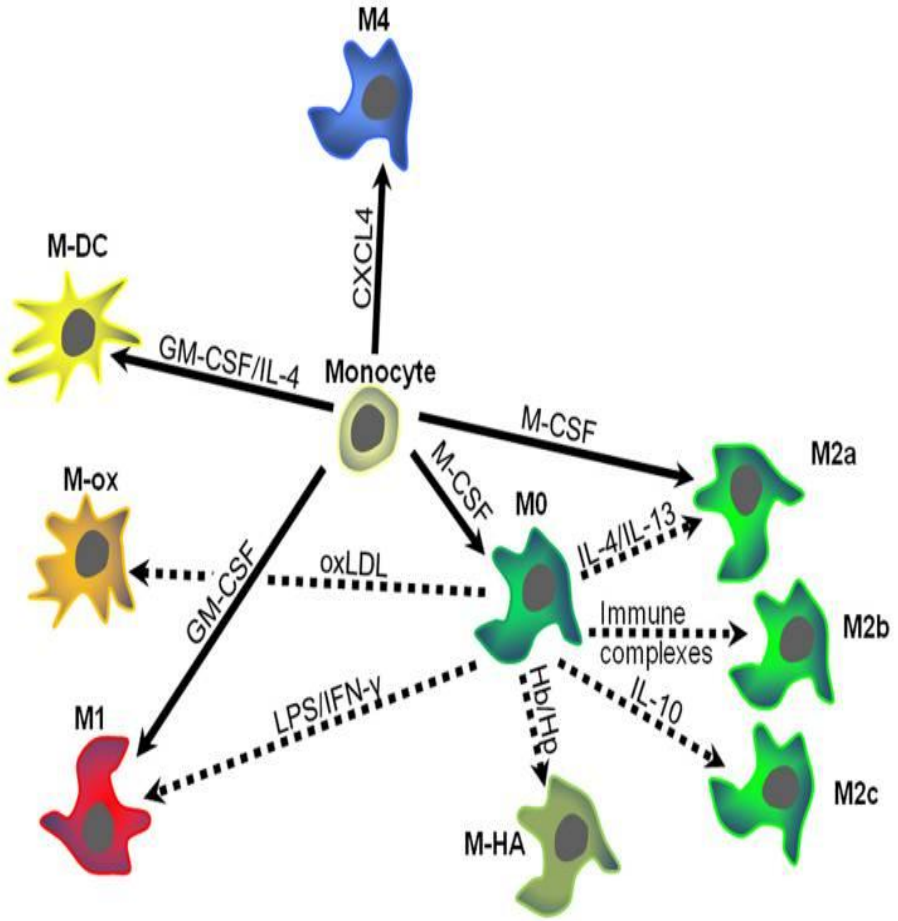


**Figure 1.6. Macrophage heterogeneity.**

Adapted from Gleissner CA. *Frontier in Physiology*. 2012.

Immunohistology studies show that macrophages are prevalent in the shoulder regions of atherosclerotic lesions of patients with unstable angina and acute myocardial infarction (Li and Glass, 2002; Tuomisto, 2003). The monocytes-derived-macrophages could differentially be polarized by the growth factors, chemokines, or lipoproteins in microenvironment. Macrophages are believed to polarize towards diverse activation status depending on T-lymphocyte-derived cytokines. The Th1 pro-inflammatory cytokine, IFN-γ, alone or in combination with LPS or other cytokines like TNF-α polarizes macrophage toward a pro-inflammatory subtype and defined as classic or M1 macrophages. On the other hand, Th2

anti-inflammatory cytokines, IL-4, IL-5, and IL-13, induce the alternative or M2 phenotype. Furthermore, M-ox that is associated with the plaque ox-LDL, M-HA that is activated by tissue hemorrhage, and M4 that is activated by CXCL4 have been proposed (Gleissner, 2012). (Figure 1.6.) M1 macrophages secrete inflammatory cytokines, such as IL-6, IL-7, IL-8, and the soluble CD40 ligand. It is suggested that M1 macrophages induce SMC proliferation; release vasoactive molecules, such as nitric oxide, endothelins; generate ROS that cause lipoprotein oxidation and cytotoxicity. M2 macrophages are considered as anti-inflammatory macrophage because of their ability to release of IL-10 (Gordon and Taylor, 2005; Woollard and Geissmann, 2010).

### 1.5. Monocytes and Macrophages as Atherosclerosis Target

Since the monocyte/macrophage has a crucial role in all stages of atherosclerotic plaque development, it is seen as an emerging candidate for therapeutic intervention. A few monocyte and macrophage activities have been targeted, including those that facilitate monocyte recruitment, cholesterol metabolism, inflammation, and oxidative stress. The heterogeneity of circulating monocytes in mice and humans also enable using the experimental strategies to manipulate the monocyte recruitment into inflammatory stimuli. Genetic ablation or reduction of chemokine receptor expression on monocyte, especially inflammatory monocytes and antibody blockades of the chemokines in mouse models of atherosclerosis induce favorable outcomes such as plaque regression, reduction of cholesterol esters and less inflammation (Leuschner *et al.*, 2011; Tiwari *et al.*, 2008). In addition, cholesterol-lowering therapy in humans leads to plaque stabilization or atherosclerosis regression, which is characterized by reduced macrophage content, though the molecular mechanisms are not fully understood

(Tsuchiya *et al.*, 2007). A better understanding of the molecular mechanisms regard to the orchestration of monocyte/macrophage biology may constitute a viable strategy to reduce plaque macrophage burden, thereby additively or synergistically improving clinical success in combating atherosclerotic diseases.

### 1.6. Interruption of Chemokines and Chemokine Receptors to Manipulate Monocyte Recruitment in Atherosclerosis

Monocyte/macrophage infiltration into the vascular wall is controlled by many factors including those from the chemokine family. Chemokines are a family of small chemotactic cytokines, which guide the migration of cells by the chemokine concentration gradient. They can be classified into four subfamilies C, CC, CXC, and CX3C depending on the arrangement of first two conserved cysteine residues involved in the disulfide bonds formation (Braunersreuther *et al.*, 2007). Chemokines can also be categorized into inflammatory or homeostatic chemokines based on their expression patterns and function. Homeostatic chemokines are constitutively secreted and shown to be involved in developmental processes. In contrary, inflammatory chemokines are secreted in response to inflammatory or immunological stimuli. Chemokine receptors belong to the GPCR superfamily and often bind to more than one chemokine and vice versa. The extracellular N-terminus contributes to ligand recognition and binding, and the transmembrane sequences, the cytoplasmic loop, and the C-terminus, are involved in ligand internalization and receptor signaling. Chemokine receptors can be functionally divided into the typical and atypical receptors based on their abilities to couple to G-proteins, trigger classical $Ca^{2+}$ signaling, and chemotactic capacity.

Among the ~40 human chemokines, the majority were pro-atherogenic. During atherosclerosis, many cells such as SMCs, endothelial cells and macrophages in response to pro-inflammatory stimuli secrete chemokines. Genetic deletion of these ligands or their receptors systematically or conditionally significantly reduces monocyte recruitment and maturation, thus support a critical role for chemokines in macrophage accumulation and disease progression in atherosclerotic lesions (Braunersreuther *et al.*, 2007). Several chemokines and their receptors have been identified to be involved in atherogenesis, including MCP-1 (CCL2)/CCR2, regulated on activation normal T cell expressed and secreted (RANTES, CCL5)/ CCR5 (Hansson, 2005; Hansson *et al.*, 2006; Saha *et al.*, 2009). In line with this notion, a recent study showed that depletion of inflammatory monocytes by lipid nanoparticles loaded *CCR2* siRNA attenuate inflammation and reduces atherosclerotic lesions size in *ApoE*−/− mice (Leuschner *et al.*, 2011). Genome wide association studies have identified 26 coronary artery disease risk loci. Among them, the gene of interest on 10q11.21 lies on the upstream of the stromal cell-derived factor-1 (SDF-1) gene (Sivapalaratnam *et al.*, 2011; Zeller *et al.*, 2012). However, whether SDF-1 is pro- or anti-atherosclerosis is unclear.

### 1.7. Chemokine SDF-1

SDF-1 or CXCL12 is a CXC chemokine subfamily that was first cloned by Tashiro *et al* in 1993 from mouse bone marrow stromal cells and later on characterized as a pre-B-cell stimulatory factor (Nagasawa *et al.*, 1994; Tashiro *et al.*, 1993). The human SDF-1 gene is uniquely located on chromosome 10q11.1 instead of 4q as a cluster of all other CXC chemokines. SDF-1 is constitutively secreted from several cell types and best known for its role in stem/progenitor cell trafficking. It is a potent chemotactic factor for T-lymphocytes,

monocytes, pre-B-cells, dendritic cells, and hematopoietic progenitor cells (Ma *et al.*, 2013). So far seven different SDF-1 isoforms, arising from alternative splicing, have been identified; SDF-1α is the dominant isoform and is present in almost all tissues in human (Yu *et al.*, 2006). The activity and concentration of SDF-1 can be modulated by CD26/dipeptidyl peptidase 4 (DPP4) via proteolytic degradation. SDF-1β possesses four more amino acids and is more resistant to degradation by CD26 (De La Luz Sierra *et al.*, 2004; Shioda *et al.*, 1998). SDF-1 is highly conserved between not only human and mice but also lower vertebrates. Mature human SDF-1 protein shares approximately 99% amino acid sequence identity with the mouse SDF-1. Regulation of SDF-1 expression was shown in the context of hypoxia in *in vivo* models for ischemia (Ceradini *et al.*, 2004). SDF-1 is secreted as monomeric and dimeric units under physiological conditions but due to the positively charged residues at the dimer interface, it preferably forms dimers at nonacidic pH when the counterions are present (Ray *et al.*, 2012a; Veldkamp *et al.*, 2005). The local concentration of SDF-1 can also be concentrated via attachment to the extracellular heparin sulfate proteoglycans (Uchimura *et al.*, 2006).

Evidence from knockout animal studies demonstrated that SDF-1-null mice died prenatally (Ma *et al.*, 1998; Tachibana *et al.*, 1998). In addition, it was found that the number of B-cell progenitors was profoundly reduced in both the fetal liver and bone marrow, whereas the myeloid lineage progenitors were only reduced in the bone marrow. Furthermore, it was found that mice lacking SDF-1 had severe cardiac septal defect (Ara *et al.*, 2005). Moreover, SDF-1 was suggested to be involved in neuronal development (Zhu *et al.*, 2002). In conclusion, these findings demonstrate the importance of SDF-1 in lymphopoiesis, heart and brain morphogenesis. However, due to the embryonic lethal phenotype, its potential functions in adults with atherosclerosis have not been fully elucidated yet.

### 1.8. SDF-1 Receptor, CXCR4: Expression, Regulation and Function

The SDF-1 receptor, chemokine (C-X-C motif) receptor 4 (CXCR4), is ubiquitously expressed in a wide variety of tissues and organs and is highly expressed on monocytes, naïve T-cells, B-cells in the circulation. It is well known for its effect on mediating migration or chemotaxis of arrested leukocytes and hematopoietic progenitors in response to SDF-1 gradient (Aiuti *et al.*, 1997; Bleul *et al.*, 1996). Additionally, other ligands have been reported for CXCR4, including macrophage migration inhibitory factor (MIF) (Bernhagen *et al.*, 2007), trefoil factor-2 (TFF2), (Dubeykovskaya *et al.*, 2009), and ubiquitin (Saini *et al.*, 2010).

Studies have shown that CXCR4 can by unregulated by pro-inflammatory cytokine TNF-α and IL-1β (Oh *et al.*, 2001), activation of hypoxia-inducible factor-1 (HIF-1) under hypoxia (Oh *et al.*, 2012; Zagzag *et al.*, 2006), growth factors like hepatocyte growth factor/scatter factor (HGF/SF) ,vascular endothelial growth factor (VEGF) (Esencay *et al.*, 2010; Hong *et al.*, 2006). In addition, increased activation of nuclear factor kappa B (NF-κB) also prompt CXCR4 expression especially in cancer (Bruhl *et al.*, 2003). CXCR4 ubiquination is a posttranslational modification regulating the expression of itself (Lapham *et al.*, 2002). DNA methylation that negatively regulates the expression of SDF-1 or CXCR4 in cancer indicates an epigenetic regulation mechanism (Ramos *et al.*, 2011; Sato *et al.*, 2005). The enhanced CXCR4 expression in cancer or hypoxia tissue but not health tissues is suggested to facilitate cancer invasion or tissue repairmen by progenitor cells.

*CXCR4* knockout mice resemble the phenotype of *SDF-1* deficient mice (Ma *et al.*, 1998). In addition, CXCR4 served as a co-receptor for HIV entry to $CD4^+$ T-cells (Patrussi and Baldari, 2011). The SDF-1/CXCR4 pathway has been suggested to play a pivotal role during development and a few conditions including hematopoiesis, blood vessel formation, cancer metastasis, angiogenesis and HIV infection. (Figure 1.7.)

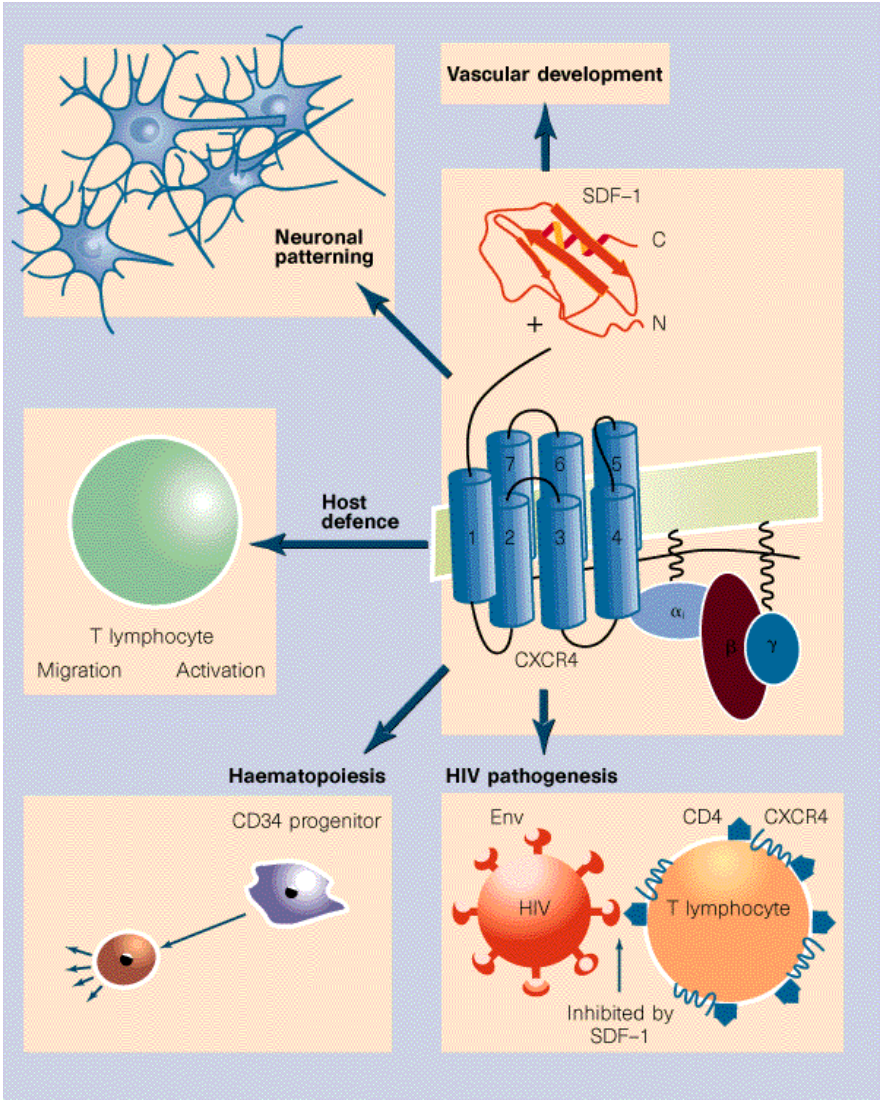


**Figure 1.7. Biological roles of the SDF-1/CXCR4 axis.**

Adapt from Richard H. *Nature*. 1998.

Upon binding of SDF-1, CXCR4 was suggested to initiate intracellular signaling through several divergent pathways that starts with dissociation of the G protein heterotrimers into α and βγ subunits. Downstream effectors include PI3K/AKT, IP3, and MAPK pathways, which promote cell survival, proliferation, and chemotaxis. Desensitization begins with the C-terminal phosphorylation of the receptor, which recruits β-arrestin and causes the clathrin-mediated internalization of the ligated chemokine receptor into vesicles for degradation or recycling (Lu *et al.*, 2009; Singh *et al.*, 2012; Thelen and Thelen, 2008). (Figure 1.8.)

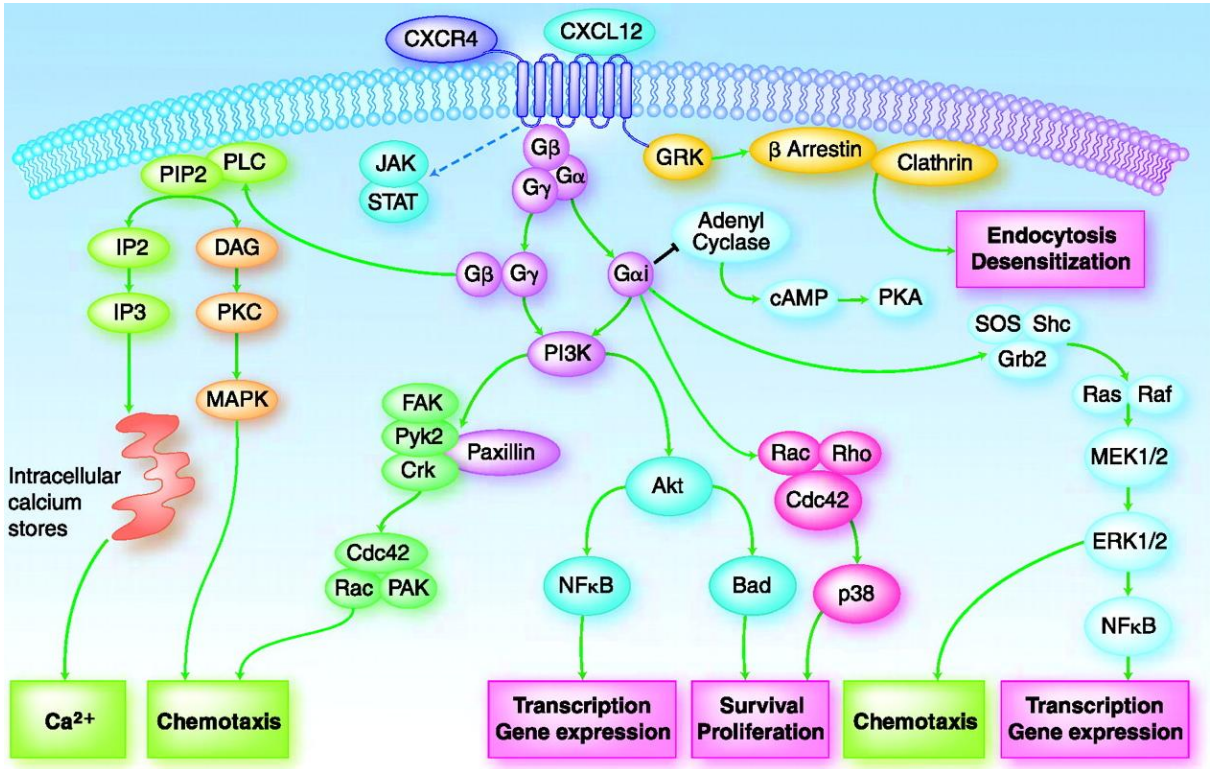


**Figure 1.8. Schematic diagram of the CXCR4/CXCL12 axis signaling pathway.**

Adapted from Teicher BA and Fricker S P. *Clinical Cancer Ressearch.* 2010.

Since the SDF-1/CXCR4 axis plays a critical role for diseases like such as HIV, cancer, WHIM (Warts, Hypogammaglobulinemia, Infections, and Myelokathexis) syndrome, and

hematopoietic progenitor cells mobilization, small molecule inhibitors of CXCR4 have been developed to block SDF-1/CXCR4 interactions that are currently under different stages of development. The first CXCR4 antagonist, AMD3100 (also known as Plerixafor, Mozobil by Genzyme), was approved by the FDA in 2008 for the mobilization of hematopoietic stem cells. It is suggested that AMD3100 inhibits CXCR4 mediated calcium signal, GTP binding and chemotactic response elicited by SDF-1 (Dar *et al.*, 2011; Debnath *et al.*, 2013; Hatse *et al.*, 2002). It is also used to mobilize progenitor cells from the bone marrow into circulation in murine and humans, and is approved for stem cell mobilization in patients with leukemia (Dar *et al.*, 2011; Fricker, 2008). However, the efficacies and specificity of these CXCR4 inhibitors were questioned after the de-orphanization of CXCR7 (Kalatskaya *et al.*, 2009).

### 1.9. The Novel SDF-1 Receptor, CXCR7

CXCR4 was once believed to monogamously interact with SDF-1, until CXCR7 is de-orphanized, and shown to bind with high affinity to SDF-1. CXCR7, formerly called RDC1, was cloned from a canine cDNA library as a putative G-protein coupled receptor for vasoactive intestinal peptide hormone (VIP). Receptor-binding studies indicate that besides SDF-1, CXCR7 also binds to interferon-inducible T cell chemoattractant (I-TAC; CXCL11). SDF-1 binds to CXCR7 with ~10 times higher affinity than to CXCR4 (Balabanian *et al.*, 2005; Burns, 2006). CXCR7 binds to SDF-1 with ~10 to 20 fold greater affinity than to I-TAC (Balabanian *et al.*, 2005). Similar with CXCR4, mouse CXCR7 displayed 91% homology to human CXCR7 (Heesen *et al.*, 1998).

As the de-orphanization of CXCR7 as a new high affinity receptor for SDF-1, tremendous effort is devoted to unveil its role and re-determine the cellular functions previously shown mediated by SDF-1/CXCR4 axis. Therefore *CXCR7* knockout mice were generated for the dissection of its *in vivo* roles. However, the *CXCR7*-null mice die after birth due to severe semilunar valve stenosis (Gerrits *et al.*, 2008; Sierro *et al.*, 2007). Despite its ligand-binding properties, it has not reached a consent regarding the exact function and expression pattern of CXCR7. CXCR7 has been suggested play a role in cell survival, adhesion, tumor growth, and development; and induced expression was demonstrated during pathological inflammation and tumor development (Hou *et al.*, 2010; Yan *et al.*, 2012).

Unlike CXCR4, CXCR7 expression was not up-regulated by hypoxia, TNF-α, IFN-γ, interleukin-1β, interleukin-6, and VEGF in human glioma cells (Hattermann *et al.*, 2010). Promoter deletion and mutation studies suggest that CXCR7 expression is regulated in an NF-κB dependent manner (Tarnowski *et al.*, 2010a; Tarnowski *et al.*, 2010b). However, CXCR7 protein may not present on the cell surface even if the intracellular CXCR7 mRNA is high, suggests a potential post-translational regulation mechanism (Burns, 2006). Since CXCR7 has an altered DRYLSIT motif, which is sufficient for $G_{\alpha}$i-protein coupling and activation of CXCR7. In addition, by binding with SDF-1, CXCR7 does not show chemotaxis, receptor mediated calcium mobilization, and the activation of intracellular signaling via AKT or MAP kinase, it is considered as an atypical GPCR (Balabanian *et al.*, 2005; Burns, 2006; Infantino *et al.*, 2006). Thus, some evidence supports the theory that CXCR7 acts as a "scavenger receptor" by constitutively internalize the ligand to lysosome for degradation and recycle back to the cell membrane (Boldajipour *et al.*, 2008; Luker *et al.*, 2010; Naumann *et al.*, 2010; Ray *et al.*, 2012b). Some studies indicate that activation of CXCR7 triggers the

β-arrestin pathway and ligand internalization, which is dependent on the Serine/Threonine residues at the carboxy terminus of CXCR7 (Canals *et al.*, 2012; Rajagopal *et al.*, 2010). It was also suggested that ligand binding of CXCR7 recruits G protein and active some of the MAPKs on some type of cells (Levoye *et al.*, 2009; Odemis *et al.*, 2010; Odemis *et al.*, 2011). In addition, the expression of CXCR7 could either enhance or abate the responsiveness to SDF-1 on different cell lines, which suggest interaction of the receptors (Singh *et al.*, 2012; Thelen and Thelen, 2008).

The novel SDF-1 receptor, CXCR7 is suggested to be involved in the maturation differentiation of B cells (Infantino *et al.*, 2006) and CXCR7 expression was found on T cells as well as on natural killer cells (Balabanian *et al.*, 2005) but not on the monocytes (Berahovich *et al.*, 2010b). However, the postnatal role of CXCR7, especially whether CXCR7 could be induced in inflammation process like atherosclerosis, has not been elucidated yet.

### 1.10. Other CXCR7 Ligand: I-TAC and its Receptor CXCR3

The SDF-1/CXCR4/CXCR7 network grows more complex with expanding evidence showing that CXCR7 also binds to another endogenous ligand I-TAC. The binding of I-TAC with CXCR7 shows lower affinity compare to SDF-1 (Burns, 2006). I-TAC is a well-established ligand for CXCR3. It is demonstrated that CXCR3 is not expressed on human peripheral monocytes but is expressed on T lymphocytes (Katschke *et al.*, 2001). CXCR3 antagonist compound 6c exhibit potent inhibition on calcium mobilization functional assay and T-cell chemotaxis (Cole *et al.*, 2006).

### 1.11. Role of SDF-1 in Atherosclerosis

Mounting evidence suggests SDF-1 is potentially involved in atherosclerosis, vascular inflammation, and neointima formation. It has been shown that in *ApoE*-null mice with atherosclerosis, the serum SDF-1 level is significantly lower than normal, and this is accompanied by the progressive loss of mobility of bone marrow derived cells due to reduced CXCR4 expression (Shen *et al.*, 2010; Xu *et al.*, 2011). In humans, the plasma levels of SDF-1 are significantly lower in patients with stable and unstable angina pectoris compared with healthy subjects, suggesting that SDF-1 is involved in atherosclerosis (Damas *et al.*, 2002). Moreover, SDF-1 protein is not detected in the healthy artery but is expressed in atherosclerotic lesions and is important for vascular repair and remodeling (Abi-Younes *et al.*, 2000). These studies indicate a natural gradient of SDF-1 across the blood vessel. (Figure 1.9.) Furthermore, chronic blocking of SDF-1 receptor, CXCR4, by a potent small antagonist,

AMD3465 or *ApoE*−/− mice deficiency in bone marrow CXCR4 accelerates diet-induced atherosclerosis by increasing circulating neutrophils and leukocytes, indicating that SDF-1/CXCR4 plays an important role on neutrophils in atherosclerotic mice (Coffield *et al.*, 2003; Zernecke *et al.*, 2008). Moreover, systematic treatment of SDF-1 promotes the stabilization of the atherosclerotic lesions by enhanced accumulation of smooth muscle progenitor cells in *ApoE*-deficient mice (Akhtar *et al.*, 2013). In addition, studies also suggest that SDF-1 is crucial in neointima formation after vascular injury in *ApoE*−/− mice by regulating neointimal SMC content through recruitment of SMC progenitors (Schober *et al.*, 2003; Zernecke *et al.*, 2005). The SDF-1/CXCR-4 axis has been intensively studied; however,

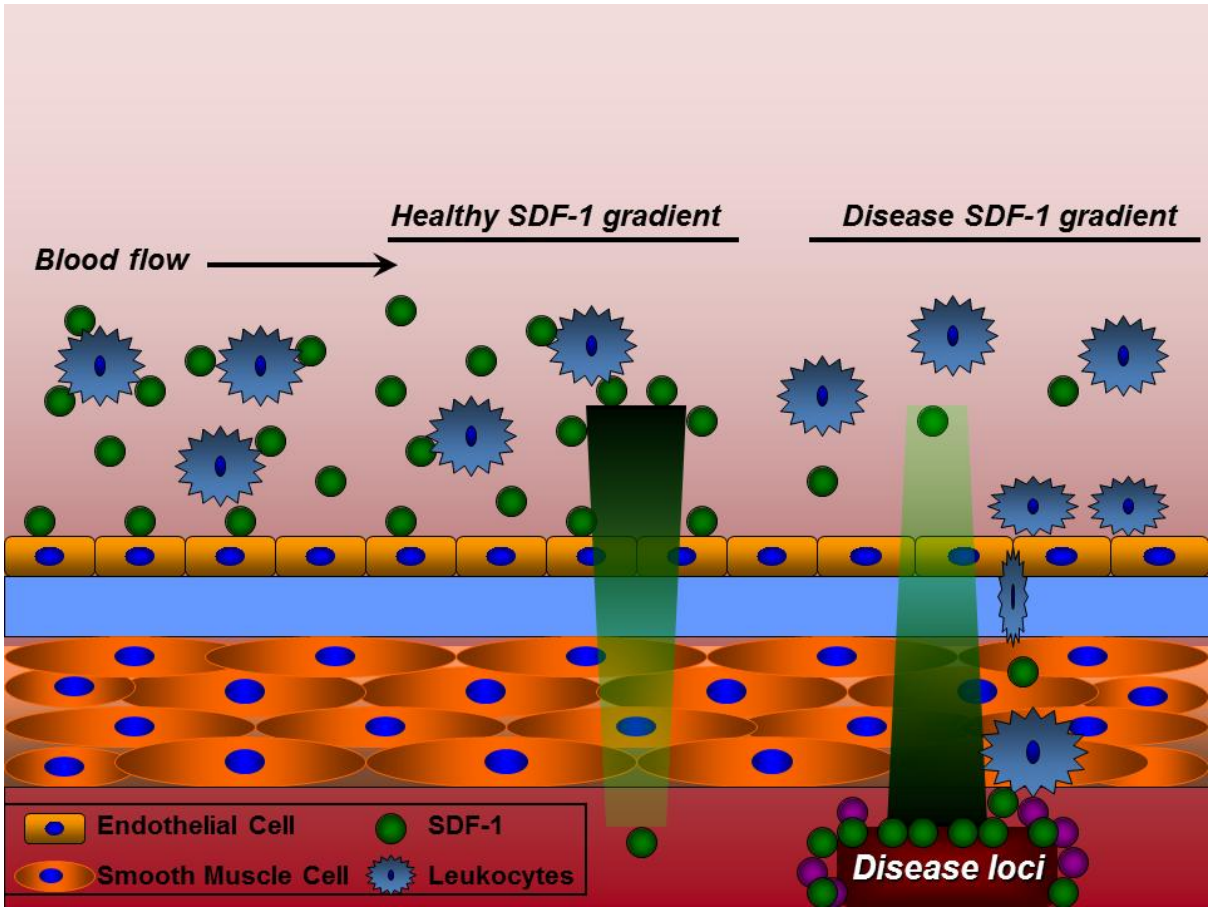


**Figure 1.9. Hypothetic SDF-1 gradient in health and atherosclerosis.**

the role of circulating SDF-1 in health and disease on circulating monocyte has not been fully addressed.

### 1.12. Aim of Study

Atherosclerotic cardiovascular disease is the leading cause of morbidity and mortality worldwide. Although lipid-lowering drugs have made a huge success story, they fail to protect more than half of patients from cardiovascular events. Thus, there is a need for better understanding of pathophysiology of atherosclerotic lesion formation and ultimately

development of novel treatment options. Monocyte/macrophage has a crucial role in the initiation and progression of atherosclerosis; this knowledge has led to the view that interruption of the recruitment and activity of these cells may represent important therapeutic targets. Although the beneficial effect of lipid-lowering therapy is associated with reduced macrophage content in atherosclerotic plaques, the underlying mechanisms are not fully understood (Puato *et al.*, 2010). Thus, it is expected to improve clinical success independently or by enhancing the efficacy of lipid-lowering medications. Unveiling the mechanisms will lead to therapies reinforcing on events that prevent monocyte recruitment and therefore reduce monocyte-derived macrophage in plaques.

Studies suggest a role of SDF-1 in atherosclerosis; however, whether the novel SDF-1 receptor, CXCR7, could be induced in inflammation process like atherosclerosis has not been elucidated yet. Our overall hypothesis is that the SDF-1 has differential roles in monocytes vs. macrophages due to dynamic expression of the CXCR4 and CXCR7 receptor. We further hypothesized that CXCR7 functionally regulates SDF-1 signaling and monocyte/macrophage function, contributing to the progression of atherosclerosis. To test these hypotheses, we used the mouse model of hyperlipidemia atherosclerosis and showed the expression of CXCR7 and a correlation with macrophage marker *in vivo*. Then the THP-1 monocyte cell line and human primary monocyte were used for *in vitro* cell culture to confirm the induction of CXCR7; and to dissect its signaling and cellular functions. Briefly, we mainly focused on the AKT, ERK, JNK, and p38 pathways, which are suggested to be involved in chemokine signaling and have been shown to play an important role in inflammation. The CXCR7 endogenous ligands, SDF-1 and I-TAC were employed to activate CXCR7. To exclude the interference of CXCR4 and CXCR3, the CXCR4 antagonist, AMD3100 and CXCR3 antagonist, compound 6c was

used. In addition, the synthetic CXCR7 agonist, TC14012, was used to confirm the effect of CXCR7. Furthermore, the effect of CXCR7 is validated by knocking down either CXCR4 or CXCR7. (Figure1.10.) To test the above central hypothesis, four specific research aims were addressed:

Aim 1: To determine whether CXCR7 is involved in monocyte-to-macrophage differentiation.

Aim 2: To explore the signaling pathway mediated by CXCR7 in macrophage.

Aim 3: To assess the CXCR7-mediated macrophage functions.

Aim 4: To dissect the mechanisms of CXCR7 expression regulation by statins.

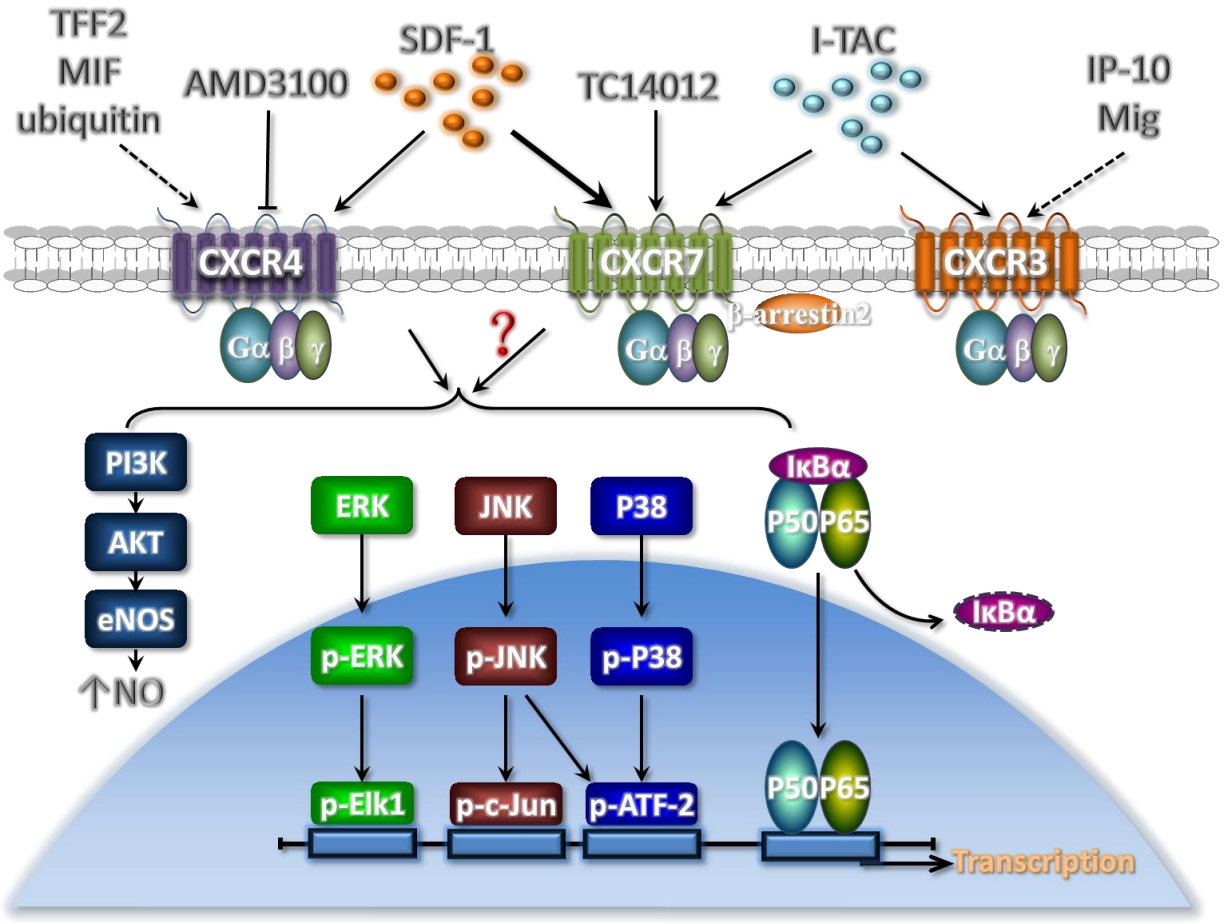


**Figure 1.10. Working model to dissect the role of CXCR4 versus CXCR7 on macrophages.**

# Chapter 2. Material and Methods

## 2.1. Materials

The commercial sources of the chemicals and recombinant proteins used in this study are listed in Table 2.1 and Table 2.2.

**Table 2.1. Chemicals**

| Items | Catalog Number | Company |
|---|---|---|
| TC14012 | 4300 | Tocris |
| AMD3100 | 239820-5MG | EMD |
| SB203580 | 1202 | Tocris |
| SP600125 | 1496 | Tocris |
| CXCR3 antagonist 6c | Axon 1800 | Axon Medchem |
| Resazurin | AR002 | R&D Systems |
| Phorbol12-myristate-13-acetate | 1201 | Tocris |
| Atorvastatin | 3776 | Tocris |

**Table 2.2. Recombinant proteins and LPS**

| Items | Catalog Number | Company |
|---|---|---|
| recombinant human SDF-1α | 350-NS | R&D Systems |

| | | |
|---|---|---|
| recombinant human I-TAC | 672-IT | R&D Systems |
| recombinant human IL-4 | 204-IL | R&D Systems |
| recombinant human IL-13 | 213-IL | R&D Systems |
| recombinant human M-CSF | 216-MC | R&D Systems |
| recombinant human GM-CSF | 215-GM | R&D Systems |
| recombinant human IFN-γ | 285-IF | R&D Systems |
| recombinant human TNF- α | 210-TA | R&D Systems |
| LPS | L 2654 | Sigma-Aldrich |

## 2.2. Cell Culture and Differentiation

### 2.2.1. Cell line and Culture

The human myelomonocytic cell line THP-1 was purchased from American Type Culture Collection (ATCC). This cell line is derived from the blood of a one-year-old boy with acute monocytic leukemia (Tsuchiya *et al.*, 1980). These cells can be continuously cultured in suspension and be further differentiated into macrophage-like cells. THP-1 cells were cultured in RPMI-1640 (HyClone, Thermo) supplemented with 10% (v/v) heat-inactivated fetal bovine serum (FBS) (HyClone, Thermo), 100U/ml penicillin, and 100 μg/ml streptomycin (Lonza) at 37 ℃ in Forma Series ii Water Jacketed incubator (Thermo) in a humidified atmosphere with 5% $CO_2$.

### 2.2.2. Passaging

The THP-1 cells were maintained in 75 $cm^2$ flask by replacing 2/3 to 3/4 of the medium when splitting. Alternatively, cells were collected and centrifuged at ~1100 rpm for 5 min and subsequently re-suspended in a concentration of ~ 2-4x$10^5$ cells/ml.

### 2.2.3. Long-term Storage

For long-time storage, confluent THP-1 cells were collected and centrifuged at ~1100 rpm for 5 min. The pellets were re-suspended in complete growth medium supplemented with 10% (v/v) DMSO (EMD Milipore) at a concentration of ~3x$10^6$ in 2 ml cryovials. The vials were transferred into an isopropanol freezing container (VWR) to reach 1 ℃/min cooling rate required for successful cryopreservation of cells, then the container was kept in -80 ℃ overnight. The following day, the frozen vials were transferred to a liquid nitrogen (-196 ℃) tank (taylor-wharton). To thaw the frozen cells, rapidly removed the cryovials into a 37 ℃ water bath and gently swirl the vials till the medium starts to thaw. Then dilute the cells suspension with pre-warmed growth medium and centrifuge at ~1100 rpm for 5 min. After the centrifugation, re-suspend the cells in complete growth medium into the appropriate culture vessel at the appropriate culture environment.

### 2.2.4. Starvation

In general, THP-1 monocytes and differentiating THP-1 macrophages were starved for 10 h in RPMI-1640 without FBS. Potential endogenous SDF-1 secreted by macrophages was minimized by changing the starvation medium 2 h before the end of starvation. Cells were pretreated with inhibitors or antagonists for 40 min before stimulation.

### 2.2.5. Cell Viability

Resazurin, a non-toxic, water soluble, redox-sensitive dye, was utilized to measure the cell viability and cytotoxicity. It changes from blue/non-fluorescent state to a pink/highly-fluorescent state via reduction by viable cells. Generally, resazurin was added directly to cultured cells in serum-supplemented medium to reach a final concentration of 10% (v/v). Fluorescence was read by Varioskan Flash Multimode Reader fluorescence (Ex/Em: 544/590).

### 2.2.6. Macrophage Differentiation and Activation

For the induction of cell differentiation, THP-1 cells were seeded at $5x10^5$ cells/well in six-well plates in RPMI-1640 supplemented with 5% FBS with 40 nM PMA for 48 h or otherwise indicated times. Alternatively, THP-1 cells were stimulated for 48 h with both IFN-γ (100 ng/ml) and M-CSF (10 ng/ml) or IFN-γ (100 ng/ml) and LPS (1 μg/ml). To obtain polarized macrophages, THP-1 cells were differentiated by treatment with 40 nM PMA for 6 h and then cultured for another 18 h with IFN-γ (20 ng/ml) and LPS (100 ng/ml) for M1 subtype, or with IL-4 (20 ng/ml), IL-13 (20 ng/ml), IL-4 (20 ng/ml) and IL-13 (20 ng/ml) to generate M 2-polarized cells. Cells only treated with PMA (40 nM) were used as controls. The non-adherent cells were removed by aspiration. Before agonist stimulation, differentiating THP-1 macrophages were starved for 10 h in RPMI-1640 without FBS.

### 2.2.7. Isolation and Culture of Human Primary Blood Monocytes

Human peripheral blood mononuclear cells (PBMCs) were separated from buffy coat (Biological Specialty Corp) by density-gradient centrifugation on Histopaque-1077 (Sigma). Briefly, 5ml buffy coat was diluted with two volumes of PBS. Then the diluted buffy coat was carefully layered on top of the same volume of Histopaque-1077. After 2000 rpm centrifuge for 30 min at room temperature, human PBMCs can be visible at PBS/ Histopaque-1077 interface. PBMCs were carefully collected and washed with PBS twice. Then untouched human primary monocytes were purified by negative selection using a Dynabeads kit (Invitrogen), yielding an average 98% purity. Freshly isolated monocytes were cultured in RPMI 1640 supplemented with 10% heat-inactivated FBS and antibiotics, and used in experiments after being stabilized for at least 2 h. In some experiments, the purified monocytes were allowed to differentiate into macrophages with the presence of recombinant human GM-CSF (50 ng/ml) plus LPS (100 ng/ml) or IFN-γ (100 ng/ml) plus LPS (1 μg/ml) for 2~3 days.

## 2.3. PCR Analysis

### 2.3.1. Isolation and Measurement of RNA and DNA

Cells were grown in six-well plates until confluence. The total RNA and DNA were extracted from THP-1 cells, human primary monocytes, THP-1-derived macrophages, and primary macrophage according to manufacturer's protocol for the RNeasy and DNeasy kits, respectively (Qiagen).

### 2.3.2. cDNA Synthesis

For the synthesis of the first strand of cDNA, 1µg of total RNA after DNase (Ambion) treatment was reverse-transcribed using Taqman reverse transcription reagents (Applied Biosystems) using the recipe in Table 2.3..

**Table 2.3. Reaction composition for cDNA synthesis**

| Component | Volume/reaction |
|---|---|
| 10xTaq RT buffer | 5µL |
| 25mM $MgCl_2$ | 11µL |
| 10mM dNTP | 10µL |
| oligo dT | 2.5µL |
| Rnase inhibitor | 1µL |
| Reverse Transcriptase or RNase free $H_2O$ | 1.25µL |
| RNA | variable |
| RNase free $H_2O$ | variable |
| Total Volume | 50µL |

The mixture of all the components was incubated at 25 ℃ for 10 min; 48 ℃ for 30 min; 95 ℃ for 5 min and then held at 4 ℃.

### 2.3.3. RT-PCR Analysis

The cDNA samples were then amplified by PCR using HotStarTaq DNA Polymerase (Qiagen) using the recipe in Table 2.4..

**Table 2.4. Reaction composition using HotStarTaq DNA polymerase**

| Component | Volume/reaction |
|---|---|
| 10xPCR buffer | 5µL |
| 10mM dNTP | 1µL |
| 5x Q-solution | 10µL |
| HotStarTaq DNA polymerase | 0.5µL |
| Rnase inhibitor | 1µL |
| Reverse transcriptase or RNase free $H_2O$ | 1.25µL |
| Forward primer | 0.5µL |
| Reverse primer | 0.5µL |
| Rnase/Dnase free $H_2O$ | 27.5µL |
| cDNA template | 5µL |
| Total Volume | 50µL |

The PCR amplification was performed using an iCycler iQ5 detection system (Bio-Rad) with jump start for 2 min at 95 ℃, followed by 40 thermal cycles of denaturation for 1 min at 95 ℃, annealing for 1 min at 56 ℃, and extension at 72 ℃ for 1 min with a final extension at 72 ℃ for 10 min. The resulting PCR products were resolved on a 1% agarose (amresco) gel with 0.01% ethidium bromide (sigma) in electrophoresis gel system (minicell primo, Thermo), and the

bands were visualized with universal hood imaging system (Bio-Rad) under ultraviolet light as we previously described (Ding *et al.*, 2011; Ma *et al.*, 2013).

### 2.3.4. Real-time PCR Analysis

Real time RT-PCR was carried out using an iCycler iQ5 detection system (Bio-Rad) with SYBR Green reagents (Applied Biosystems), as we previously described (Ding *et al.*, 2011; Ma *et al.*, 2013). The PCR mixture (20 μL) contained 0.5 μM concentration of each primer, 4 μl of water, 10 μL of SYBR Green mixture, and 5 μL of cDNA template from previous step. The samples were placed in 96-well plates that were sealed with optical clear cap (Fisher) with the following reaction condition: initial PCR activation step (5 min at 95 ℃), and cycling steps (denaturation for 1 min at 95 ℃, annealing for 1 min at 60 ℃, extension for 2 min at 72 ℃; 40 cycles). Internal controls, GAPDH or β-actin were amplified in separate wells. For data analysis, we used the comparative cycle threshold method (ΔΔCt method) for relative quantitation of gene expression. Basically, the cycle threshold (Ct) for the target amplicons and internal controls were determined. The fold change in the target gene relative to the endogenous control gene is determined by:

$$\text{Fold Change} = 2^{-\Delta(\Delta Ct)}$$

where $\Delta Ct = Ct\ (\text{target genes}) - Ct\ (\text{internal controls})$

and $\Delta(\Delta Ct) = \Delta Ct\ (\text{stimulated}) - \Delta Ct\ (\text{control})$

Thus, all values for experimental samples were expressed as differences (n-fold) between the sample mRNA and the calculator mRNA. The sequences of primers are listed in the Table 2.5..

**Table 2.5. Primers used for PCR assay**

| Gene | Forward Primer | Reverse Primer |
|---|---|---|
| h CXCR4 | 5'-CACTTCAGATA-ACTACACCG-3' | 5'-ATCCAGACGCCAACATAGAC-3' |
| h CXCR7 | 5'-TGGTCAGTCTCGTGCAGCAC-3' | 5'-GCCAGCAGACAAGGAAGACC-3' |
| h CXCR3 | 5'-CCCTCCTGGAGAACTTCAG-3' | 5'-GTATTGGCAGTGGGTGGCG-3' |
| h SDF-1 | 5'-GACCCGCGCTCGTCCGCC-3' | 5'-GCTGGGCTCCTACTGTAAGGG-3' |
| h β-actin | 5'-ATTGCCGACAGGATGCAGAA-3' | 5'-GCTGATCCACATCTGCTGGAA-3' |
| h GAPDH | 5'-TCAACAGCGACACCCACTCC-3' | 5'-TGAGGTCCACCACCCTGTTG-3' |

## 2.4. Western Blotting

### 2.4.1. Solutions

The commercial sources of the buffers and chemicals used in this study for Western blotting are listed in Table 2.6.

**Table 2.6. Buffers used for Western blot**

| Items | Catalog Number | Company |
|---|---|---|
| 10x Tris Glycine Buffer | 75894 | USB Affymetrix |

| | | |
|---|---|---|
| 10x Tris/Glycine/SDS Buffer | 161-0732 | Bio-Rad |
| 20x Tris-Buffered Saline and Tween 20 | 77500 | USB Affymetrix |
| Western Lightning® Plus-ECL | NEL105001EA | PerkinElmer |
| Blotto (non-fat dry milk) | sc-2324 | Santa Cruz Biotechnology |
| Albumin, Bovine Fraction V | 9048-46-8 | Research Products International Corp. |

Milli-Q purified water was used to dilute the buffers. Electrophoresis buffer was diluted from 10x Tris/Glycine/SDS Buffer and the dilution contains 25mM Tris, 192mM Glycine and 0.1% (w/v) SDS at PH 8.3. Transfer buffer was diluted from 10x Tris Glycine buffer and 20% (v/v) methanol with a final concentration of 25 mM Tris, 192 mM Glycine at PH 8.3. Tris-Buffered Saline and Tween 20 (TBS-T) buffer was made from 10x TBS-T buffer and containing 500 mM Tris, 60 mM KCl, 2.8 mM NaCl, and 1.0% Tween-20. Blocking buffer was made with 5% non-fat dry milk in TBS-T buffer. Primary antibody was diluted in 5% bovine serum albumin (BSA) in TBST buffer.

### 2.4.2. Sampling

Cells were cultured in six well plates and serum-deprived for 10 h before stimulation with agonists at the indicated concentration. Then the supernatant was removed directly or by centrifuge and cells were solubilized in 250μL Laemmli sample buffer (sigma-aldrich) and scratched with rubber policeman on ice followed by being heated in boiling water for 5 min.

### 2.4.3. Blotting

Precision plus protein dual color standard (Bio-Rad) was used as a reference to identify the approximate molecular weight. Samples were loaded and separated on 12% Mini-PROTEAN® TGX™ Precast Gel (Bio-Rad) in a SDS-PAGE gel chamber (Bio-Rad) in electrophoresis buffer for 45 min with the voltage of 110 V. After running the gel, assemble the stack in the order of two layers of absorbent paper, which was thoroughly soaked in transfer buffer; the SDS-PAGE gel; a wet polyvinylidene difluoride (PVDF) membrane (Thermo); two layers of absorbent paper, which was thoroughly soaked in transfer buffer. Gels were blotted using a semi-dry blotting apparatus (Bio-Rad) for 35 min with the voltage of 20 V. After transfer, the stack was carefully disassembled. The membrane was blocked for 1 h (room temperature, shaking) in Western blot blocking solution. The membrane was probed with the primary antibody overnight in 5% BSA in TBS-T buffer. The primary antibodies used for Western in this study are listed in Table 2.7.. Next day, the blots were washed in TBS-T buffer for four times 10 min each time. A horseradish-conjugated secondary antibody (Cell Signaling) was incubated for 1 h at room temperature (5 % dry milk in TBS-T buffer). Unbound antibodies were washed in TBS-T buffer four times for 10 min each time. The bound antibody was detected by incubating the blots in Western Lightning® Plus-ECL (PerkinElmer). The image was captured on a sensitive photographic film (research products international corp.), placed against the membrane, and visualized by medical film processor (Konica Minolta medical & graphic Inc.).

**Table 2.7. The primary antibodies used for Western blot**

| Items | Catalog Number | Clone | Company |
|---|---|---|---|
| anti-human CXCR7 mAb | MAB42273 | 11G8 | R&D Systems |

| | | | |
|---|---|---|---|
| anti-human CXCR7 mAb | K0223-3 | 9C4 | MBL |
| anti-human CXCR7 mAb | 331110 | 8F11-M16 | BioLegend |
| anti-human CXCR4 mAb | MAB171 | 44708 | R&D Systems |
| P-p44/42 MAPK | 4370 | D13.14.4E | Cell Signaling |
| P-p38 MAPK | 4511 | D3F9 | Cell Signaling |
| P-SAPK/JNK | 4668 | 8.1E+12 | Cell Signaling |
| P-AKT | 4060 | D9E | Cell Signaling |
| GAPDH | 2118 | 14C10 | Cell Signaling |
| α-tubulin | 2125 | 11H10 | Cell Signaling |
| β-tubulin | 2128 | 9F3 | Cell Signaling |

### 2.4.4. Imaging Analysis

The images on the films were then scanned into the computer for presentation and analysis. The intensity of signals was acquired in the linear range of the digital images using specific densitometric software, Quantity One. Images were calibrated against the background and given in relative density units.

### 2.4.5. Stripping and Re-probing

Equal protein loading was verified by stripping off the original antibodies and re-probed with the primary antibodies. Blots were rinsed with TBS-T buffer and incubated for 15 min at room temperature in restore PLUS Western blot stripping buffer (Thermo). After which, the membrane was extensively rinsed with TBS-T buffer three time for 1 min each time, and

blocked for 30 min in 5% non-fat dry milk in TBS-T buffer. Subsequently, the blots were re-probed with desired primary antibodies as described previously (Ding *et al.*, 2011; Ma *et al.*, 2013).

### 2.5. Immunofluorescence Assay

THP-1 cells and primary human blood monocytes were seeded in 8-chamber glass slides (Nalge Nunc International) with or without differentiation into macrophages using the methods in the previous section. After 48 h, the medium was aspirated and cells were fixed in cold methanol for 10 min. The fixed cells were washed with PBS buffer (Calbiochem) three times and blocked with 3% horse serum (Sigma-aldrich) for 1 h at room temperature. Then the cells were incubated with mouse monoclonal anti-hCXCR7 antibody (1:100, 11G8, R&D Systems) overnight at 4 ℃ in humid chamber followed by incubation with FITC-conjugated anti-mouse IgG for 90 min at room temperature in dark. For negative controls, cells were incubated with non-immune IgG in place of the specific primary antibody or just the FITC-conjugated second antibody. Images with fluorescent signals in random fields were acquired and captured using EVOS® digital inverted multi-functional microscope (AMG) as we previously reported (Ding *et al.*, 2011; Ma *et al.*, 2013).

.

### 2.6. Flow Cytometry Assay

The antibodies and isotype controls used for flow cytometery in this study are listed in Table 2.8..

**Table 2.8. The fluorescence-conjugated antibodies used for flow cytometry.**

| Items | Flurophore | Clone | Catalog Number | Company |
|---|---|---|---|---|
| anti-h/m CXCR7/RDC-1 | phycoerythrin | 11G8 | FAB4227P | R&D Systems |
| mouse $IgG_1$ isotype control | phycoerythrin | 11711 | IC002P | R&D Systems |
| anti-h CXCR4 fluorescein | fluorescein | 12G5 | FAB170F | R&D Systems |
| mouse $IgG2_a$ isotype control | fluorescein | 20102 | IC003F | R&D Systems |
| anti-human CD36 | FITC | 5-271 | 336203 | Biolegend |
| mouse $IgG2_a$ isotype control | FITC | MOPC-173 | 400209 | Biolegend |
| anti-human CD68 | FITC | Y1/82A | 333806 | Biolegend |
| mouse $IgG_{2b}$ isotype control | FITC | MPC-11 | 400310 | Biolegend |
| anti-human CD206(MMR) | Alexa Fluor 488 | 15_2 | 321113 | Biolegend |
| mouse $IgG_1$ isotype control | Alexa Fluor 488 | MOPC-21 | 40132 | Biolegend |
| anti-human CD206(MMR) | perCP-eFluro 710 | 19.2 | 46-2069-41 | eBioscience |
| mouse $IgG_{1\kappa}$ isotype control | perCP-eFluro 710 | p3.6.2.8.1 | 46-4714-80 | eBioscience |

For determining cell surface CXCR4, CXCR7, and CD36 cells were washed twice with flow cytometry staining buffer (Biolegend) and suspended in the same buffer to a final concentration of $4x10^6$ cells/ml. After which, 25 µl cell aliquots were transferred for Fc receptor blocking with human IgG (R&D Systems) for 15 min at room temperature. Then the cells were stained with fluorescence conjugated antibodies or non-immune IgG isotype controls as listed in Table 2.8. at 10 µg/ml on ice for 30 min in dark and then rinsed with cold buffer (PBS containing 2% FBS). For intercellular staining of CD68, the cells were washed twice with flow cytometry staining buffer and fixed for 10 min at room temperature in 4%

paraformaldehyde (v/v). After twice washing, the cells were resuspended in 100 µl 0.5% triton X in PBS buffer plus 0.5 µg/ml FITC-labeled anti-human CD68. After incubation for 30 min at room temperature in dark, cells were washed again and analyzed. After rinsing, cells were re-suspended in the same buffer for flow analysis in the Accuri C6 Flow Cytometer®.

### 2.7. Detection of *In Vivo* CXCR7 in Plaque Macrophages of *ApoE*-null Mice

Normally, mice do not develop atherosclerosis. The *ApoE*-/- mouse spontaneously develop hyperlipidemia and atherosclerotic lesions in a way that is very similar to humans. Thus *ApoE*-/- mouse provides an excellent model for studies of atherosclerosis. *ApoE*-deficient mice and genetically matched C57BL/6 normal control mice (Jackson Laboratory) with same ages and genders were employed in this study as we previously described (Shen *et al.*, 2010). Mice were housed in specific pathogen-free animal facilities of Auburn University. Mice were kept under 12 h dark / 12 h light cycles and were administered fresh water and pellet food. Mice were fed standard chow diet with 4.5% fat (PMI Feeds, St. Louis, MO). All mice were maintained in a facility free of well-defined pathogens under the supervision of the Biological Resource Unit at Auburn University. All animal protocols were approved by Auburn Institutional Animal Care and Use Committee; and the investigation conforms to the Guide for the Care and Use of Laboratory Animals published by the United States National Institutes of Health.

We fed mice with normal chow diet for 16 weeks, and then evaluated atherosclerotic lesions in aortic sinus by oil red O staining as reported previously (Shen *et al.*, 2010). The mice hearts and aorta were perfused, dissected, and subjected to determination of atherosclerosis, as

previously described (Shen *et al.*, 2010). Briefly, mice requiring aortic tissue analysis were euthanized by deep anesthesia with ketamine/xylaxine (170 mg/kg and 5 mg/kg, respectively, intraperitoneal injection once) prior to intracardiac perfusion with 4% paraformaldehyde in PBS. The hearts were embedded in optimal cutting temperature (OCT) medium and frozen, after which serial sections (10 μm) were taken from the aortic sinus.

### 2.8. Immunohistochemistry Analysis

Mouse aortic sections were fixed in cold methanol for 10 min and rinsed twice in PBS. Sections were blocked with 5% horse serum at room temperature for 1 h. The anti-F4/80 or anti-mCXCR7 mAb (11G8) or isotype control antibodies were added to the sections at 10 μg/ml and incubated at room temperature for 1.5 h. Sections were rinsed thoroughly in PBS and incubated with Dylight 488-conjugated anti-rat IgG (Biolegend) or NL637-conjugated anti-sheep IgG (R&D Systems) for 45 min. Sections were then counterstained with H&E and oil red O, rinsed thoroughly in PBS, and cover slipped with Vectashield Mounting Medium (Vector laboratories), as previously reported(Ding *et al.*, 2011; Ma *et al.*, 2013). All images were acquired and captured on EVOS. The CXCR7-positive and F4/80-positive areas were determined in 4 sections from each mouse, using 80 μm intervals between the sections; the results were confirmed in three *ApoE*-null and control mice.

### 2.9. Silencing of CXCR4/CXCR7 Receptor by siRNA

To knockdown the CXCR7 and CXCR4 receptor, THP-1 cells were transfected with the four-sequence pool (ON-TARGET plus CXCR7 siRNA: L-013212-00-0005; ON-TARGET

plus CXCR4 siRNA: L-005139-00-0005; ON-TARGET plus Non-targeting scramble control siRNA: D-001810-10-05, Dharmacon) by electroporation using the Lonza Nucleofector technology (4D-Nucleofector®). We followed an optimized protocol reported recently by Schnoor et al (Schnoor *et al.*, 2009). Briefly, a human monocyte nucleofector kit (Lonza) was used for the transfection and the number of THP-1 cells was $2.5x10^6$ per transfection cuvette. THP-1 cells were recovered 4 h after transfection in Human Monocyte Nucleofector Medium (Lonza) supplemented with 20% FBS. Transfected cells per cuvette were transferred into single well of 6-well plates containing 1.5 ml fresh Human Monocyte Nucleofector Medium supplemented as described above and containing PMA 40 nM or IFN-γ (100 ng/ml) plus LPS (1 μg/ml) for macrophage differentiation for 24~48 h. Real-time RT-PCR assay was performed to confirm the decrease or suppression of CXCR7 mRNA after 24 h post-transfection. For cell stimulation, transfected and differentiated cells were starved for at least 8 h before stimulated by SDF-1 or TC14012 for the indicated times.

**2.10. Macrophage Phagocytosis**

Macrophage phagocytic activity was measured using the Vybrant Phagocytosis Assay Kit (Invitrogen) and fluorescently labeled acetylated low-density lipoprotein, Dil-Acetylated LDL (Ac-LDL) (Invitrogen). Briefly, human primary monocytes were differentiated into macrophages in 96-well plate as described above and starved for 10 h. The cells in four replicates were stimulated with agonists for 2 h with or without pre-treatment with inhibitors. The cells were further incubated with heat-inactivated, fluorescein-labeled *E. coli* K-12 BioParticles for 2 h, after which extracellular fluorescence was quenched by trypan blue and phagocytic activity was quantified by measuring fluorescence of the uptaken particles emission

at 520 nm with an excitation at 485 nm using a microplate reader (FLUOstar). To assay Dil-Ac-LDL uptake, PMA driven macrophages in 96-well were preincubated for 2 h with the indicated concentrations at 37℃ followed by a further incubation of 10 μg/ml Dil-Ac-LDL. Then the cells were washed twice in PBS and the fluorescence was read by Varioskan Flash Multimode Reader fluorescence (Ex/Em: 554/571).The negative controls were prepared by adding vehicles and fluorescence labeled particles without cells; and macrophages without stimulation were used as positive controls. Results were expressed as the percentage of increase compared to positive controls after deduction of negative controls as suggested by the kit instruction.

### 2.11. Gene Expression Profiling

The Human Atherosclerosis RT ² Profiler PCR Array and Human Inflammtion RT ² Profiler PCR Array (Qiagen), which profiles the expression of 84 genes related to atherosclerosis or inflammation, were used. Total RNA was prepared from the PMA-derived macrophage with or without SDF-1 300 ng/ml treatment for 1 h then total RNA was extracted as described in the previous section. 1 μg total RNA from each group was reverse transcribed, and the realtime-PCR analysis of 84 atherosclerosis related genes was performed per the manufacturer's protocol. Data analysis was performed using the manufacturer's integrated web-based software package for the PCR Array System using ΔΔCt based fold-change calculations.

### 2.12. Optical Microscopy Imaging for Cell Counting

Single color fluorescent images were obtained by capturing the Calcein AM stained cells using an EVOS® digital inverted multi-functional microscope. Automatic cell counting was performed using the ImageJ software, version 1.4 (NIH). In each group at least five images obtained from randomly views were first converted to 16-bit grayscale using the Image > Type > 16-bit command. Next, the background was set using the Image > Adjust > Threshold command followed by cell counting using the Analyze > Analyze Particles command. All images in the same series were processed using the same analysis parameters. The numbers shown in the graphs represent the average number of cells per image for each treatment.

### 2.13. Macrophage Adhesion Assay

THP-1 cells were differentiated and starved for 10 h. Cells were stained with 5 uM Calcein AM for 30 min at 37 ℃ before detachment with accutase. The cells were resuspended and seeded in 6-well plates to reach a final concentration of $5 \times 10^4$ cells/well in triplicate and allowed to adhere at 37 ℃ for 5 min. The unattached cells were then gently rinsed off twice with warmed phosphate-buffered saline (PBS) and fixed for 15 min in cold methanol. Images of adherent macrophages were captured under the fluorescent microscope with five random fields. A researcher who was blinded to the experimental protocols counted the number of adherent cells as described in the previous section. Data are expressed as the average number of adherent cells compared to control.

### 2.14. Boyden Chamber Cell Migration Assay

Cell migration was performed with the modified Boyden chamber trans-well system (BD Biosciences). Briefly, pre-coated cell culture inserts having 8 μm pore size membranes were placed into 24-well plates. Differentiated THP-1 cells were starved for 10 h and detached by accutase, then re-suspended in RPMI 1640 medium without FBS. Cell suspensions (150 μL, $10^4$ cells) were added to the upper chambers (the inserts) of the Boyden chamber system. The lower chamber was filled with 500 μl RPMI 1640 medium with starvation medium, SDF-1, TC14012, I-TAC or RPMI 1640 medium without 10% FBS in different concentrations. Cells were stimulated overnight, after which the cells remaining on the upper surface of the membrane were removed by cotton swab. Inserts were then washed 3 times with PBS and cells on the underside of the membrane were fixed with cold methanol for 15 min. The membranes were washed again, removed, and mounted on glass slides before stained with DAPI. Cells were counted from ten random fields by a blinded manner using Image J as described previously. The assays were performed in triplicate wells for each condition, and each experiment was repeated at least 3 times.

**2.15. Data Analysis**

Data are expressed as the mean ± S.E.M.. The means of two groups were compared using Student's t test (unpaired, two tailed), and one-way analysis of variance was used for comparison of more than 2 groups with $p < 0.05$ considered to be statistically significant. Unless otherwise indicated, all experiments were repeated at least three times. Statistical analysis was performed with Graphpad Prism 5.0.

# Chapter 3. Results

## 3.1. *In Vivo* Expression of CXCR7 in Atherosclerotic Plaques of *ApoE*-null Mice

To determine whether CXCR7 is involved in atherosclerosis, we assessed the aorta sections from atherosclerotic lesions *ApoE*-null mice and the gender and age-controlled C57BL6/J mice. Our immunohistology assay showed that the normocholesterolemic control mice did not develop atherosclerosis and the morphology of aorta was normal and lipid-free. However, the hypercholesterolemic *ApoE*-null mice gained atherosclerosis and the atheroma were featured with remodeled intima and lesion with accumulated lipids, as defined by the Oil-Red O staining. (Figure 5.1.A, top) Immunofluorescent analysis on serial sections of mouse aorta from *ApoE*-null mice showed that CXCR7 protein was expressed in the intima of the atherosclerotic lesions. In addition, CXCR7 protein expression was co-localized with F4/80-positive macrophage areas of the atheroma (Figure 5.1.A right). In contrast, the parallel analysis of the aorta sections from control C57BL6/J mice did not detect any noticeable CXCR7 protein and were F4/80-negative in the atheroma (Figure 5.1.A left). Figure 5.1.B shows that the fluorescence conjugated control IgG for either F4/80 or CXCR7 did not exhibit significant staining, indicating the specificity of the assay system. Based on this study, it was speculated that CXCR7 is induced during atherogenesis on macrophages in mice.

## 3.2. CXCR7 mRNA is Induced During Monocyte-to-Macrophage Differentiation

As mentioned earlier, studies have shown that CXCR7 is not expressed on monocytes, but whether CXCR7 could be induced on macrophages during inflammation has been omitted (Berahovich *et al.*, 2010b). To investigate whether CXCR7 is induced during monocyte-to-macrophage differentiation, THP-1 cells were treated with PMA, a well-established macrophage inducer (Daigneault *et al.*, 2010; Tsuchiya *et al.*, 1982). As expected, the THP-1 cells which were floating in the cell culture medium acquired a macrophage-like morphology and became adherent on the flask after stimulation by PMA (40 nM) for 48 h (Figure 5.2.A). In addition, we analyzed changes in the expression of the macrophage differentiation markers the class D receptor CD68 and cluster of differentiation 36 (CD36) (Figure 5.2.B). Our results suggested that consistent with morphology change, the macrophage markers, scavenger receptors CD36 and CD68, were up-regulated on PMA-derived macrophages.

RT-PCR analysis showed that undifferentiated THP-1 cells expressed high level of CXCR4, but not CXCR7 mRNA; treatment of the cells with PMA dose-dependently induced CXCR7 mRNA expression, with a simultaneous down-regulation of CXCR4 mRNA (Figure 5.3.A). Real-time PCR assay confirmed that CXCR7 mRNA was induced as early as 2 h in response to 40 nM PMA, reached maximal level at 24~48 h, and then declined to a level still significantly higher than that of time-controlled undifferentiated cells (Figure 5.3.B). In contrast, the same differentiation protocol suppressed CXCR4 mRNA expression more than 50% in the observation window (Figure 5.3.B). These data indicate that during monocyte-to-macrophage differentiation, the two SDF-1 receptors CXCR4/7 mRNA change their expression patterns in opposing directions.

### 3.3. Induced CXCR7 mRNA is not Affected by Starvation or Autocrine SDF-1

To determine whether serum starvation affect the CXCR7 mRNA, the PMA driven macrophage were starved for another 10 h. Real-time PCR assay showed that starvation of the macrophage for 10h did not cause significant difference of CXCR7 mRNA compared to the macrophage with extended treatment with PMA (Figure 5.4.A) suggesting the starvation of macrophage does not cause loss of CXCR7 in this study.

In addition, studies have suggested that SDF-1 is constitutively secreted by monocytes and modulates monocyte-to-macrophage differentiation (Sanchez-Martin *et al.*, 2011). To determine whether the autocrine SDF-1 influence macrophage differentiation in our system, the macrophages were induced by PMA with or without SDF-1 neutralizing antibodies or its isotype control. As shown in Figure 5.4.B, the morphology of macrophages was not affected by SDF-1 neutralization. Moreover, we analyzed the expression of the macrophage differentiation marker, CD68 and macrophage mannose receptor (MMR or CD206). Our results suggested that in line with our previous data, the CD68 and CD206 were up-regulated on PMA-derived macrophages as expected, but SDF-1 neutralization has negligible effects on the expression of CD68 and CD206 (Figure 5.4.C), suggesting autocrine of SDF-1 by THP-1 macrophage does not play a significant role in this study.

### 3.4. CXCR7 Protein Expression in Monocytes versus Macrophages

To assess whether the induced CXCR7 mRNA is translated into protein, we performed Western blotting assay. Our data further showed that during monocyte-to-macrophage

differentiation, CXCR7 total protein was detected by three different specific mouse monoclonal antibodies at the predicted size (Berahovich *et al.*, 2010a), whereas CXCR4 protein level was down-regulated as compared to control cells (Figure 5.5.A). To determine whether CXCR7 induction is applicable to primary cells, we isolated and purified primary human periphery blood $CD14^+$ monocytes. Our immunofluorescence assay clearly showed that CXCR7 was expressed in macrophages differentiated from primary human peripheral blood monocytes after 48 h treatment with IFN-γ + LPS as well as THP-1 macrophages (Figure 5.5.B). Consistent with our observation in THP-1 cells, CXCR7 protein was not detected in normal primary human monocytes. Of notes, no positive staining was observed once CXCR7 monoclonal antibody 11G8 was replaced by its IgG control antibody or when only FITC-conjugated secondary antibody was used, indicating the specificity of immunofluorescent staining of CXCR7 protein (Figure 5.5.B).

To confirm whether CXCR7 is present on cell surface, we performed flow cytometry assays. Figure 5.6.A. shows that CXCR7 was not expressed in THP-1 cells or in primary monocytes; however, upon differentiation by PMA or IFN-γ + LPS for 48 h, cell surface CXCR7 antigen was significantly increased in THP-1 macrophages or in macrophages differentiated from primary cells. In contrast, cell surface CXCR4 antigen decreased during the differentiation process as measured by mean fluorescence intensity (Figure 5.6.B). We found a similar change when the percentages of CXCR4-positive or CXCR7-positive cells were determined (Figure 5.6.C&D). Together, these suggested the induced CXCR7 mRNA is translated into protein and present on the cell surface on macrophages.

### 3.5. CXCR7 is Differentially Up-regulated in M1 versus M2 Macrophages

To determine whether CXCR7 up-regulation in THP-1 cells is limited to the reagent PMA, we treated the cells with alternative differentiation factors that are more pathologically relevant. Figure 5.7.A shows that CXCR7 mRNA was similarly induced in response to IFN-γ + LPS, but not to IFN-γ + M-CSF. To investigate whether CXCR7 is differentially expressed on polarized macrophages, especially the M1 and M2 macrophages, the macrophages are polarized into M1 (IFN-γ + LPS; M-CSF + LPS; GM-CSF + LPS) or M2 macrophages (IL-4; IL-13). As shown in Figure 5.7.B, similar pattern of CXCR4/7 mRNA expression change was observed in human primary monocytes when they were differentiated into M1 and M2 macrophages with a more robust induction of CXCR7 in M1 cells than in M2 cells. In addition, our flow cytometry data indicated that both IFN-γ + LPS polarized M1 and IL-4 polarized M2 primary macrophages exhibited increased CD68; more CXCR7 antigen was detected on M1 macrophages than did M2 macrophages (Figure 5.7.C).

### 3.6. SDF-1 Activates ERK and AKT Pathways, but not JNK, p38, and NF-κB Pathways on Monocytes

To determine whether CXCR7 plays a role in SDF-1 signaling, we first compared SDF-1 signaling profiles in human primary monocytes versus macrophages. As shown in Figure 5.8.A, stimulation of THP-1 cells with SDF-1 dose-dependently activated the ERK and AKT pathways with negligible or no effects on the p38 and JNK pathways. Notably, the physically level of SDF-1 as detected in healthy subjects was around 3.5 ng/ml, which elicited a strong pro-survival ERK and AKT signal in our study; on the contrary, the inflammatory cytokine,

TNF-α, mainly activated pro-inflammatory p38 and JNK pathways. A similar pattern of ERK and AKT activation was found on human primary monocytes (Figure 5.8.B).

To further confirm the ERK and AKT activation were mediated by CXCR4, the monocytes were treated with or without different doses of CXCR4 antagonist, AMD3100 before SDF-1 activation. Our data suggest that the maximal dose of AMD3100 did not activate ERK or AKT, but AMD3100 dose-dependently inhibited the ERK and AKT elicited by physiological level of SDF-1 (3.5 ng/ml). (Figure 5.9.)

It is well established that NF-κB is an inflammatory cytokine that induces the expression of pro-coagulatory tissue factor expression (Ding *et al.*, 2011). To investigate whether this pathway is involved in CXCR4 mediated signaling pathways, the IκBα and phosphorylated p65 levels were analyzed when the cells were treated with physiological level of SDF-1 at different time intervals. Figure 5.10. shows that SDF-1 did not induce IκBα degradation or increase of p65 phosphorylation; however, TNF-α as a positive control greatly reduced total IκBα and increased p65 phosphorylation. (Figure 5.10.) These data suggest that the NF-κB pathway is not involved in CXCR4-mediated NF-κB pathways on monocytes.

### 3.7. Induction of CXCR7 during Monocyte-to-Macrophage Differentiation Switches SDF-1 Signaling to JNK and p38

Surprisingly, once the cells were differentiated into macrophages, the ERK and AKT pathways were not activated by SDF-1. Interestingly, on these macrophages, SDF-1 became a strong activator of the p38 and JNK pathways. Our time dependent study showed that the maximal

activation of p38 and JNK was observed at 15 min, and the activation was in a level comparable to a maximal dose of LPS (Figure 5.11.A). So 15 min was chosen to observe the effect of SDF-1 on CXCR7 positive macrophages activation. The activation of p38 and JNK by SDF-1 was dose-dependent and was further confirmed on THP-1 macrophages and primary macrophages (Figure 5.11.B&C&D). These data suggest that CXCR7 induction may switch SDF-1 signaling from pro-survival ERK and AKT to pro-inflammatory JNK and p38 pathways during monocyte-to-macrophage differentiation.

### 3.8. CXCR7 Agonists Activate JNK and p38 via CXCR7 but not CXCR4

To further evaluate the role of CXCR7 in SDF-1 signaling in macrophages, we stimulated the cells with the CXCR7-selective peptide agonist TC14012. Figure 5.12.A showed that TC14012 activated p38 and JNK pathways in a time-dependent manner, which began as early as 5 min, peaked at 15-30 min, which was comparable to the maximal dose of LPS. Figure 5.12.B indicated that TC1402 is a potent CXCR7 agonist, which dose-dependently triggered p38 and JNK signals at 0.01 μM and reached a plateau at 0.1 μM, with a slight inhibition on the ERK and AKT pathways, suggesting a potential role of CXCR7 in SDF-1 signaling in macrophages.

To verify the contribution of CXCR7, we silenced *CXCR7* gene in THP-1 cells using siRNA techniques. Figure 5.13.A show that CXCR7 mRNA and protein expression were significantly suppressed by transfection of *CXCR7*-selective siRNA, but not by scramble control siRNA. Of note, transfection of *CXCR7*-selective siRNA did not affect CXCR4 expression (Figure 5.13.B). In addition, silencing CXCR7 abolished the effect of SDF-1 and TC14012 on p38 and

JNK activation in these macrophages, with no impact on LPS signaling (Figure 5.13.C). Furthermore, the ERK and AKT pathways were not changed in response to SDF-1, TC14012 or LPS after silencing CXCR7 (Figure 5.13.C).

To further assess the contribution of CXCR4 in SDF-1 signaling in macrophages, we knocked down *CXCR*4 by siRNA. Figure 5.14.A shows that *CXCR4*-selective siRNA suppressed CXCR4, but not CXCR7 or GAPDH protein expressions. In addition, SDF-1- or TC14012-induced p38 and JNK activations were not affected by silencing of *CXCR4*, indicating that CXCR7 can signal independent of CXCR4 in macrophages (Figure 5.14.B).

### 3.9. I-TAC-induced JNK and p38 on Macrophages

Since I-TAC is the other endogenous agonist for CXCR7, we evaluated whether the I-TAC/CXCR7 pathway has a same role as SDF-1 did. Figure 5.15.A showed that neither monocytes nor macrophages express detectable level of cell surface CXCR3, another receptor for I-TAC, but it is highly expressed in blood lymphocytes. Consistent with this, stimulation of monocytes by I-TAC did not induce any effect on the ERK, AKT, p38, and JNK pathways, but SDF-1 strongly activated ERK and AKT as expected (Figure 5.15.B). However, I-TAC significantly activated p38 and JNK in macrophages in a time-dependent manner, albeit not as efficacious as SDF-1 (Figure 5.15.C). Of note, like SDF-1, I-TAC had no effect on the ERK and AKT pathways in macrophages. Figure 5.15.C shows that pretreatment of macrophages with the compound 6c, a CXCR3-selective antagonist, had no impact on I-TAC-induced p38 and JNK activation. In contrast, *CXCR7* silencing by siRNA almost abolished the effect of I-TAC on p38 and JNK in macrophages (Figure 5.15.E), indicating a role for CXCR7 in I-TAC

signaling.

### 3.10. CXCR7 Prompts Macrophage Phagocytosis of *E.coli* and Uptake of Ac-LDL

Next, we evaluated whether CXCR7 plays a role in macrophage functions. Firstly, we focused on phagocytosis, the primary function of macrophages. Figure 5.16.A shows that stimulation of macrophages by either SDF-1 or TC14012 significantly increased cellular phagocytosis as evidenced by increased uptake of FITC-labeled *E.coli*. Of note, we observed that TC14012 was more efficacious than SDF-1, and both are more efficacious than IFN-γ (Figure 5.16.B). In addition, treatment of the cells with CXCR4-selective antagonist AMD3100 had no inhibition on SDF- 1's effect (Figure 5.16.C). In contrast, siRNA silencing of *CXCR7* almost eliminated the effect of either SDF-1 or TC14012, but not that of IFN-γ (Figure 5.16.D), suggesting a role for CXCR7 in macrophage phagocytosis. To explore the role of JNK and p38 in CXCR7-mediated cellular phagocytosis, well-established selective inhibitors for p38 and JNK were employed. Figure 5.16.E shows that inhibition of either JNK or p38 significantly suppressed SDF-1- or TC14012-induced cellular phagocytosis. Together, these data suggest that SDF-1 promotes macrophage phagocytosis via CXCR7-mediated JNK and p38 pathways.

We further extended the study to a more atherosclerosis relevant context. Figure 5.16.A shows that SDF-1 and TC14012 increased macrophage uptake of Dil-ac-LDL, and the efficacy of SDF-1 was comparable to that of IgG, activator of Fcγ receptors. In addition, we confirmed that this effect was not affected by CXCR4 blockade (Figure 5.16.C), but was abated by *CXCR7* siRNA (Figure 5.16.D), and CXCR7 mediated activation of JNK and p38 pathways were required for this effect (Figure 5.16.E).

### 3.11. Role of CXCR7 in I-TAC-induced Macrophage Phagocytosis

Finally, we verified whether I-TAC promotes macrophage phagocytosis through CXCR7. Figure 5.17.A-C shows that stimulation of macrophages with I-TAC increased macrophage uptake of *E.coli* particles, which was suppressed by siRNA silencing of *CXCR7* or blocking the p38/JNK pathways, but not by CXCR3 blockade. Similarly, we found that I-TAC increased macrophage uptake of Dil-ac-LDL in a CXCR7 and p38/JNK-dependent but CXCR3-independent mechanism (Figure 5.17.D-E).

### 3.12. Potential Role of CXCR7 in Macrophage Adhesion and Migration

To determine whether CXCR7 activation is pro-migratory on macrophages, we starved THP-1 derived macrophage and then the macrophage suspension was loaded in the upper chamber of Boyden chamber system. The chemotactic capacity of SDF-1, TC14012 and I-TAC was evaluated by visualizing and counting the number of cells that migrated beneath the membrane. (Figure 5.19A) Our data indicate that SDF-1, TC14012, and I-TAC facilitated the THP-1 macrophage migration. Notably, the effect of 100 ng/ml SDF-1 and 30uM TC14012 on macrophage was comparable and was more robust than 100 ng/ml I-TAC. (Figure 5.19B)

To determine whether CXCR7 is involved in macrophages adhesion, THP-1macrophages were treated with SDF-1 or TC14012 and cell adhesion activity was assayed. Figure 5.20 showed that macrophage adhesion to six well plate was low if un-stimulated *in vitro*. However, when

stimulated with CXCR7 agonists, SDF-1 or TC14012, macrophage adhesion was profoundly increased in a dose dependent manner.

### 3.13. Candidate Genes Regulated by CXCR7 Activation

To acquire initial insights into the potential mechanisms mediating the increased inflammatory activity via CXCR7 activation, we analyzed the expression profile of 84 atherosclerosis- or inflammation-related genes on control macrophages or SDF-1 activated macrophages using commercially available RT arrays. RT arrays indicated that SDF-1 modulated the expression of the atherosclerosis-related molecules on THP-1 macrophages such as elastin; IL-3; IL-4; leukemia inhibitory factor; nitric oxide synthase 3; Nuclear receptor subfamily 1, group H, member 3;VCAM-1. In addition, it also regulated the inflammatory factors, including CCL11, CCL13, CCL16, CCL17,CCL4, CCR4, C reactive protein, Fas ligand, interferon-γ, IL-18 receptor accessory protein, interleukin 1 family member 10, IL-22, IL22 receptor-α2, IL-23 receptor, IL-6, CXCR1, IL-9, kininogen 1 (Figure 5.18), suggest that a potential SDF-1-dependent regulation on macrophage in response to *in vivo* with high local SDF-1 level. Further quantitative RT-PCR is required to confirm the fold change of these candidate genes.

### 3.14. Atorvastatin Treatment Inhibits CXCR7 Expression Induced in Macrophage

As mentioned earlier, independent of the lipid lowering effect statins also show anti-atherosclerosis properties including inhibition of chemokine receptors on monocytes (Greenwood *et al.*, 2006). To investigate whether statins could regulate SDF-1 receptors expression especially CXCR7 induction during monocyte-to-macrophage differentiation,

THP-1 cells were differentiated with PMA in the presence or absence of the physiological relevant dose of atorvastatin. Interestingly, the induction of CXCR7 by PMA on macrophages is blunted by atorvastatin pre-treatment. On the other hand, the lowered CXCR4 level on macrophages was not rescued by atorvastatin treatment. (Figure 5.22.) Real-time PCR assay confirmed that in line with previous study, CXCR7 mRNA was induced to the maximal level at 24~48 h, atorvastatin treatment showed significant CXCR7 inhibition at ~12h and kept in the same level within the observation window (Figure 5.23.A). In addition, atorvastatin dose dependently inhibited CXCR7 expression during monocyte-to-macrophage differentiation, but did not significantly change the CXCR4 level (Figure 5.23.B&C). Our data suggest that atorvastatin has a potential modulation on CXCR7 expression in macrophages.

To find out whether this phenomenon can be generalized to other statins, we pretreated the monocyte with a physiological relevant dose of atorvastatin, pravastatin, fluvastatin, mevastatin, and simvastatin before differentiation with PMA. The RT-PCR analysis showed that all the statins employed in this study showed CXCR7 inhibition effect to some extent but only atorvastatin treatment showed a statistically significant reduction of the CXCR7 mRNA expression (Figure 5.24.).

### 3.15. Atorvastatin Treatment Inhibits CXCR7 Protein Expression

To assess whether the CXCR7 protein is also decreased upon atorvastatin treatment, we performed Western blotting assay. Our data further showed that during monocyte-to-macrophage differentiation, CXCR7 total protein was reduced by atorvastatin compared to PMA only. The total CXCR7 from breast cancer cell line MBA-MD-231 was

shown to express CXCR7 and used as positive control. To confirm whether the surface CXCR7 is also lessened, we performed flow cytometry assays. Consistent with our previous finding, Figure 5.25.B&C. showed that CXCR7 was not expressed in THP-1 monocytes but was induced upon differentiation, which was reversed by atorvastatin treatment. In contrast, cell surface CXCR4 antigen decreased during the differentiation process and was not altered by atorvastatin. Together, these results suggest the atorvastatin specifically inhibits CXCR7 but not CXCR4 mRNA and protein expression, leading to less CXCR7 on macrophage surface.

### 3.16. The Inhibitory Effect of Atorvastatin on CXCR7 Induction is not Caused by Cytotoxicity or Macrophage Differentiation

To determine if the inhibition of CXCR7 by atorvastatin is caused by non-specific cytotoxicity, the cell viability and morphology were evaluated. Our data suggest that atorvastatin showed no increased cytotoxicity until 10μM. (Figure 5.26.A) To further determine whether atorvastatin treatment influences macrophage differentiation, the macrophages were induced by PMA with or without atorvastatin. As shown in Figure 5.26.B, the morphology of macrophages was not affected by atorvastatin treatment. Moreover, we analyzed the expression of the macrophage differentiation marker, CD36 and CD68. Our results suggest that the CD36 and CD68 were up-regulated on PMA-derived macrophages as expected, but atorvastatin had no significant change on the expression of CD36 and CD68 (Figure 5.26.C&D), suggesting the inhibition of CXCR7 expression by atorvastatin is independent of cytotoxicity and macrophage differentiation.

### 3.17. The Effect of Atorvastatin on CXCR7 Induction is Partially Mediated by Cholesterol Synthesis but is Independent of Protein Geranylation

To explore the mechanism by which atorvastatin regulated CXCR7 expression, we first determined whether the effect of atorvastatin is depend on the activity of HMG-CoA reduactase. Our data suggest that inhibition of CXCR7 by atorvastatin was completely rescued by mevalonate to an extent that was comparable to PMA alone. In addition, blockade of cholesterol synthase, the enzyme committed for cholesterol biosynthesis, by squalestatin also inhibited the effect of CXCR7 induction, albeit not as efficacious as atorvastatin. These data suggest that the inhibition of CXCR7 induction during PMA-driven monocyte-to-macrophage differentiation by atorvastatin is partially via the inhibition of cholesterol synthesis. On the other hand, mevalonate, atorvastatin, or squalesatin individually showed negligible effect on CXCR7 expression, indicating that the effect of atorvastatin is specific and depend on HMG-CoA reduactase activity.

To determine whether the prevention of isoprenoids and activation of Ras/Rho protein by atorvastatin is also involved in modulation of CXCR7 expression, we employed the protein geraylation inhibtors, GGTI-286, FTI-276, and Rho kinase inhibitor Y-27632. Our data suggest that inhibition of downstream mevalonate pathways such as synthesis of GGPP and FPP did not mimic the effect of atorvastatin on CXCR7 expression, suggesting that the isoprenoid synthesis and Rho activity is not involved in atorvastatin mediated CXCR7 inhibtion on THP-1 macrophages. Taken together, our data suggest the inhibitory effect of atorvastatin on CXCR7 expression is not mediated via isoprenoid synthesis but is, at least, partially through cholesterol synthesis.

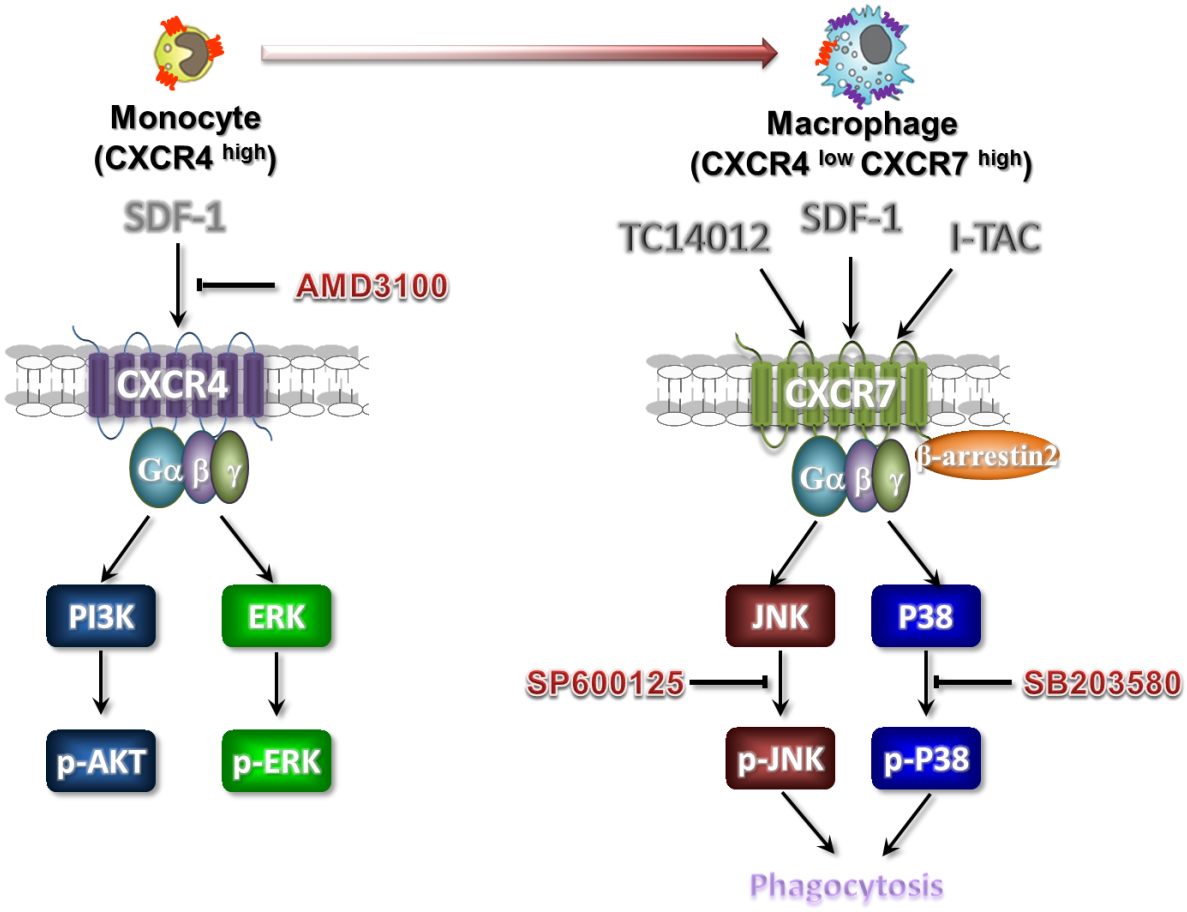


**Figure 4.1. Summary of the study.**

Here we show for the first time that CXCR7 is expressed in macrophage-positive areas of mouse aortic atheroma and CXCR7 is induced during monocyte-to-macrophage differentiation. Furthermore, we have demonstrated that CXCR7 is required for SDF-1 and I-TAC activation of the JNK and p38 pathways in macrophages, leading to enhanced cellular phagocytosis and

also play a potential role in macrophage migration and adhesion. Moreover, we identified a few candidate genes that could be modulated by CXCR7 activation on macrophages. In addition, our data indicate that the atorvastatin dose dependently inhibit CXCR7 expression on macrophage, via a mechanism that is independent of posttranslational modification of proteins by isoprenoids, suggesting a CXCR7 dependent mechanism to benefit atherosclerosis treatment independent of lipid lowering.

The role of SDF-1 in the biology of leukocytes and stem/progenitor cells has been extensively investigated. It has been established that SDF-1 is one of the most efficacious chemoattractant for multiple leukocytes, including monocytes (Sun *et al.*, 2010). For a while, it was thought that CXCR4 is the only receptor that mediates various functions of SDF-1. This concept was supported by the fact that genetic knockout of the *CXCR4* gene recaptured the lethal phenotype initially observed in *SDF-1*-deficent mice (Ma *et al.*, 1998). This knowledge led to the development of the FDA-approved drug plerixafor (DiPersio *et al.*, 2009), which is currently used for efficient mobilization of bone marrow stem cells (Fricker, 2008). However, Balabanian et al. recently showed that the orphan RDC1 receptor binds to SDF-1 with an even higher affinity than CXCR4 (Balabanian *et al.*, 2005). CXCR7 mRNA has been found on leukocytes, but the CXCR7 protein cannot be detected by flow cytometery (Berahovich *et al.*, 2010b). Few other studies generate conflicting data regarding CXCR7 expression in leukocytes (Infantino *et al.*, 2006; Sanchez-Martin *et al.*, 2011; Tarnowski *et al.*, 2010b). A recent, more sophisticated study convincingly demonstrated that normal peripheral blood leukocytes in humans or mice do not express CXCR7, and further pointed out that the conflicting earlier observations were due to nonspecific staining of poly-clonal CXCR7 antibodies (Berahovich *et al.*, 2010a; Berahovich *et al.*, 2010b). Another study suggested that

the isolation method also largely affect the detection of surface chemokine receptors which partially explain the discrepancy of the CXCR7 expression (Nieto *et al.*, 2012). In the present study, by using three specific CXCR7 monoclonal antibodies, we confirmed by multiple approaches that the monocytic THP-1 cells and human primary monocytes do not express CXCR7. This is supported by our RT-PCR analysis, which shows no significant CXCR7 mRNA expression in these monocytes. However, we found unexpectedly that CXCR7 is induced during monocyte-to-macrophage differentiation. This notion is supported by several lines of evidence: 1) PMA treatment of THP-1 cells induced up-regulation of CXCR7 mRNA along with cell differentiation into macrophage-like morphology and expression of macrophage markers; 2) CXCR7 induction is not limited to the pharmacological reagent PMA, and indeed can be mimicked by a few inflammation relevant factors; 3) We confirmed by Western blotting and immunofluorescence assays that CXCR7 mRNA induction is accompanied by CXCR7 protein up-regulation; 4) We verified by flow cytometry that monocyte surface has no or negligible amount of CXCR7 antigen, and once differentiated into macrophages, their cell surface CXCR7 antigen is up-regulated; and 5) We found more CXCR7 induction in M1 macrophages than M2 cells. Thus, we have provided compelling evidence indicating that during monocyte-to-macrophage differentiation, CXCR7 is induced at mRNA, total protein, and cell surface levels. Our finding reinforces the idea that CXCR7 induction may be a more broadly related phenomenon for terminal cell differentiation, since a prior study found that CXCR7 is induced during B cell maturations (Infantino *et al.*, 2006).

Although CXCR4 is not the focus of this study, we consistently observed that this SDF-1 receptor was down-regulated during macrophage differentiation. This result indicates that the two SDF-1 receptors exhibit dynamic regulation in opposite directions during

monocyte-to-macrophage differentiation. Similar pheromone was reported on glioma stem-like cell line 25/07 and oligodendroglial precursor cell, which CXCR4 is preferentially down-regulated upon differentiation, whereas CXCR7 induced drastically (Göttle *et al.*, 2010; Hattermann *et al.*, 2010). Prior study found that isolated monocytes showed decreased responsiveness to SDF-1 through unknown mechanism (Seeger *et al.*, 2007). Our finding suggests that this could be attributed to decreased CXCR4 expression and/or CXCR7 induction. We and others reported that plasma level of SDF-1 in normal mice or humans is around 3.5 ng/ml, (Damas *et al.*, 2002; Shen *et al.*, 2010) which based on this study is high enough to achieve a steady-state activation of cell signaling pathways such as ERK and AKT. This finding suggests that in normal physiology, blood SDF-1 may function as a pro-survival factor. The mechanism(s) responsible for CXCR7 induction and CXCR4 down-regulation are unknown and beyond the scope of this report. However, prior study found that there are NF-κB binding sites in the *CXCR7* gene promoter (Tarnowski *et al.*, 2010a). Thus, it is conceivable that in our system, PMA or IFN-γ plus LPS activated the NF-κB pathway, leading to CXCR7 gene induction.

Debate continues regarding whether CXCR7 acts as a signaling or non-signaling "decoy" receptor (Sun *et al.*, 2010; Thelen and Thelen, 2008). In general, two models have been proposed: 1) CXCR7 is a non-signaling receptor and functions as a scavenger to remove extracellular SDF-1, thereby indirectly controlling CXCR4 signaling (Boldajipour *et al.*, 2008; Luker *et al.*, 2010; Naumann *et al.*, 2010; Wang *et al.*, 2012); 2) CXCR7 acts as typical signaling receptor either as an independent entity or via hetero-dimerization with CXCR4 (Decaillot *et al.*, 2011; Grymula *et al.*, 2010; Hartmann *et al.*, 2008; Hattermann *et al.*, 2010; Levoye *et al.*, 2009; Odemis *et al.*, 2010; Odemis *et al.*, 2011; Rajagopal *et al.*, 2010; Wang *et*

*al.*, 2008; Wang *et al.*, 2011; Zabel *et al.*, 2009). Of note, even for dimerization, both positive and negative impacts of CXCR7 on CXCR4 signaling have been reported (Decaillot *et al.*, 2011; Levoye *et al.*, 2009; Zabel *et al.*, 2009). Although, the CXCR4/CXCR7 forms a heterodimer in the transfected cells, there is no evidence that the heterodimer exist *in vivo*. Indeed, a recent study did not detect the dimer in primary human CD19+ B cells that express both receptors (Naumann *et al.*, 2010). Currently, there is no clear explanation for these contradictions; however, cell type or cell context difference may be a contributing factor. In the current study, we found that the up-regulated CXCR7 receptor is a functional signaling receptor at least during monocyte-to-macrophage differentiation. Several lines of evidence support this notion: 1) SDF-1 activated p38 and JNK pathways in differentiating macrophages bearing both CXCR4 and CXCR7 receptors; 2) In monocytes expressing only CXCR4, SDF-1 was unable to activate p38 and JNK; 3) The effect of SDF-1 on p38/JNK in macrophages was fully mimicked by the CXCR7-selective agonist TC14012; and 4) siRNA silencing of *CXCR7*, but not *CXCR4*, abolished SDF-1-induced p38 and JNK activation. Thus, we provide strong evidence indicating that CXCR7 is required for SDF-1 signaling to p38 and JNK pathways and CXCR4 is dispensable in this process in macrophages. This interpretation is further supported by our finding that I-TAC, which does not bind to CXCR4, can activate p38 and JNK pathways as well in a CXCR7-dependent, but CXCR3-independent manner in macrophages.

HMG-CoA reductase inhibitors (statins) are generally used for hyperlipidemia treatment to ameliorate atherosclerotic diseases. Recent studies have suggested that the beneficial effects of statins may be extended beyond cholesterol lowering, including the reduction of vascular inflammation, improvement of endothelial function, inhibition of the proliferation of SMCs, and stabilization of atherosclerotic plaques. These pleiotropic effects are thought to be based

on blocking the synthesis of isoprenoid intermediates, which are important for post-translational modification of intracellular signaling molecules. In our present study, we extended our knowledge about the CXCR7 receptor by determing whether statins could modulate CXCR7 expression. Our data suggest that CXCR7 but not CXCR4 was downreuglated by the most widely used statin, atorvastatin, on THP-1 macrophages. We further demonstrated that only atorvastatin but no other statins used in this study significantly inhibited CXCR7 expression on THP-1 macrophages. We observed that the effect of atorvastatin on CXCR7 expression was dose-dependent in THP-1 macrophages. Moreover, the effect of atorvastatin is independent of the macrophage differentiation process. Interestingly, atorvastatin achieved the significant inhibition at a low dose that does not cause cytotoxicity and is close to the blood concentration during statin therapy. Importantly, atorvastatin also reduced the CXCR7 total and cell surface protein and potentially reduces the inflammatory and phagocytic effects mediated by CXCR7.

Studies have shown the anti-inflammatory and immunomodulatory properties of statins. The blockage of L-mevalonic acid synthesis by statins not only inhibits the cholesterol synthesis but also reduces, and not limited to, the conversion of mevalonate to farnesylpyrophosphate and geranylgeranylpyrophosphate. It is well known that isoprenylation of protein is critical for the activation of small G-proteins mediated signal transduction, such as Ras. These small G proteins are suggested to be implicated in the regulation of some cytokines and chemokines for intracellular signaling molecules. Thus, many studies suggest that the pleiotropic effects are mediated by inhibition of isoprenylation of G proteins. We observed that supplement of L-mevalonic acid could reverse the effect of atorvastatin, suggesting HMG-CoA reductase activity is important for CXCR7 inhibition. However, inhibition of squalene synthesis, a more

direct precursor of cholesterol, showed an inhibitory effect that was not as potent as atorvastatin. In addition, farnesyl transferase inhibitor, geranylgeranyl transferase inhibitor or Rho kinase inhibitor did not mimic atorvastatin induced CXCR7 inhibition. These data suggest that synthesis of isoprenoid intermediates is not involved in modulating CXCR7 expression. The inconsistent extent of inhibition on CXCR7 expression by atorvastatin and squalestatin suggests that other mechanism(s) are involved. Although the exact mechanism is unknown so far, we cannot rule out the possibility that atorvastatin has direct effects independent of cholesterol and isoprenoids synthesis.

In our study, all statins inhibited PMA-induced CXCR7 expression on THP-1 macrophages but only the inhibitory effect of atorvastatin was statistically significant. Studies have suggested that statins shows differential anti-inflammatory properties. Despite their differential hydrophilic properties, one study showed that statin differentially inhibited LPS-induced NF-κB binding activity in human primary blood monocytes with a potency order of Atorvastain> Pravastatin> Fluovastatin, which was reversed by mevalonate supplement (Hilgendorff *et al.*, 2003). As mentioned earlier, studies suggested that there are NF-κB binding sites in the *CXCR7* gene promoter; it is speculated that the differential ability of different statins on NF-κB binding activity may partially explain the inconsistency of their effect on inhibition of CXCR7 expression.

The *in vivo* relevance of our findings to the pathogenesis of atherosclerosis can be envisioned in several aspects as shown in Figure 4.2 : 1) We found that SDF-1 activates the pro-survival ERK and AKT pathways, but not the pro-inflammatory p38 and JNK pathways in primary blood monocytes. This result implies that normal blood level of SDF-1 may be beneficial for

vascular homeostasis through nurturing blood monocytes and keeping them inside bloodstream via CXCR4 signaling; 2) Once blood SDF-1 moves down to the threshold level, blood monocytes may be more prone to emigrate into sub-endothelial space and differentiate into macrophages. During this process, CXCR4 is down-regulated and CXCR7 is up-regulated, the latter of which may promote vascular inflammation by activation of the pro-inflammatory p38 and JNK pathways; 3) Our data clearly show that CXCR7 is detectable in aortic atheroma of *ApoE*-null, but not normal mice, with a restricted expression in macrophage-positive area, suggesting a potential involvement of macrophage CXCR7 in atherogenesis; 4) We found that activation of CXCR7 increased phagocytosis (uptake of bacterial and modified LDL), evidently mediated by the p38 and JNK pathways, since blocking either of these two pathways has a negative impact on cellular phagocytosis; and 5) We found that a physiological relevant dose of atorvastatin inhibits CXCR7 expression on macrophage, thus an *in vivo* relevance of a novel beneficial effect of atorvastatin via CXCR7 inhibition may be assumed. However, macrophage phagocytosis is a complicated process that involves a variety of receptors, signaling pathways, and cytoskeleton proteins (Ley *et al.*, 2011). It will be of interest to determine whether CXCR7 employs the same or different mechanism(s) to promote uptake of bacterial versus modified-LDL. Nonetheless, given the fact that both SDF-1 and I-TAC promote macrophage phagocytosis in a CXCR7-dependent manner, it is imperative to further study the role of CXCR7 in macrophage biology.

In summary, we report the first evidence that during monocyte-to-macrophage differentiation, CXCR7 is induced while CXCR4 is down-regulated. Also, CXCR7 is primarily responsible for SDF-1 and I-TAC stimulation of pro-inflammatory signaling pathways such as JNK and p38, leading to enhanced capability of macrophage phagocytosis. The lipid lowering

atorvastatin may also benefit atherosclerosis treatment via inhibition of CXCR7 expression. These findings suggest that SDF-1 may play dual roles in atherosclerosis via its two receptors. This concept is supported by a recent study showing that *in vivo* delivery of CXCR4 antagonist exaggerates atherosclerosis (Zernecke *et al.*, 2008). In addition, identification of CXCR7 activation of JNK and p38 pathways may also have significant implications for better understanding of the role of CXCR7 in other cells expressing this receptor.

Furthermore, future studies using conditional *CXCR7*-null mice may provide a better understanding of *in vivo* roles of this receptor in vascular/leukocyte biology.

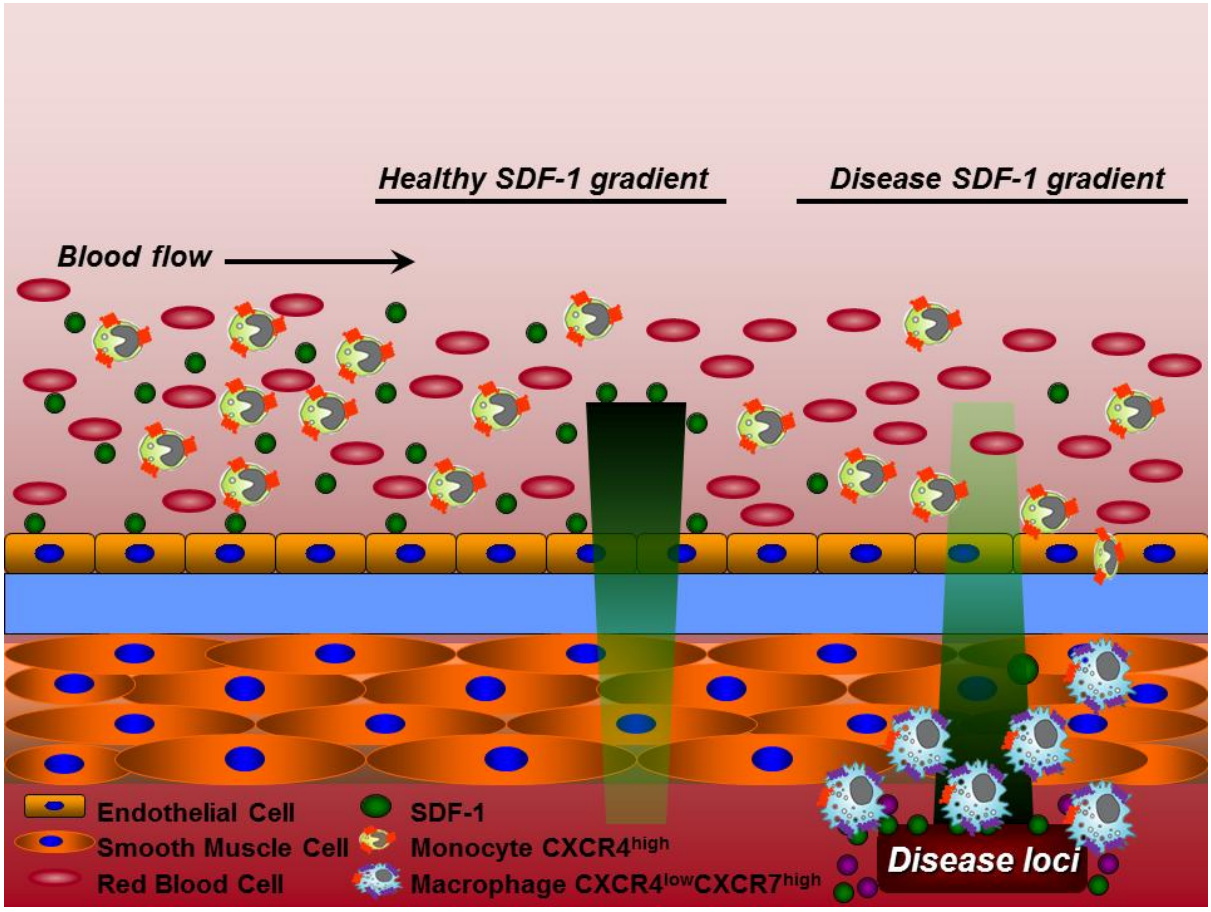


**Figure 4.2. *In Vivo* relevance of this study.**

Chapter 5. Figures and Legends

**Figure 5.1. Detection of CXCR7 in macrophage-positive area of aortic atheroma in *ApoE*-null mice.**

(A) Atherosclerotic plaque was revealed by oil red O staining with H&E counterstain on aortic sinus sections from 16-week old female *ApoE*-null mice, but not from age-matched female control C57BL/6 mice (top). Immunofluorescent detection of mice macrophage marker F4/80 (green), CXCR7 (red), and their co-localization in atheroma. Nuclei were visualized by DAPI staining (blue, bottom). Representative images from three mice in each group were shown (original magnification: 20 X).

(B) Specificity of fluorescence conjugated isotype control antibodies for F4/80 and CXCR7 was confirmed by negative stain on serial sections. The morphology of sections was revealed by a phase-contrast mode.

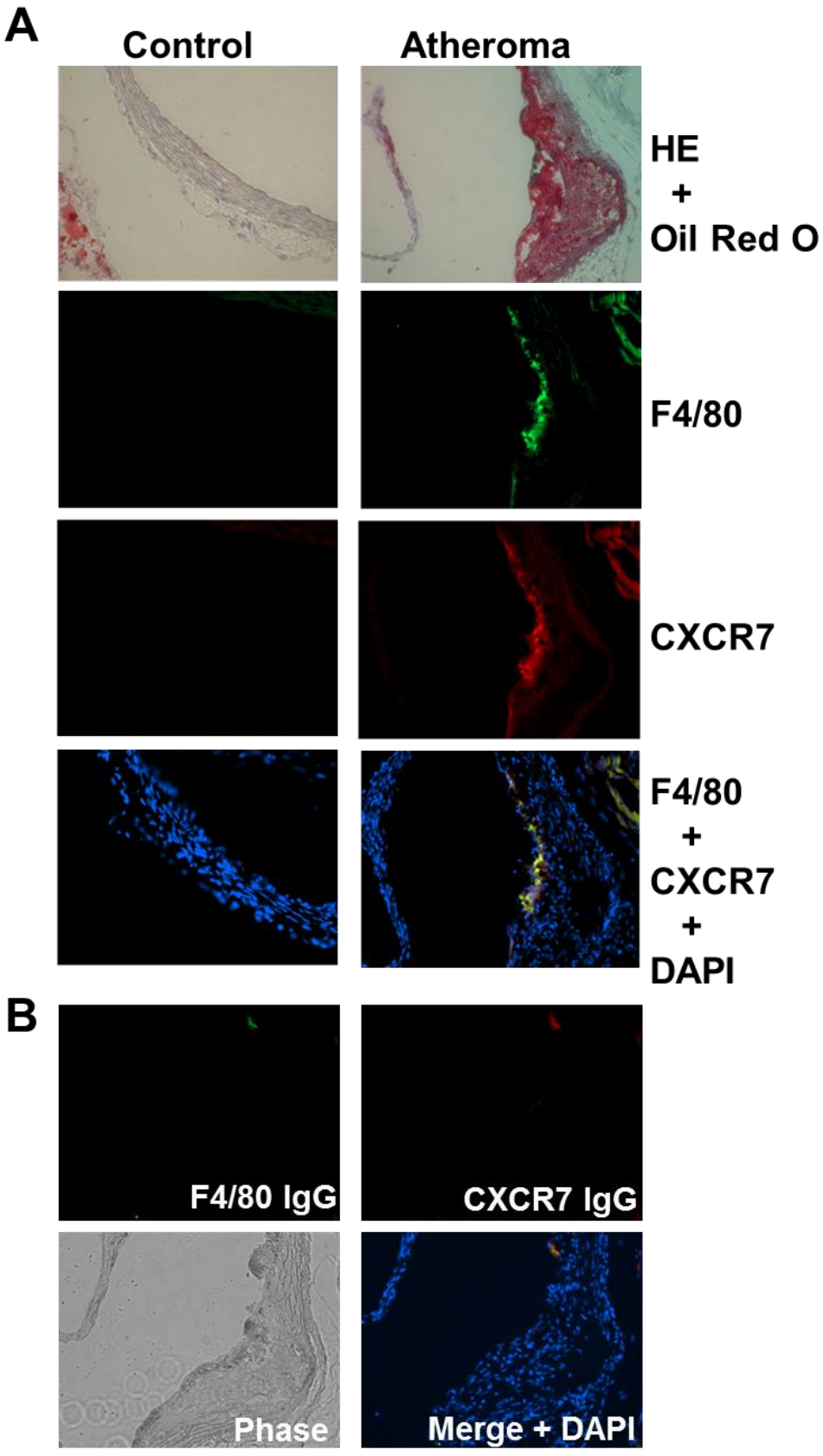
A
Control
Atheroma
HE
+
Oil Red O
F4/80
CXCR7
F4/80
+
CXCR7
+
DAPI
B
F4/80 IgG
CXCR7 IgG
Phase
Merge + DAPI

**Figure 5.2. Validation of PMA induced monocyte-to-macrophage differentiation.**

(A) Treatment of THP-1 cells (floating cells) with 40 nM PMA for 48 h induced monocyte differentiation with morphological changes into macrophage-like cells (adherent cells). Images magnification: 20 X.

(B) Detection of cell surface CD68 and CD36 by flow cytometry on THP-1 monocytes versus THP-1 macrophages. THP-1 monocytes and PMA-driven THP-1 macrophages were stained with CD68 or CD36 antibodies and the respective isotype-matched IgG controls before analyzed by a standard flow cytometry assay. Monocytes and macrophages were identified and gated by their forward and side scatter characteristics. Flow cytometry plots are representative results from three independent experiments showing fluorescence intensity of isotype control antibodies (black or red line) compared to the CD68- or CD36-selective antibodies (blue or yellow line). (n = 3)

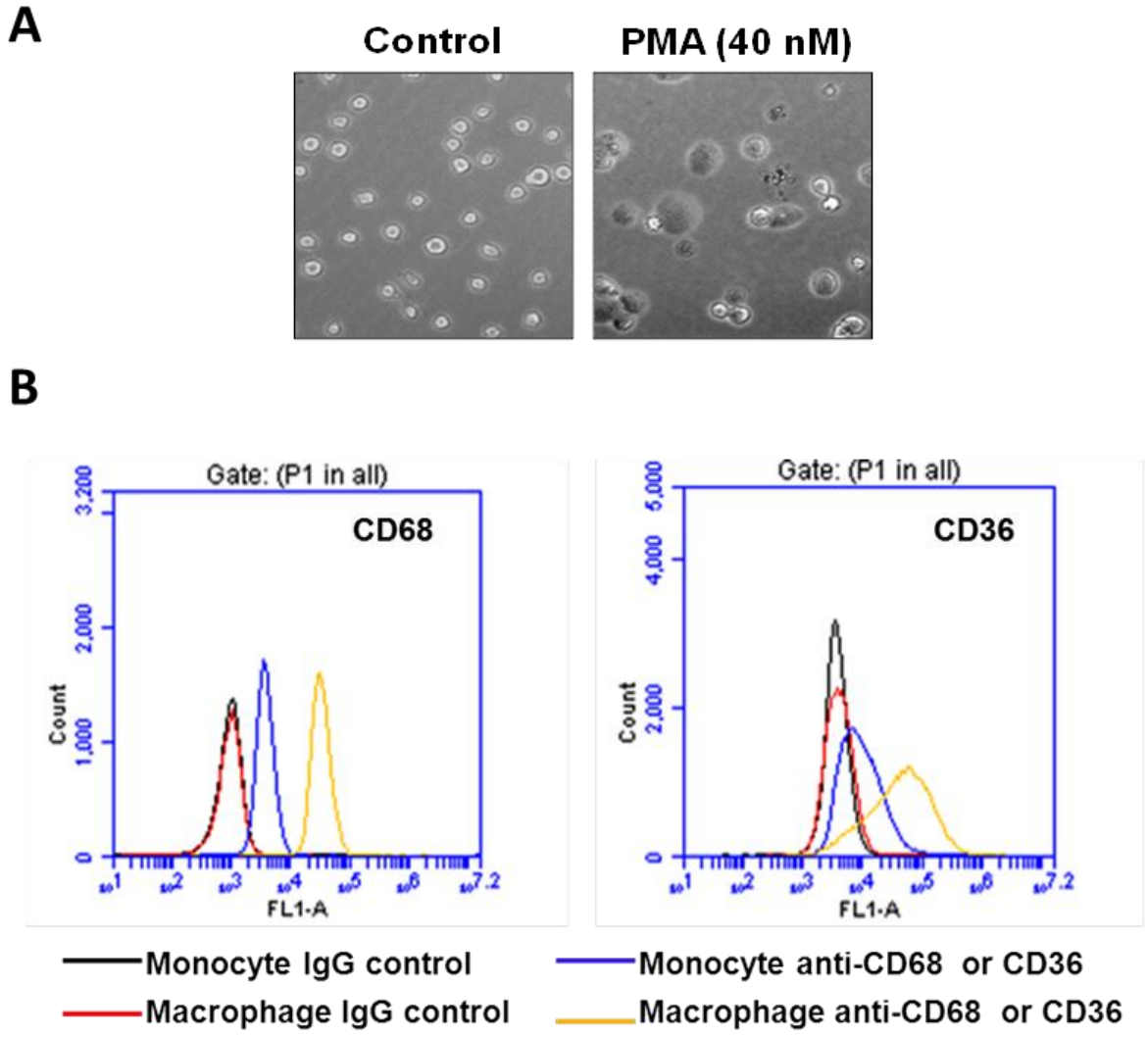
A
Control
PMA (40 nM)
B
Gate: (P1 in all)
CD68
Count
FL1-A
Gate: (P1 in all)
CD36
Count
FL1-A
Monocyte IgG control
Macrophage IgG control
Monocyte anti-CD68 or CD36
Macrophage anti-CD68 or CD36

**Figure 5.3. SDF-1 receptors expression during monocyte-to-macrophage differentiation.**

(A) mRNA expression of CXCR4 and CXCR7 in vehicle-treated cells (control), and in cells treated with 10nM or 40 nM PMA for 48 h. RT-PCR performed without reverse transcriptase (RT−) and genomic DNA was used as negative controls and positive controls, respectively. (n = 3)

(B) Kinetics of CXCR4 and CXCR7 mRNA expression during monocyte-to-macrophage differentiation induced by 40 nM PMA for the indicated time periods. The mRNA levels were determined by real-time PCR and presented as relative fold changes compared with control cells after normalized to GAPDH. (n = 5)

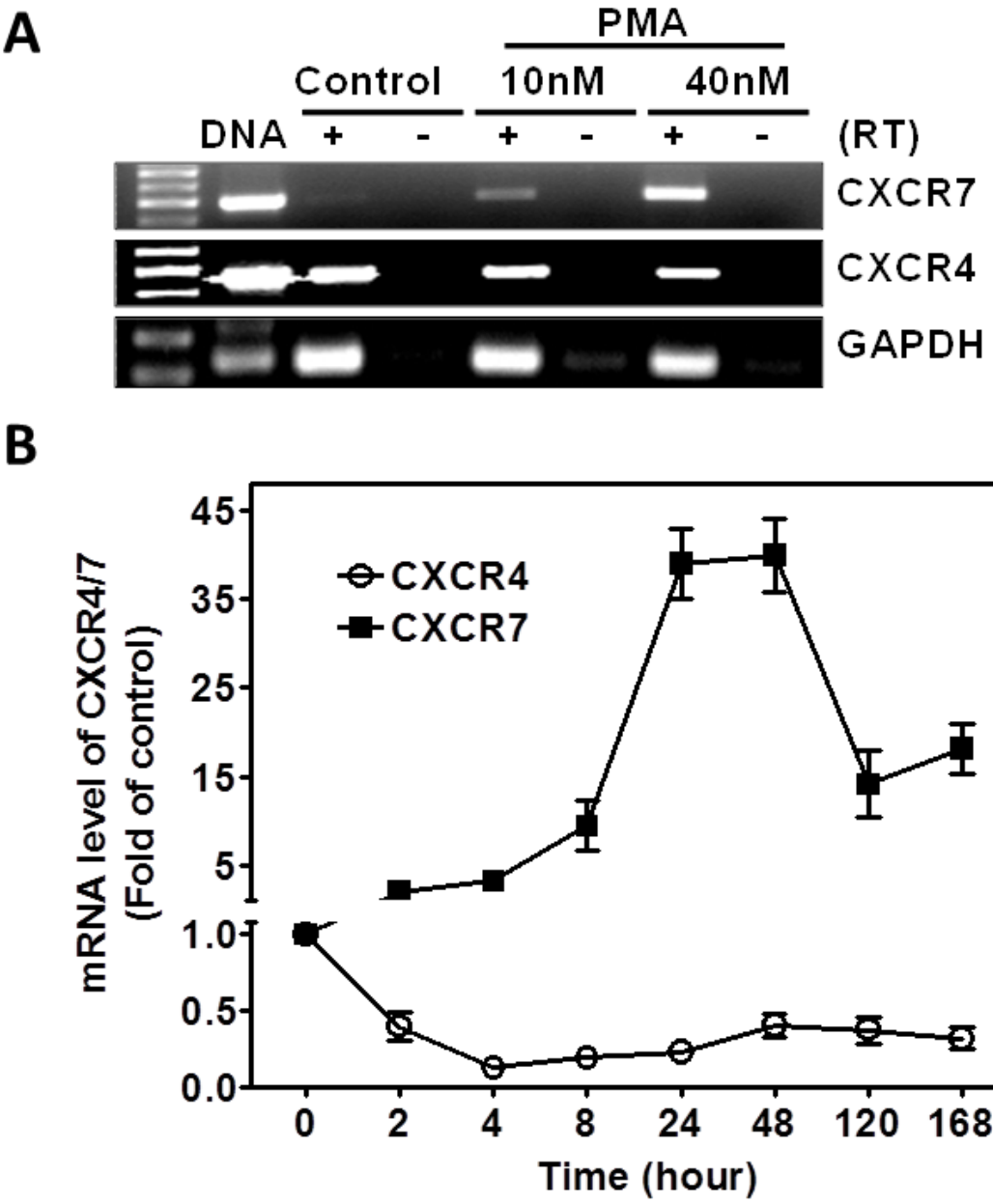
A
PMA
Control
10nM
40nM
DNA
+
-
+
-
+
-
(RT)
CXCR7
CXCR4
GAPDH
B
mRNA level of CXCR4/7
(Fold of control)
CXCR4
CXCR7
45
35
25
15
5
1.0
0.5
0.0
0
2
4
8
24
48
120
168
Time (hour)

**Figure 5.4. Effect of starvation and autocrine SDF-1 on macrophage differentiation and CXCR7 expression.**

(A) No effect of cell starvation on CXCR7 expression in PMA-driven THP-1 macrophages. THP-1 monocytic cells were either un-treated (control) or treated with PMA (40 nM) for the indicated times to induce macrophage differentiation. After 24 h, some cells were starved in serum-free medium for 10 h, and then total cellular RNAs were isolated for real-time PCR assay to determine the relative change of CXCR7 mRNA levels among different groups. Data are averaged from three independent experiments. No statistic difference was observed between starved and non-starved THP-1 macrophages.

(B) Effect of SDF-1 neutralization on macrophage differentiation. Macrophages were induced from THP-1 monocytes by treating the cells with PMA (40 nM), or PMA plus a SDF-1-neutralizing mouse anti-human monoclonal antibody (anti-SDF-1 mAb, 50 μg/ml), or PMA plus $IgG_1$ (50 μg/ml). Shown are the representative macrophage morphologies after 48 h differentiation. Magnification: 10 X.

(C). Expression levels of macrophage marker CD68 and mannose receptor CD206 were determined by standard flow cytometry assays as detailed in "Experimental Procedures". The mean fluorescence intensity data were normalized after subtracting the values from the respective isotype-matched IgG staining. "Control" stands for undifferentiated THP-1 monocytes treated with vehicle for 48 h. N.S. stands for statistic non-significance (n=5)

A

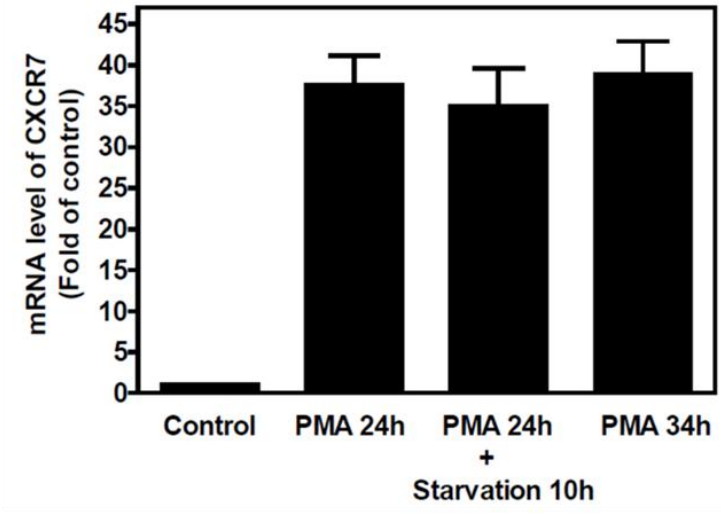
mRNA level of CXCR7
(Fold of control)
45
40
35
30
25
20
15
10
5
0
Control
PMA 24h
PMA 24h
+
Starvation 10h
PMA 34h

B

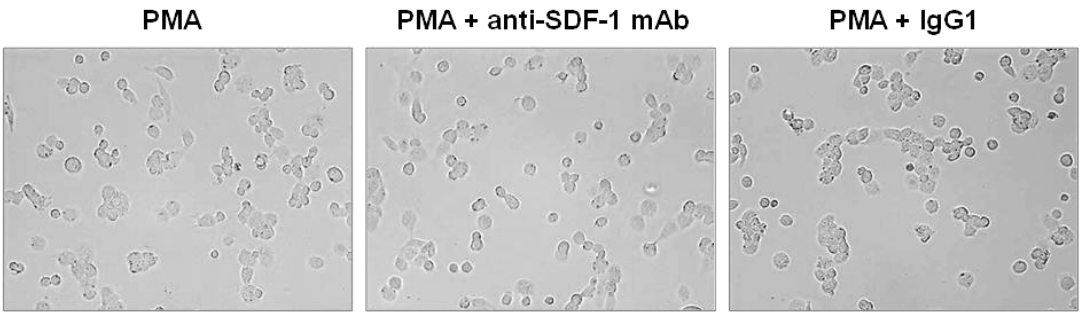
PMA
PMA + anti-SDF-1 mAb
PMA + IgG1

C

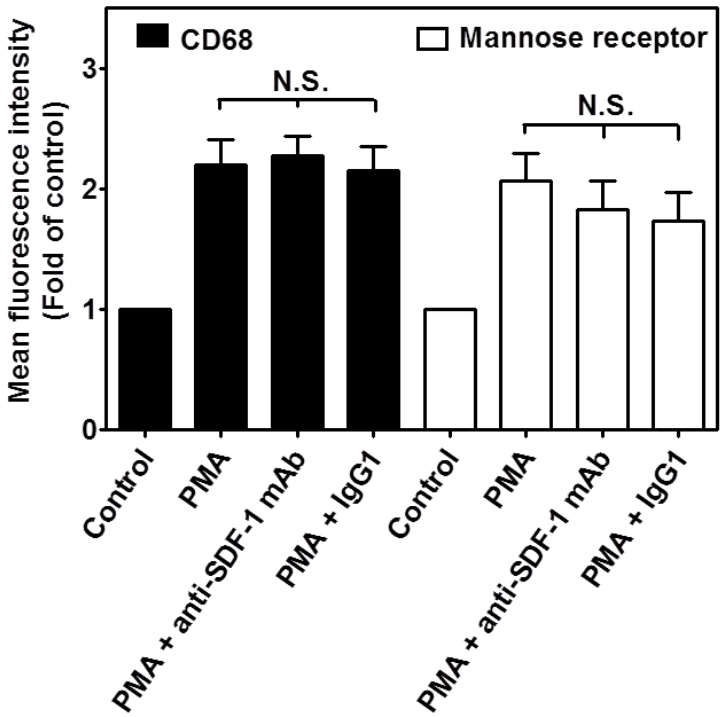
Mean fluorescence intensity
(Fold of control)
CD68
Mannose receptor
N.S.
N.S.
3
2
1
0
Control
PMA
PMA + anti-SDF-1 mAb
PMA + IgG1
Control
PMA
PMA + anti-SDF-1 mAb
PMA + IgG1

**Figure 5.5.Differential expression of CXCR7 protein on monocytes versus macrophages.**

(A) Total cellular CXCR7 protein was detected by standard Western blotting assays using three different mouse anti-human CXCR7 monoclonal antibodies: clone 11G8; clone 8F11; and clone 9C4. A ~47 KD band for CXCR7 was detected in macrophages differentiated from THP-1 cells treated with PMA (40 nM) for 48 h, but not in vehicle-treated undifferentiated THP-1 monocytes. Equal loading was verified by re-probing with anti-GAPDH antibody after stripping the original membranes. Data represent three independent experiments.

(B) Immunofluorescent detection of CXCR7 (green) on macrophages differentiated by IFN-γ (100 ng/ml) and LPS (1 μg/ml) from human primary monocytes (human macrophage). Nuclei were shown by DAPI staining (blue). Representative images from three healthy blood donors were shown. Macrophages differentiated from PMA-driven THP-1 cells were used as positive controls. Isotype-matched first antibodies (IgG) and FITC-conjugated secondary antibodies were used for negative controls. CXCR7 was not detected in THP-1 monocytes and primary monocytes (human monocyte). Original magnification: 60 X.

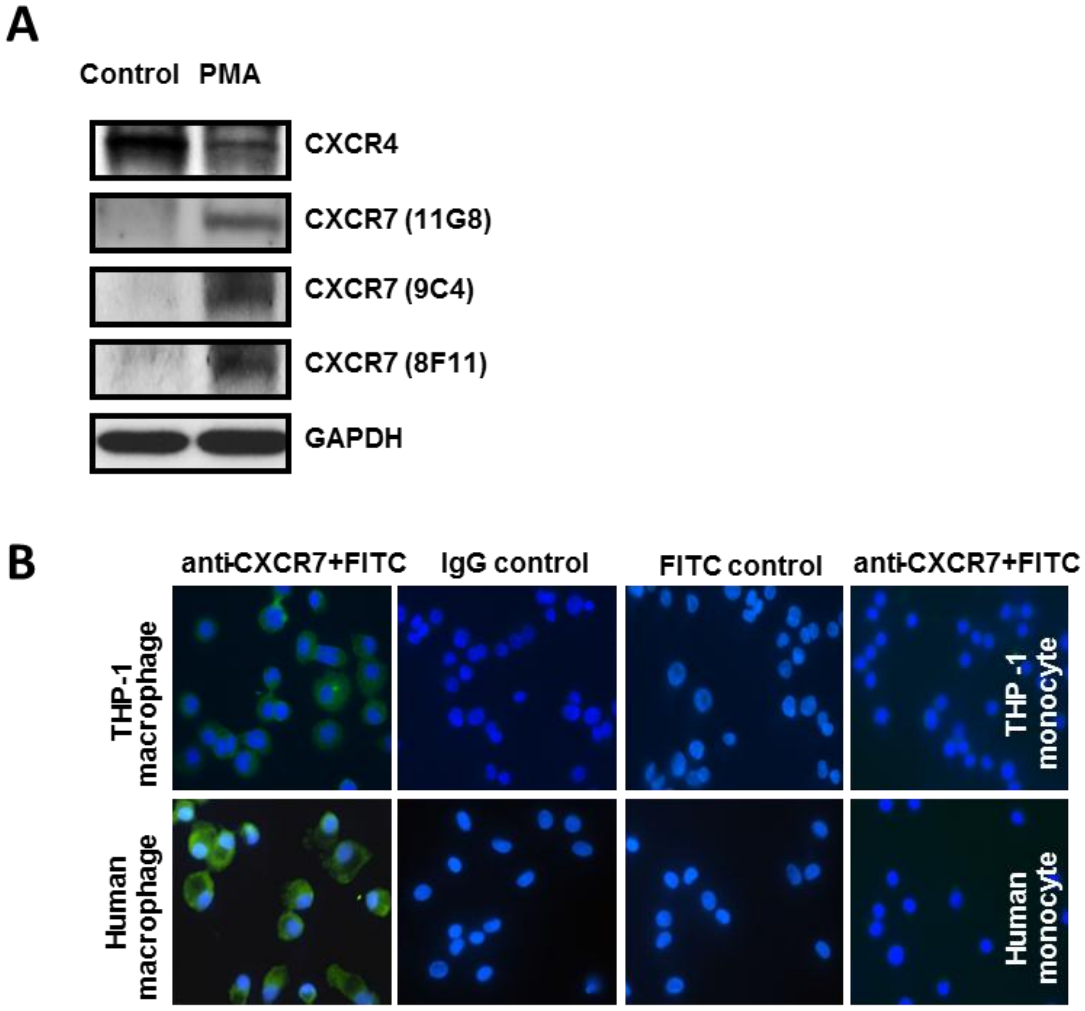
A
Control
PMA
CXCR4
CXCR7 (11G8)
CXCR7 (9C4)
CXCR7 (8F11)
GAPDH
B
anti-CXCR7+FITC
IgG control
FITC control
anti-CXCR7+FITC
THP-1 macrophage
Human macrophage
THP -1 monocyte
Human monocyte

**Figure 5.6. Detection of CXCR4 and CXCR7 surface expression on monocytes versus macrophages.**

(A)THP-1 monocytes, PMA-driven THP-1 macrophages, primary monocytes, and their differentiated macrophages (100 ng/ml IFN-γ + 1 μg/ml LPS) were stained with CXCR4 or CXCR7 antibodies and the respective isotype-matched IgG controls before analyzed by flow cytometry. Flow cytometry plots are representative results from three independent experiments showing fluorescence intensity of isotype control antibodies (black line) compared to the CXCR4- or CXCR7-selective antibodies (red line).

(B) Summarized quantitative data for panel A. *, $p<0.05$; **, $p<0.01$.

(C)THP-1 monocytes, PMA-driven THP-1 macrophages, primary monocytes, and their differentiated macrophages (100 ng/ml IFN-γ + 1 μg/ml LPS) were stained with CXCR4 or CXCR7 antibodies and their respective isotype-matched IgG controls before analyzed by flow cytometry assays. Flow cytometry plots are representative results from three independent experiments.

(D) Summarized quantitative data for panel A. *, $p<0.05$; **, $p<0.01$.

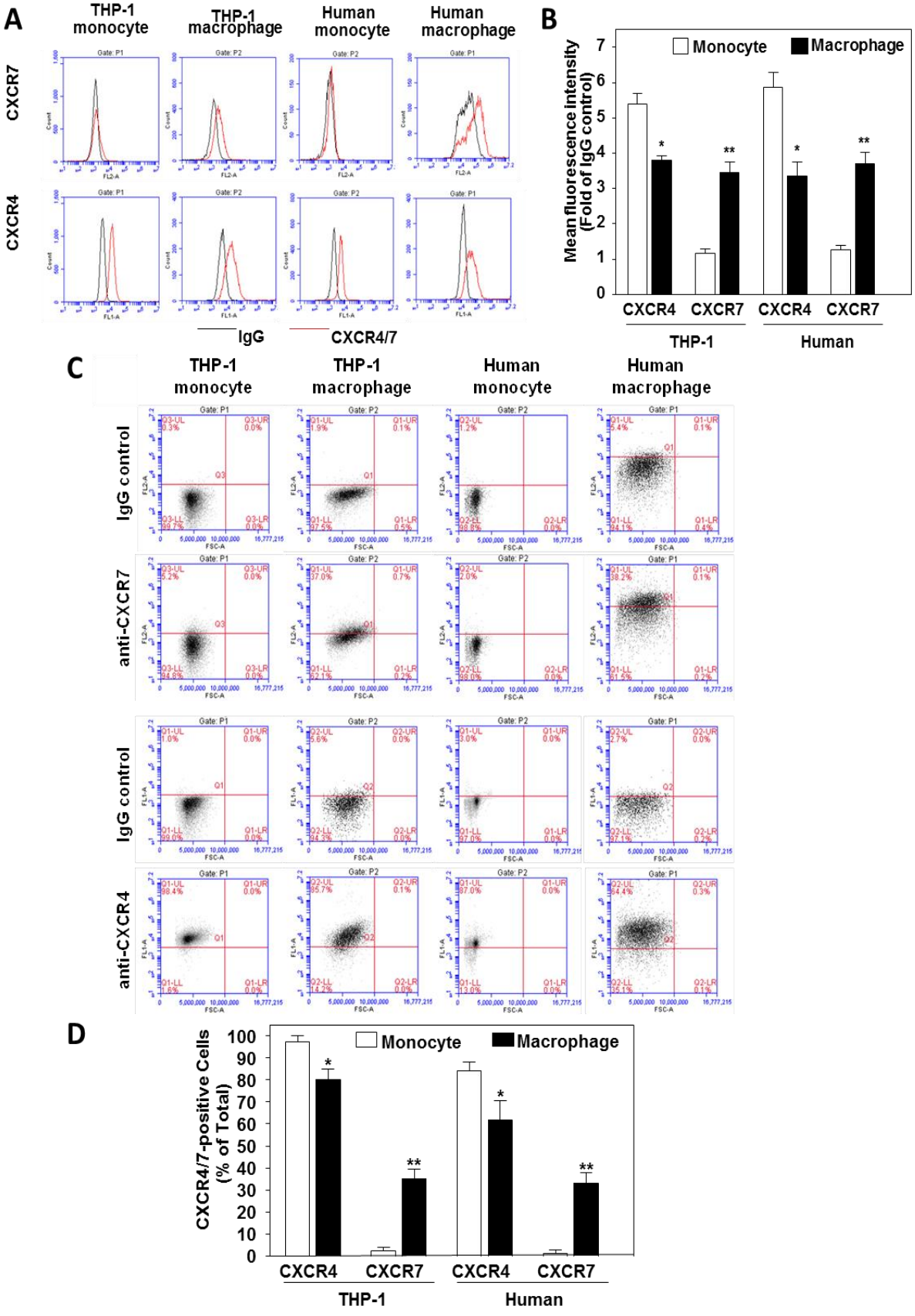
A
THP-1 monocyte
THP-1 macrophage
Human monocyte
Human macrophage
CXCR7
CXCR4
IgG
CXCR4/7
B
Monocyte
Macrophage
Mean fluorescence intensity (Fold of IgG control)
CXCR4
CXCR7
CXCR4
CXCR7
THP-1
Human
C
THP-1 monocyte
THP-1 macrophage
Human monocyte
Human macrophage
IgG control
anti-CXCR7
IgG control
anti-CXCR4
D
Monocyte
Macrophage
CXCR4/7-positive Cells (% of Total)
CXCR4
CXCR7
CXCR4
CXCR7
THP-1
Human

**Figure 5.7. CXCR7 expression on macrophage subtypes.**

(A) CXCR7 mRNA was induced in THP-1 macrophages polarized by IFN-γ (100 ng/ml) and LPS (1 μg /ml), but not by IFN-γ (100 ng/ml) and M-CSF (10 ng/ml).

(B) Differential change of cell surface CXCR4 versus CXCR7 during monocyte-to-macrophage differentiation. Cell surface CXCR4 or CXCR7 antigen levels were determined by flow cytometry assays after the human primary monocytes were differentiated into macrophages by indicated reagents for 48 h. Mean fluorescence intensity for CXCR4 or CXCR7 antigen was determined after normalization with respective IgG controls. (n=5). *, $p<0.05$; **, $p<0.01$.

(C) CXCR7 expression in M1 versus M2 macrophages. Human primary monocytes were differentiated into M1 or M2 phenotype by IFN-γ + LPS (M1) or IL-4 (M2) respectively for 48 h. Then, the cells were stained with CD68, CD206 (mannose receptor), or CXCR7 antibodies and the respective isotype-matched IgG controls before analyzed by a standard flow cytometry assay. Macrophages were identified and gated by their forward and sidescatter characteristics. Flow cytometry plots were representative results from three independent experiments showing fluorescence intensity of isotype control antibodies (black line) compared to the CD68, CD206, or CXCR7-selective antibodies (blue or red line).

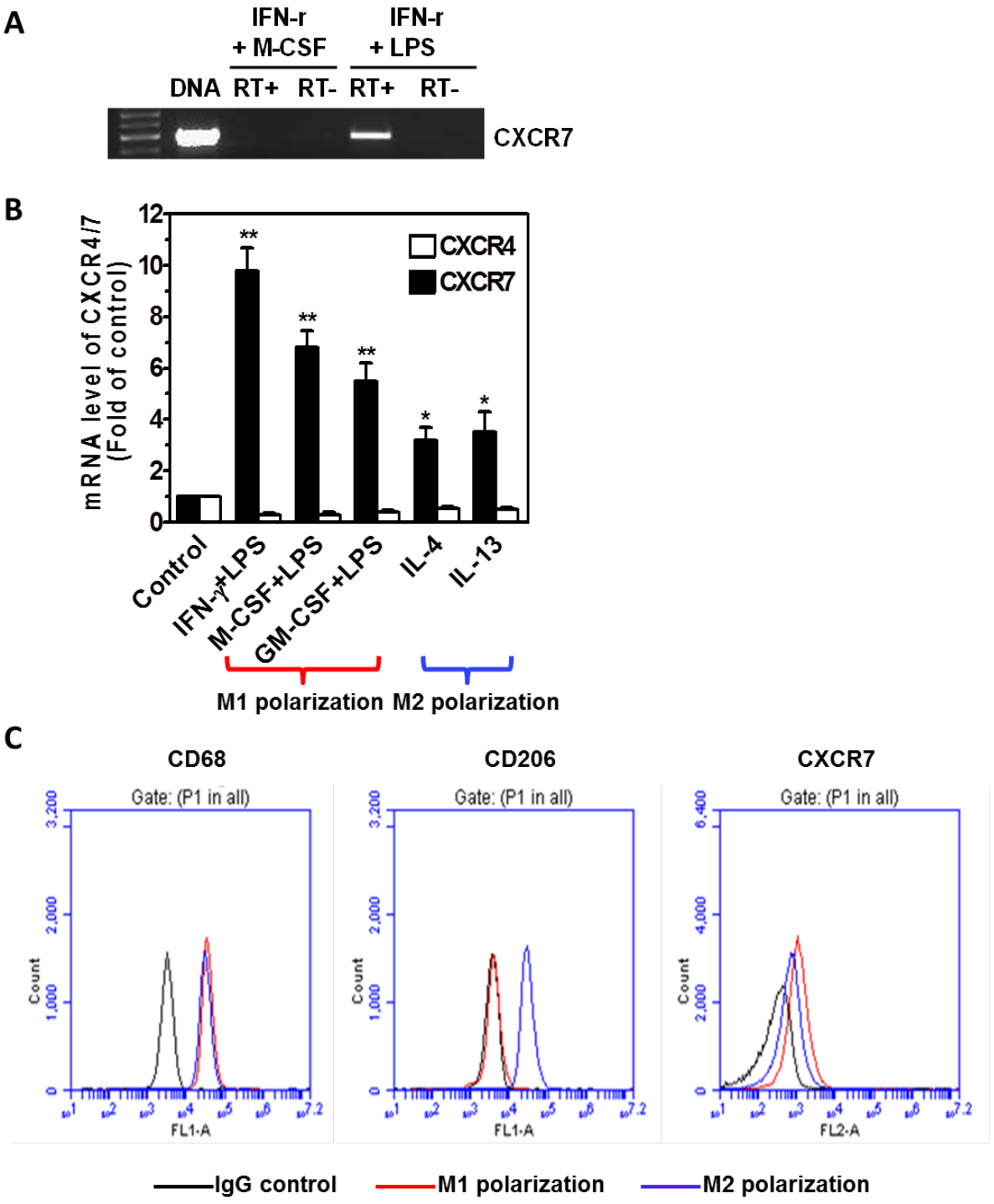
A
IFN-r + M-CSF
IFN-r + LPS
DNA RT+ RT- RT+ RT-
CXCR7
B
mRNA level of CXCR4/7 (Fold of control)
CXCR4
CXCR7
Control
IFN-γ+LPS
M-CSF+LPS
GM-CSF+LPS
IL-4
IL-13
M1 polarization
M2 polarization
C
CD68
CD206
CXCR7
Gate: (P1 in all)
Count
FL1-A
FL2-A
IgG control
M1 polarization
M2 polarization

**Figure 5.8. SDF-1 signaling in monocytes.**

(A) Cellular phosphorylation levels of ERK, AKT, p38, and JNK in THP-1 monocytes were determined by Western blotting after the cells were stimulated by SDF-1 or TNF-α for 15 min at the indicated concentrations.

(B) Dose-dependent effect of SDF-1 on the phosphorylation of p38, JNK, ERK, and AKT in primary human monocytes.

(C) The mean densitometric analysis of three separate experiments in panel B is normalized to respective total kinase loading controls and the summarized data were shown in the graph. For clarity, only tubulin loading controls were shown, and the error bars with markers for the statistical significance have been omitted.

A THP-1 monocytes

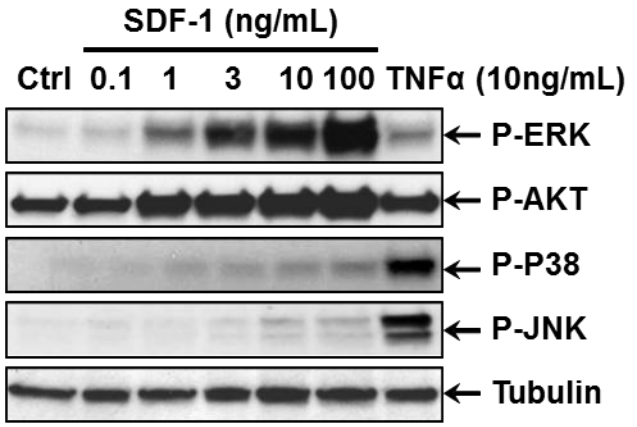


B Primary human monocytes

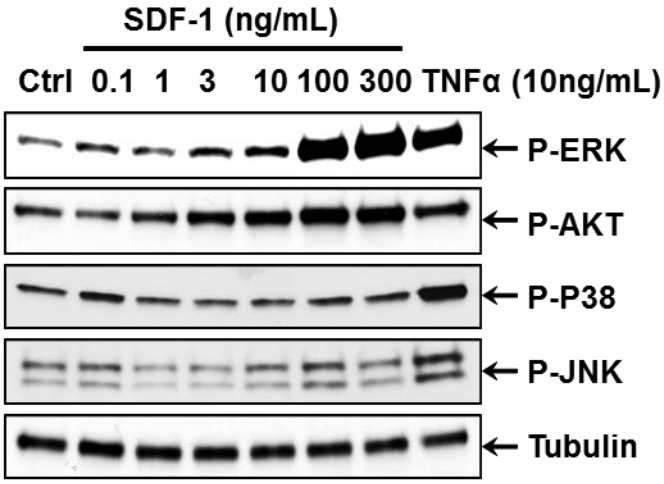


C

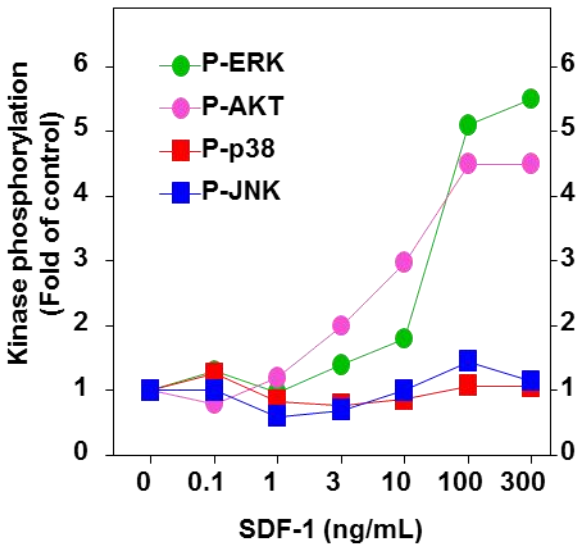

**Figure 5.9. Effect of AMD3100 on SDF-1 signaling in monocytes.**

(A) Cellular phosphorylation levels of ERK and AKT in human monocytes were determined by Western blotting after the cells were stimulated by SDF-1 for 15 min with or without pretreatment of the cells with indicated concentrations of AMD3100.

(B) The mean densitometric analysis of three separate experiments is normalized to respective total kinase loading controls (not shown) and the summarized data were shown in the bottom graph. For clarity, only tubulin loading control was shown; and the error bars with markers for the statistical significance have been omitted.

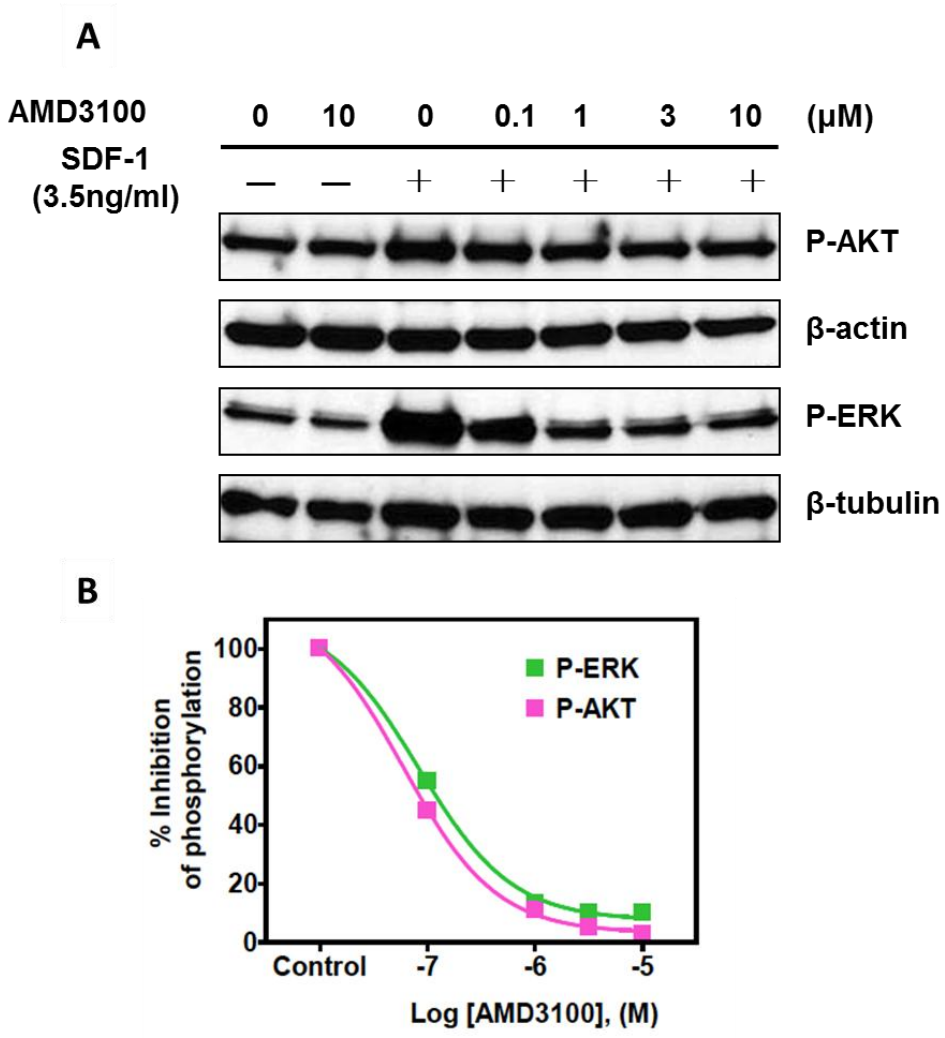

**Figure 5.10. Effect of SDF-1 on NF-κB pathway in monocytes.**

Cellular phosphorylation levels of IκBα and p65 in human monocytes were determined by Western blotting after the cells were stimulated with or without 3.5 ng/ml SDF-1 for the indicated time intervals. TNF-α is used as positive control and tubulin is for loading controls. Similar data were obtained in three independent experiments.

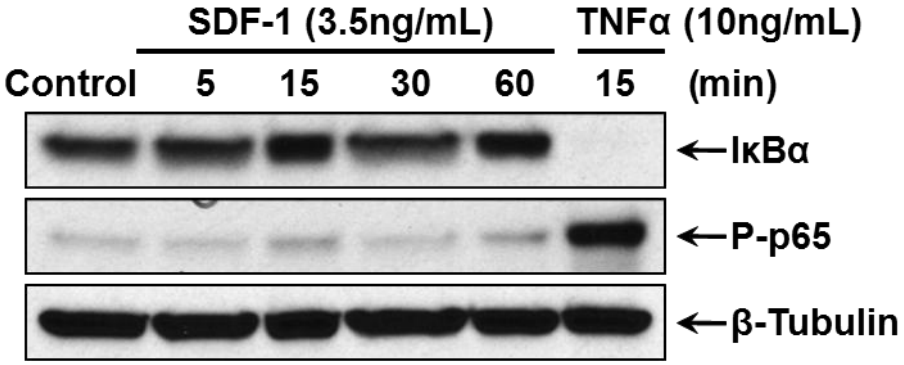

**Figure 5.11. Cellular phosphorylation levels of p38, JNK, ERK, and AKT in macrophages.**

(A) Cellular phosphorylation levels of p38, JNK, ERK, and AKT in macrophages differentiated from primary human monocytes (100 ng/ml IFN-γ + 1 μg/ml LPS for 48 h) were determined by Western blotting after the cells were stimulated by SDF-1 or LPS (15 min) for the indicated concentrations and times. Individual total kinase levels were determined after stripping and re-probing the Western blot membranes. Tubulin level were also detected and used as an additional loading control. Data are representative of three independent experiments.

Cellular phosphorylation levels of ERK, AKT, p38, and JNK in THP-1 macrophages (B) and human primary macrophages (C) were determined by Western blotting after the cells were stimulated by SDF-1 or LPS for 15 min at the indicated concentrations.

(D) The mean densitometric analysis of three separate experiments is normalized to respective total kinase loading controls (not shown) and the summarized data were shown in the bottom graphs. For clarity, only tubulin loading controls were shown; and the error bars with markers for the statistical significance have been omitted.

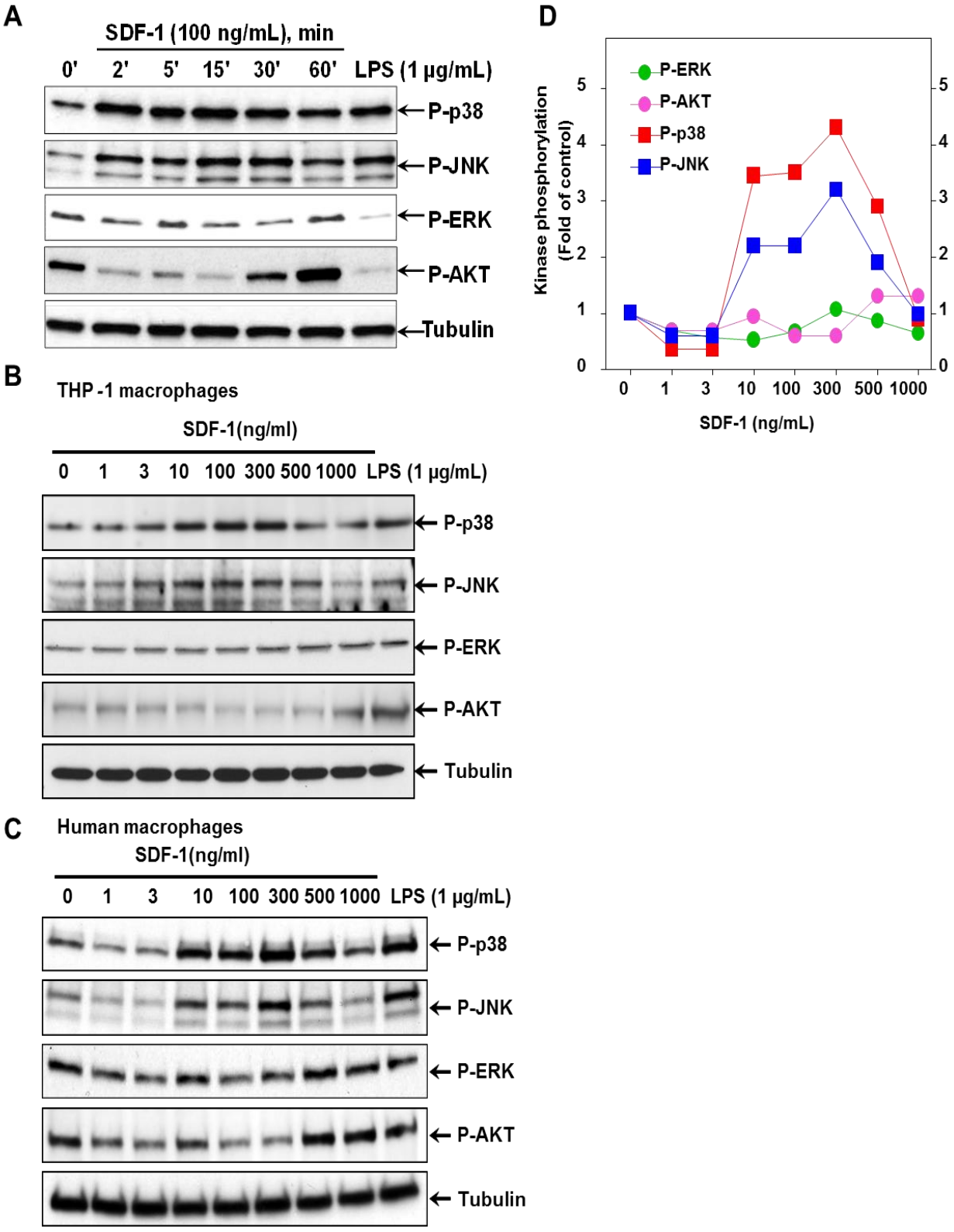
A
SDF-1 (100 ng/mL), min
0' 2' 5' 15' 30' 60' LPS (1 μg/mL)
P-p38
P-JNK
P-ERK
P-AKT
Tubulin
B
THP-1 macrophages
SDF-1(ng/ml)
0 1 3 10 100 300 500 1000 LPS (1 μg/mL)
P-p38
P-JNK
P-ERK
P-AKT
Tubulin
C
Human macrophages
SDF-1(ng/ml)
0 1 3 10 100 300 500 1000 LPS (1 μg/mL)
P-p38
P-JNK
P-ERK
P-AKT
Tubulin
D
Kinase phosphorylation (Fold of control)
P-ERK
P-AKT
P-p38
P-JNK
0 1 3 10 100 300 500 1000
SDF-1 (ng/mL)

**Figure 5.12. Evidence of CXCR7 signaling in macrophages.**

(A) Cellular phosphorylation levels of p38, JNK, ERK, and AKT in macrophages differentiated from human primary monocytes (100 ng/ml IFN-γ + 1 μg/ml LPS for 48 h) were determined by Western blotting after the cells were stimulated by TC14012 or LPS (15 min) for the indicated concentrations and times.

(B) Dose-dependent effect of TC14012 on the phosphorylation of p38, JNK, ERK, and AKT in macrophages as determined by Western blotting after the cells were stimulated by TC14012 or LPS for 15 min at the indicated concentrations.

(C)The mean densitometric analysis of three separate experiments in B is normalized to respective total kinase loading controls (not shown) and the summarized data were shown in the graph. For clarity, only tubulin loading controls were shown; and the error bars with markers for the statistical significance have been omitted.

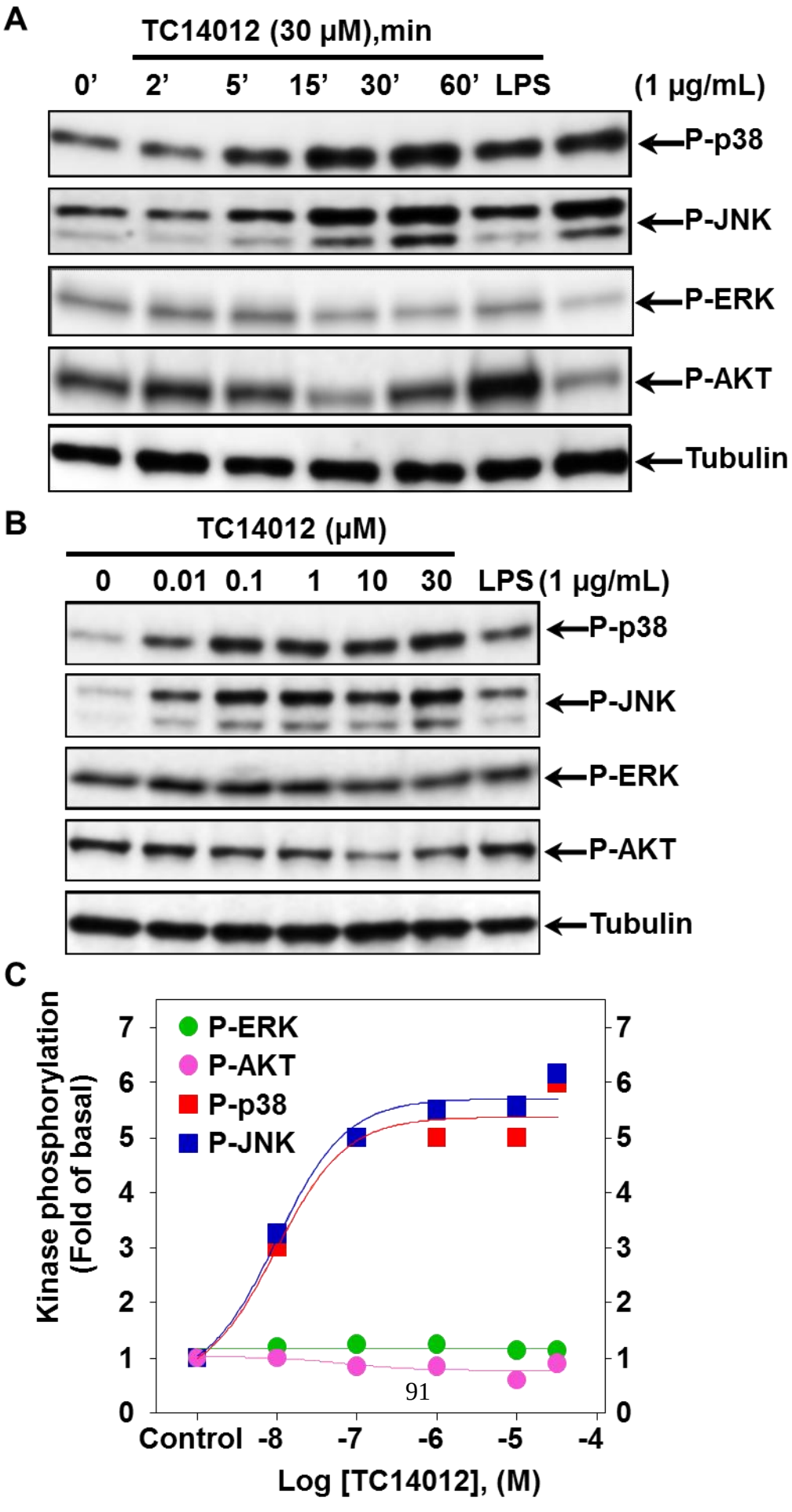
A
TC14012 (30 μM),min
0'
2'
5'
15'
30'
60'
LPS
(1 μg/mL)
P-p38
P-JNK
P-ERK
P-AKT
Tubulin
B
TC14012 (μM)
0
0.01
0.1
1
10
30
LPS (1 μg/mL)
P-p38
P-JNK
P-ERK
P-AKT
Tubulin
C
Kinase phosphorylation
(Fold of basal)
P-ERK
P-AKT
P-p38
P-JNK
0
1
2
3
4
5
6
7
Control
-8
-7
-6
-5
-4
Log [TC14012], (M)

**Figure 5.13. Effect of CXCR7 knockdown on signaling in macrophages.**

(A) Real-time PCR analysis of CXCR7 mRNA expression after the THP-1 cells were nucleofected with CXCR7 siRNA or scramble siRNA with or without (control) further PMA-induced macrophage differentiation (48 h). (n= 4)

(B) Knockdown of CXCR7 protein expression was confirmed by Western blotting using two different antibodies (11G8 and 9C4). CXCR7 siRNA had no effect on CXCR4 and GAPDH expression.

(C) Impact of CXCR7 knockdown by siRNA on SDF-1- and TC14012-induced effect on p38, JNK, ERK and AKT pathways in THP-1 macrophages. Scramble siRNA and LPS serve as respective controls. Blots are representative data from three independent experiments showing similar results.

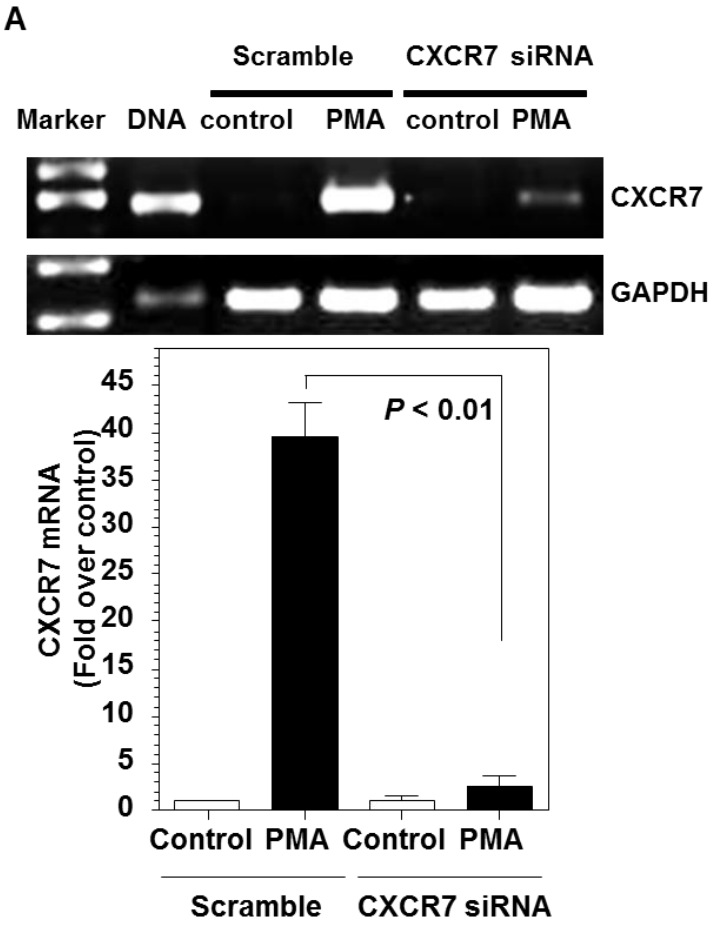
A
Scramble
CXCR7 siRNA
Marker
DNA
control
PMA
control
PMA
CXCR7
GAPDH
CXCR7 mRNA (Fold over control)
45
40
35
30
25
20
15
10
5
0
P < 0.01
Control
PMA
Control
PMA
Scramble
CXCR7 siRNA

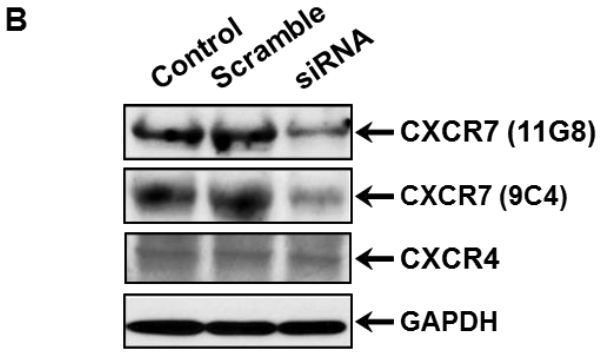
B
Control
Scramble
siRNA
CXCR7 (11G8)
CXCR7 (9C4)
CXCR4
GAPDH

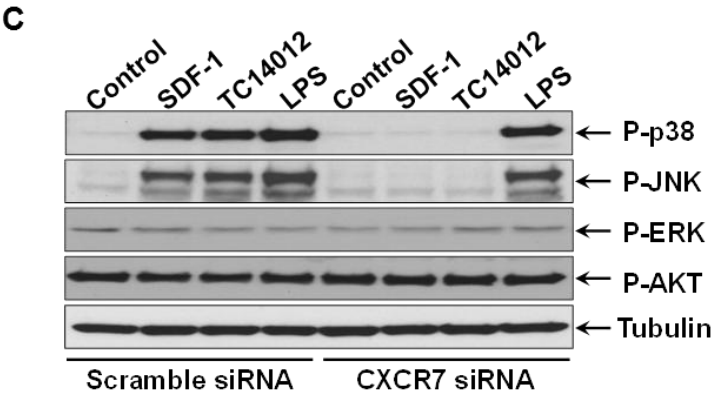
C
Control
SDF-1
TC14012
LPS
Control
SDF-1
TC14012
LPS
P-p38
P-JNK
P-ERK
P-AKT
Tubulin
Scramble siRNA
CXCR7 siRNA

**Figure 5.14. Effect of CXCR4 knockdown on signaling in macrophages.**

(A) CXCR4-selective siRNA suppressed CXCR4, but not CXCR7 (11G8) and GAPDH protein expression.

(B) No impact of CXCR4 knockdown by siRNA on SDF-1- and TC14012-induced effect on p38, JNK, ERK, and AKT pathways in THP-1 macrophages. Blots are representative data from three independent experiments showing similar results.

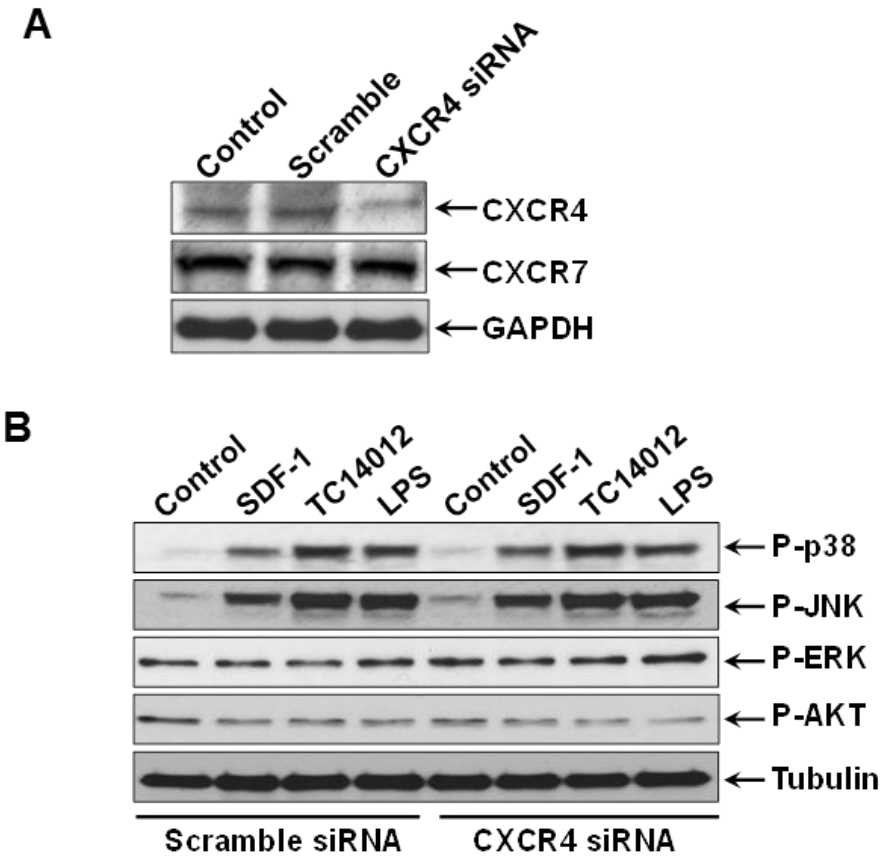

**Figure 5.15. Role of CXCR7 in I-TAC signaling in monocytes versus macrophages.**

(A) THP-1 monocytes, PMA-driven THP-1 macrophages, and human blood lymphocytes were stained with CXCR3 antibody and the isotype-matched IgG control before analyzed by flow cytometry. Flow cytometry plots are representative results from three independent experiments showing fluorescence intensity of isotype control antibody (black line) compared to the CXCR3-selective antibody (red line).

(B) Cellular phosphorylation levels of ERK, AKT, p38, and JNK in THP-1 monocytes were determined by Western blotting after the cells were stimulated by I-TAC for the indicated times. SDF-1 (100 ng/ml) stimulation for 15 min as a positive control.

(C) Time-dependent effect of I-TAC on the phosphorylation of ERK, AKT, p38, and JNK in THP-1 macrophages. SDF-1 (100 ng/ml) stimulation for 15 min as a positive control.

(D) No effect of CXCR3-selective antagonist compound 6c (10 μM) on I-TAC (100 ng/ml)-induced p38 and JNK activation.

(E) Effect of CXCR7-selective siRNA on I-TAC (100 ng/ml)- and LPS (1 μg/ml)-induced activation of p38 and JNK. For clarity, only tubulin loading controls were shown. Blots are representative data from three independent experiments showing similar results.

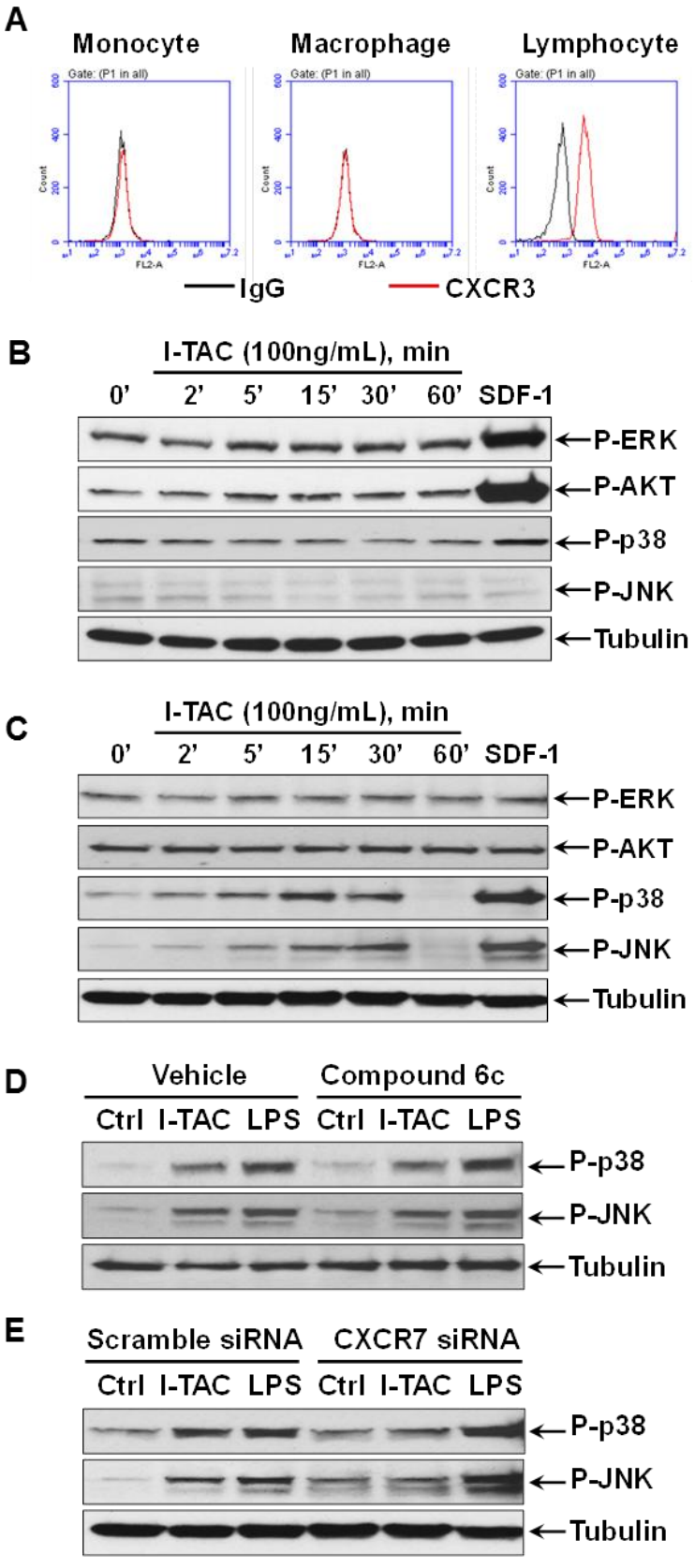
A
Monocyte
Macrophage
Lymphocyte
Gate: (P1 in all)
Count
FL2-A
IgG
CXCR3
B
I-TAC (100ng/mL), min
0'
2'
5'
15'
30'
60'
SDF-1
P-ERK
P-AKT
P-p38
P-JNK
Tubulin
C
I-TAC (100ng/mL), min
0'
2'
5'
15'
30'
60'
SDF-1
P-ERK
P-AKT
P-p38
P-JNK
Tubulin
D
Vehicle
Compound 6c
Ctrl
I-TAC
LPS
Ctrl
I-TAC
LPS
P-p38
P-JNK
Tubulin
E
Scramble siRNA
CXCR7 siRNA
Ctrl
I-TAC
LPS
Ctrl
I-TAC
LPS
P-p38
P-JNK
Tubulin

**Figure 5.16. Role of CXCR7 in the phagocytic activity of macrophages.**

(A) Macrophages differentiated from THP-1 monocytes were starved and activated by vehicle (control), SDF-1, TC14012, or IFN-γ for 2h, after which FITC-labeled *E. coli* were added and further incubated for 2h. Then phagocytic index was determined by measuring green fluorescence intensity emitted by the uptaken particles. Shown are merged images of macrophages (phase contrast) with internalized FITC-*E.coli* particles (green) and DAPI-positive nuclei (blue). Images magnification: 20 X.

(B)The summarized data of dose-dependent effect of CXCR7 activation on SDF-1-and TC14012- induced phagocytic activities in THP-1 macrophages. Then phagocytic index was determined by measuring green fluorescence intensity emitted by the uptaken particles. * $p<0.05$, ** $p<0.01$ compared to the control. (n = 5)

(C) Effect of CXCR4 blockage knockdown on 100ng/ml SDF-1-induced phagocytic activities in THP-1 macrophages. THP-1 macrophages were starved and activated by vehicle (control) or SDF-1 with or without AMD3100 pretreatment for 40 min, after which FITC-labeled *E. coli* were added and further incubated for 2 h. (n = 5)

(D) Effect of CXCR7 knockdown by siRNA on 300 ng/ml SDF-1- and 30μM TC14012-induced phagocytic activities in macrophages. N.S. stands for statistic non-significance. (n = 5)

(E) After pretreating the cells with or without SP600125 (30μM) or SB200358 (10 μM) for 40 min, cells were stimulated by TC14012 (30 μM) or SDF-1 (300 ng/ml) for 2h. Then

phagocytosis assay was performed as described above. * p<0.05, ** p<0.01 compared to the corresponding controls. (n = 6)

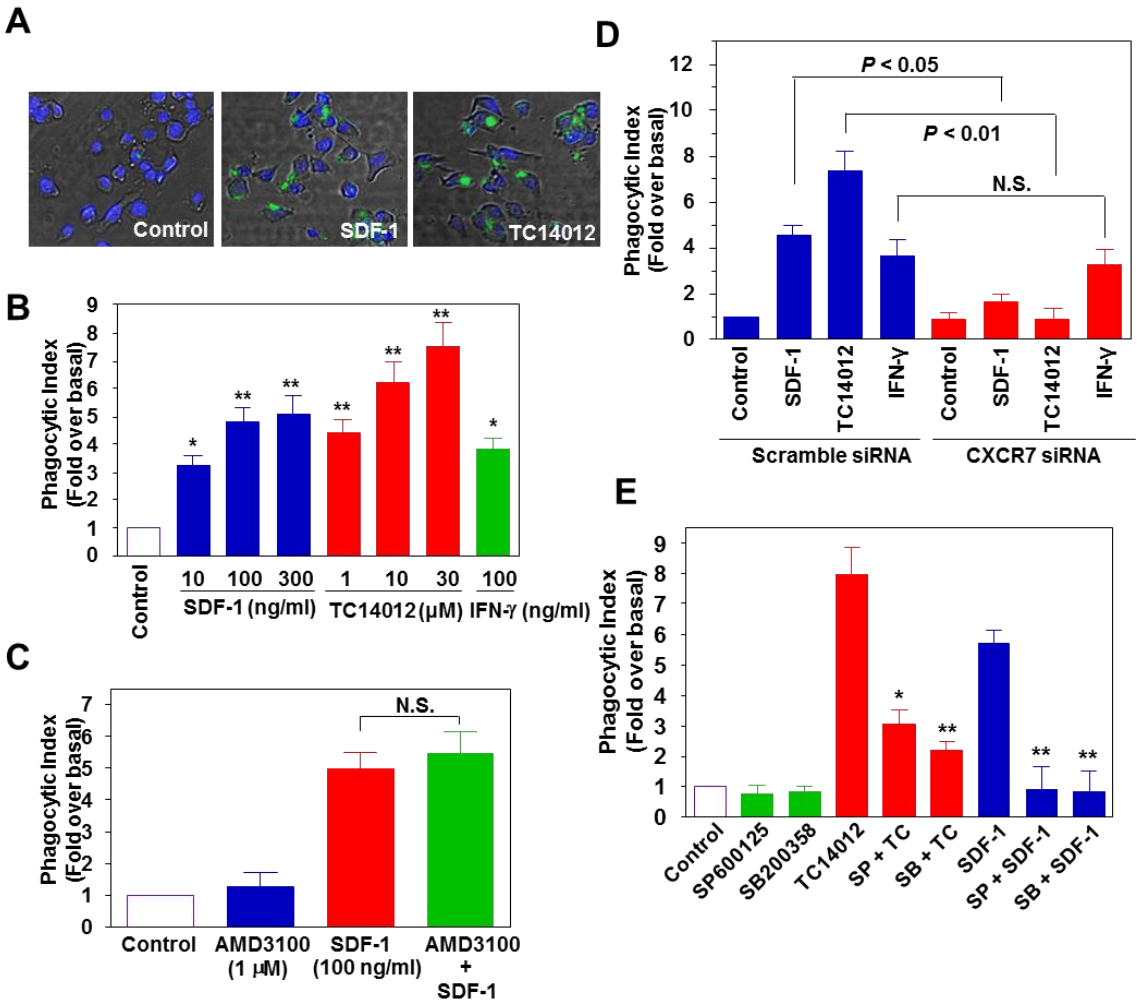

**Figure 5.17. Role of CXCR7 in the uptake of ac-LDL in macrophages.**

(A) Macrophages differentiated from THP-1 monocytes were starved and activated by vehicle (control), SDF-1, TC14012, or IgG for 2h, after which F Dil-labeled *ac-LDL* were added and further incubated for 2 h. Then phagocytic index was determined by measuring red fluorescence intensity emitted by the uptaken particles. (n = 5) Shown are merged images of macrophages (phase contrast) with internalized Dil-labeled *ac-LDL* particles (red) and DAPI-positive nuclei (blue). Images magnification: 20 X.

(B) Effect of SDF-1, TC14012, and IgG (FcγR agonist) on the uptake of Dil-ac-LDL in THP-1 macrophages. (n=5). Then phagocytic index was determined by measuring green fluorescence intensity emitted by the uptaken particles. (n = 5) * $p<0.05$, ** $p<0.01$ compared to the control.

(C) After pretreating the cells with or without AMD3100 for 40 min, cells were stimulated by SDF-1 for 2 h. Then Dil-ac-LDL uptake was measured as described in "Methods" (n=5). N.S. stands for statistic non-significance.

(D) Effect of CXCR7 knockdown by siRNA on 300 ng/ml SDF-1- and 30 μM TC14012-induced uptake of Dil-ac-LDL in human macrophages. N.S. stands for statistic non-significance. (n = 5)

(E) After pretreating the cells with or without SP600125 (30 μM) or SB200358 (10 μM) for 40 min, cells were stimulated by TC14012 (30 μM) or SDF-1 (300 ng/ml) for 2 h. Then Dil-ac-LDL uptake was measured as described in "Experimental Procedures". * $p<0.05$ compared to the controls. (n = 5)

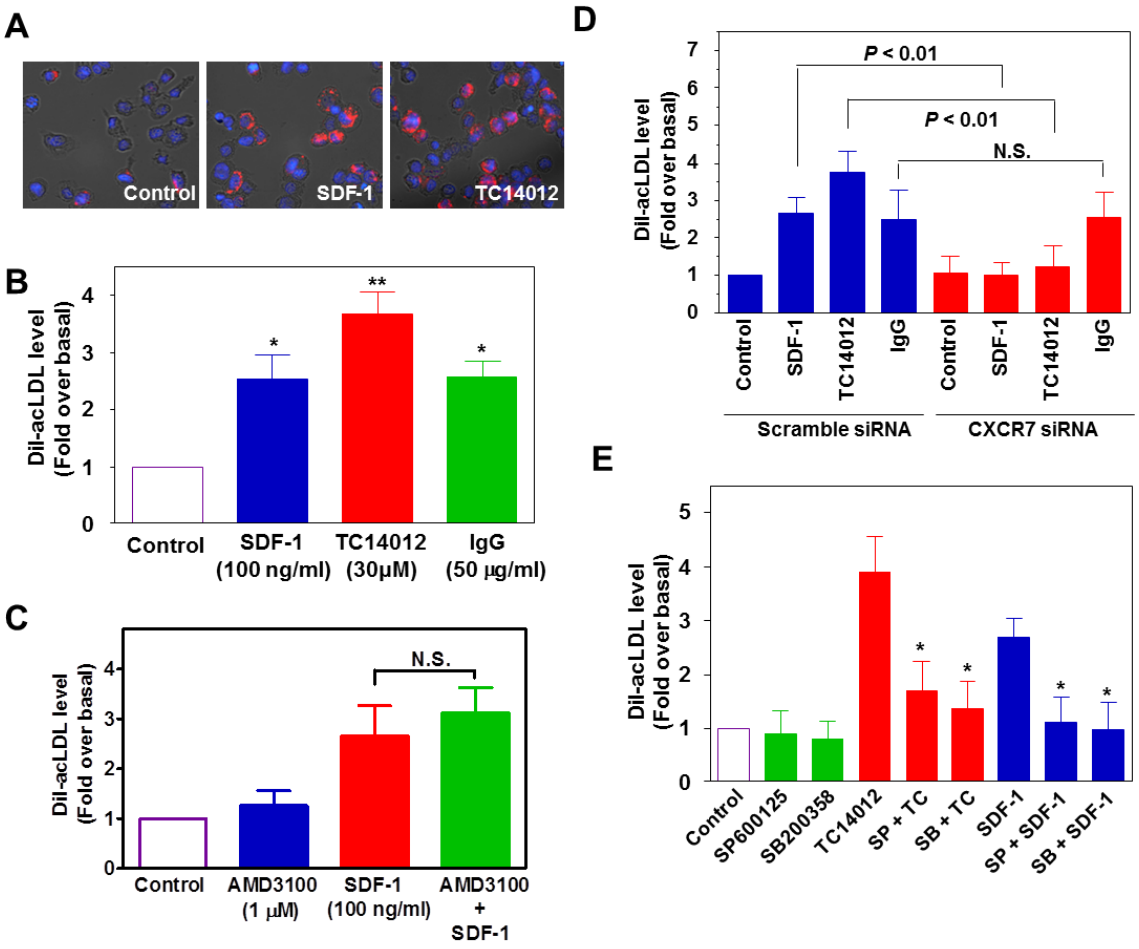
A
Control
SDF-1
TC14012
B
Dil-acLDL level
(Fold over basal)
Control
SDF-1
(100 ng/ml)
TC14012
(30μM)
IgG
(50 μg/ml)
C
N.S.
Control
AMD3100
(1 μM)
SDF-1
(100 ng/ml)
AMD3100
+
SDF-1
D
P < 0.01
P < 0.01
N.S.
Control
SDF-1
TC14012
IgG
Scramble siRNA
CXCR7 siRNA
E
Control
SP600125
SB200358
TC14012
SP + TC
SB + TC
SDF-1
SP + SDF-1
SB + SDF-1

**Figure 5.18. Role of CXCR7 in I-TAC-induced macrophage phagocytosis.**

(A) THP-1 macrophages were starved and activated by vehicle (control), I-TAC (100 ng/mL) or IFN-γ (100 ng/mL) for 2h, after which FITC-labeled *E. coli* were added and further incubated for 2h. Then phagocytic index was determined by measuring green fluorescence intensity emitted by the uptaken particles. Shown are merged images of macrophages (phase contrast) with internalized FITC-*E.coli* particles (green) and DAPI-positive nuclei (blue). Images magnification: 20 X.

(B) Effect of CXCR7 knockdown by siRNA on I-TAC- or IFN-γ-induced phagocytic activities in THP-1 macrophages. N.S. stands for statistic non-significance (n=5).

(C) After pretreating the cells with or without SP600125 (30 μM), SB200358 (10 μM), or compound 6c (10 μM) for 40 min, cells were stimulated by I-TAC (100 ng/ml) for 2h. Then phagocytosis assay was performed as described above. * $p<0.05$, ** $p<0.01$ compared to the corresponding controls. (n = 5)

(D) Effect of I-TAC and IgG (FcγR agonist) on the uptake of Dil-ac-LDL in THP-1 macrophages. Images magnification: 20 X.

(E) Effect of CXCR7 knockdown by siRNA on I-TAC (100 ng/mL)- or IgG (50 μg/mL)-induced uptake of Dil-ac-LDL in THP-1 macrophages. N.S. stands for statistic non-significance. (n = 5)

(F) After pretreating the cells with or without SP600125 (30 μM), SB200358 (10 μM) or compound 6c (10 μM) for 40 min, cells were stimulated by I-TAC (100 ng/mL) for 2 h. Then

Dil-ac-LDL uptake was measured as described in “Experimental Procedures”. * p<0.05, ** p<0.01 compared to the controls. (n = 5)

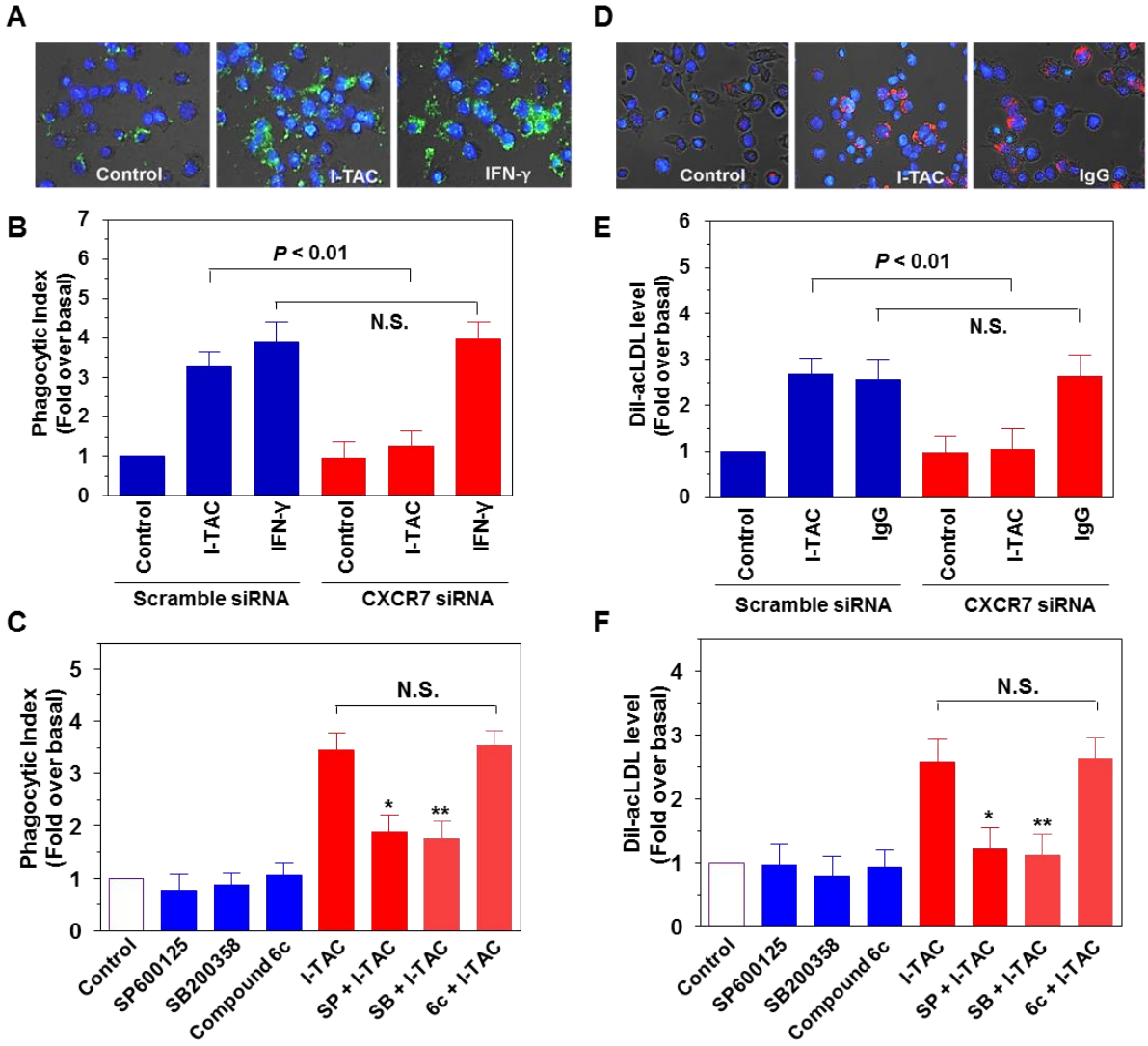

**Figure 5.19. Effect of different CXCR7 agonists on macrophage migration.**

(A) PMA-driven THP-1 macrophages were starved for 10 h, after which the cells were seeded on the top inserts of the Boyden Chamber system. Starved macrophages were then stimulated by adding vehicle (control), SDF-1 (100 ng/mL), TC14012 (30 μM), or I-TAC (100 ng/mL) into the bottom chamber of the system. After 12 h, the cells migrated beneath the pore-containing membranes were fixed and stained with DAPI. Ten random fields were selected for cell counting.

(B) Figure depicts summarized results from five independent experiments. * $p<0.05$, ** $p<0.01$.

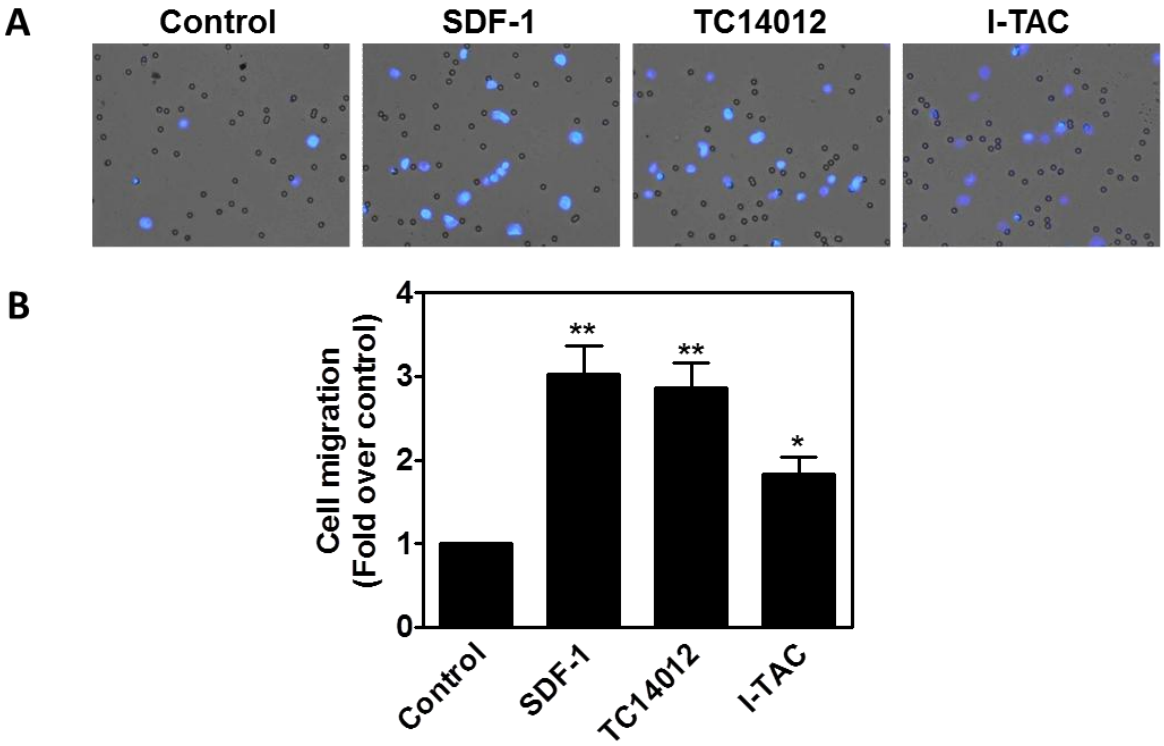

**Figure 5.20. Role of SDF-1 and TC14012 in the adhesion of human macrophages.**

(A) Calcin AM-stained THP-1 macrophages were seeded and allowed to attach to 6-well plate with or without activation by SDF-1, TC14012 at the dose indicated for 5 min. The attached cells were imaged. Representative images from 3 experiments were shown.

(B) The attached cells were counted by Image J and presented as the fold change of attached cell in the treatment groups over control group. *, $p<0.05$; **, $p<0.01$ as compared with control.(n = 5)

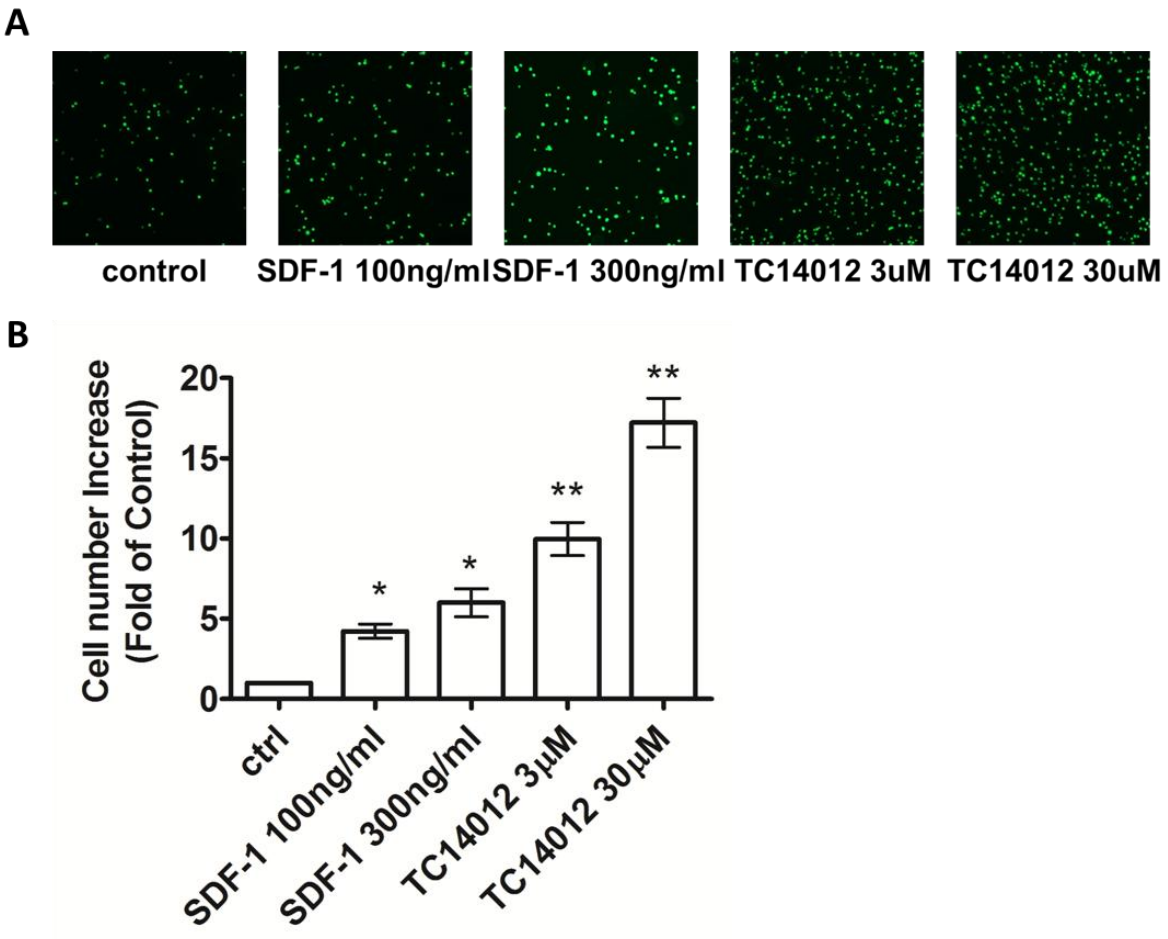

**Figure 5.21. Gene expression profiles in SDF-1-treated THP-1 macrophages.**

Microarray heat map of genes regulated specifically in response to SDF-1 treatment on THP-1 macrophages. The fold change of expression of the 84 genes related to atherosclerosis (A) or inflammation (B) compared to untreated macrophage is shown. Red indicates that the induction of expression while green indicates inhibition.

**A**

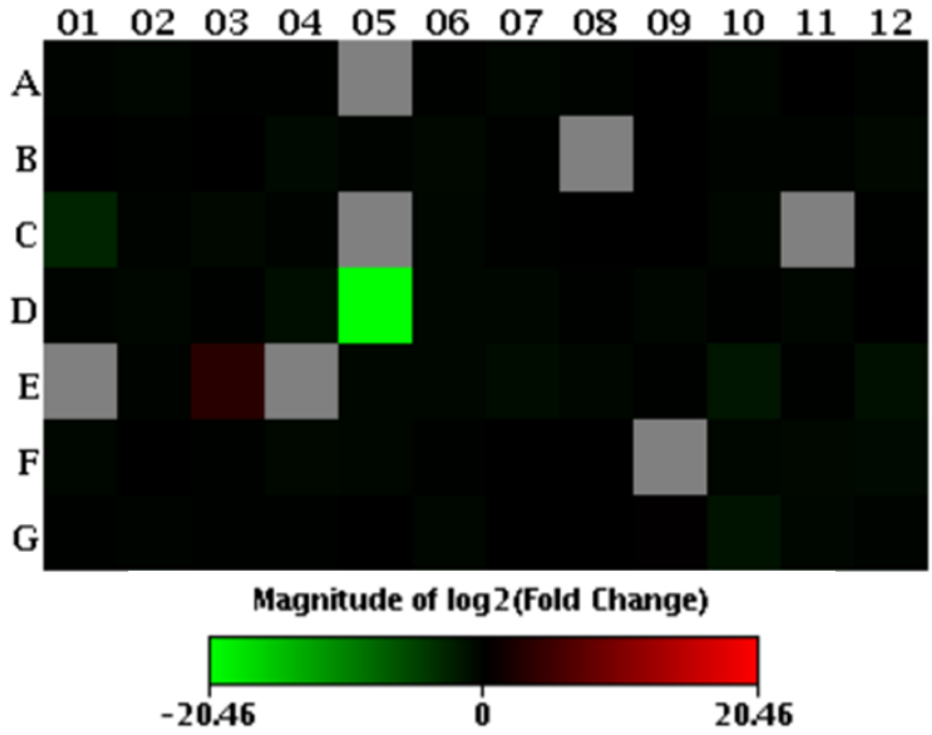
01 02 03 04 05 06 07 08 09 10 11 12
A
B
C
D
E
F
G
Magnitude of log2(Fold Change)
-20.46
0
20.46

**B**

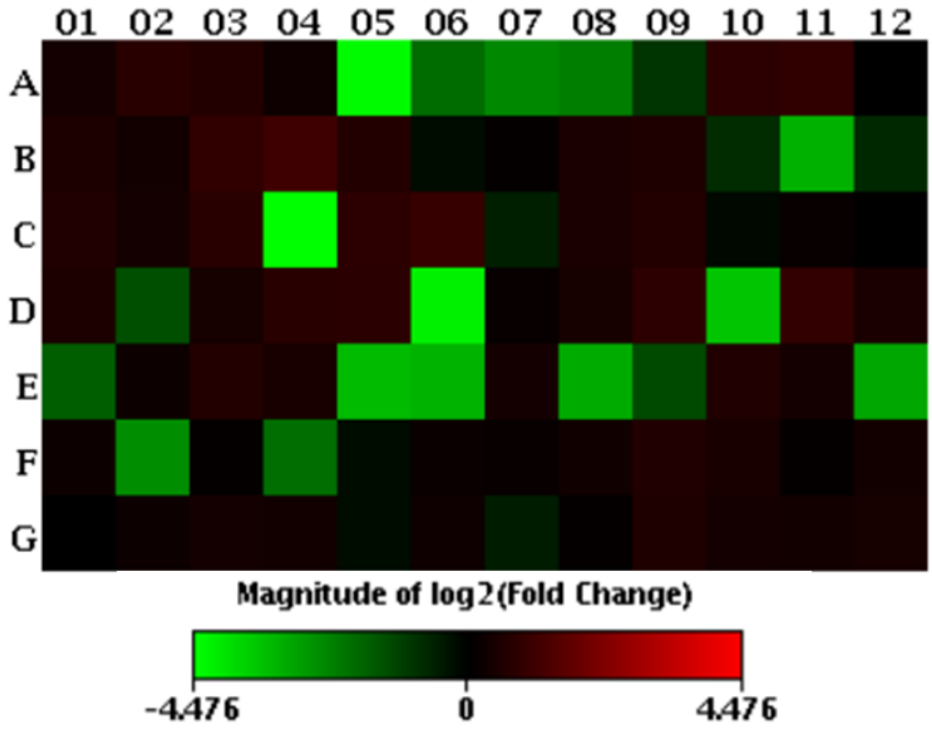
01 02 03 04 05 06 07 08 09 10 11 12
A
B
C
D
E
F
G
Magnitude of log2(Fold Change)
-4.476
0
4.476

**Figure 5.22. Atorvastatin treatment inhibits CXCR7 mRNA expression.**

(A) CXCR4 and CXCR7 mRNA was determined on vehicle treated THP-1 monocyte and THP-1 macrophages differentiated with 40 nM PMA for 48 h in the presence or absence of 1 μM atorvastatin pre-treatment. Genomic DNA was used as positive controls. Figures depict representative results from three independent experiments.

(B) Figures depict summarized results of CXCR7 mRNA from three independent experiments in duplicate. * $p<0.05$, ** $p<0.01$.

(C) Figures depict summarized results of CXCR4 mRNA from three independent experiments in duplicate. * $p<0.05$, ** $p<0.01$.

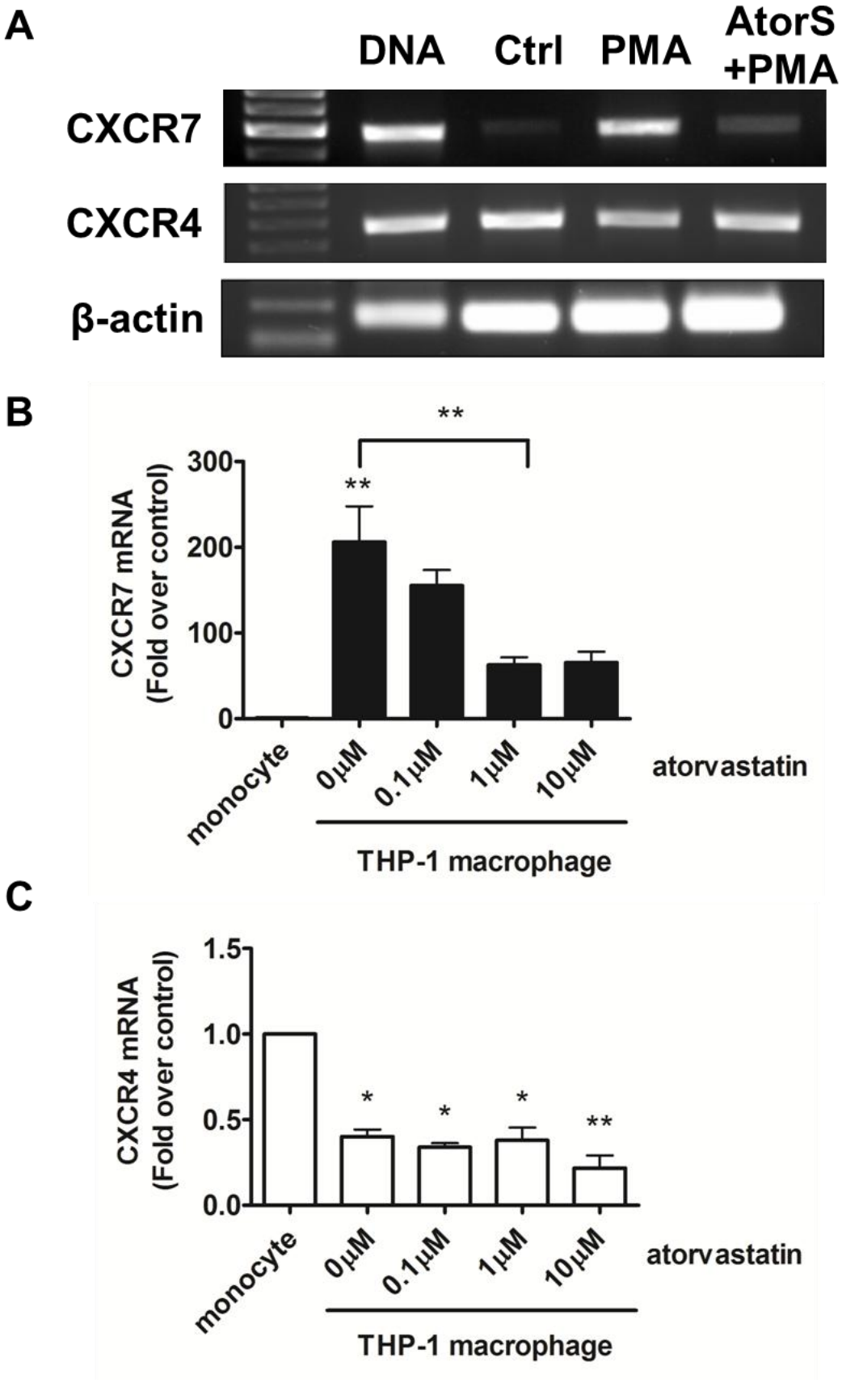
A
DNA
Ctrl
PMA
AtorS +PMA
CXCR7
CXCR4
β-actin
B
CXCR7 mRNA (Fold over control)
300
200
100
0
**
**
monocyte
0μM
0.1μM
1μM
10μM
atorvastatin
THP-1 macrophage
C
CXCR4 mRNA (Fold over control)
1.5
1.0
0.5
0.0
*
*
*
**
monocyte
0μM
0.1μM
1μM
10μM
atorvastatin
THP-1 macrophage

**Figure 5.23. Statins show differential inhibition on CXCR7 expression in macropahges.** CXCR7 mRNA was determined on vehicle treated THP-1 monocyte , THP-1 macrophages, THP-1 macrophages pretreated with 1 μM of atorvastatin, pravastatin, fluvastatin, mevastatin, and simvastatin, respectively, for 30 min. Figure depicts summarized results from three independent experiments. ** $p<0.01$.

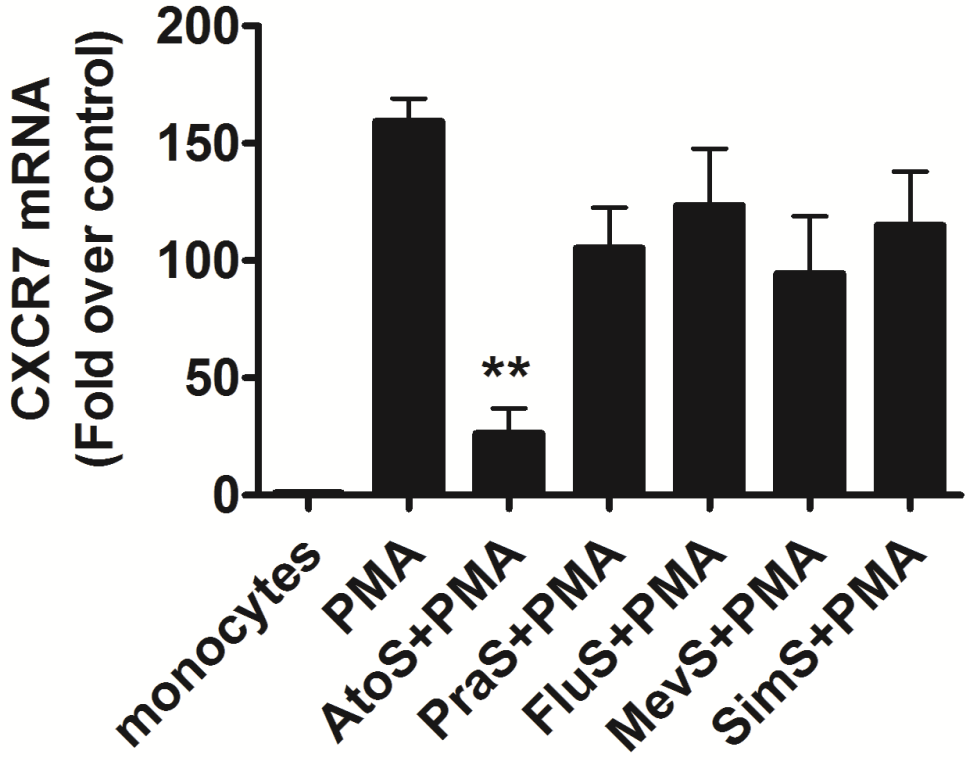

**Figure 5.24. Atorvastatin treatment inhibits CXCR7 mRNA expression in a time- and dose-dependent manner.**

(A) Kinetics of CXCR7 mRNA expression during monocyte-to-macrophage differentiation induced by 40 nM PMA with or without 1 μM atorvastatin for the indicated time periods. The mRNA levels were determined by real-time PCR and presented as relative fold changes compared with control cells after normalized to β-actin. (n = 5)

(B) CXCR7 mRNA in monocytes and 40 nM PMA-driven macrophages with or without atorvastatin at the indicated doses were studies. Similar data were obtained in three independent experiments. * $p<0.05$, ** $p<0.01$.

(C) CXCR4 mRNA in monocytes and 40 nM PMA-driven macrophages with or without atorvastatin at the indicated doses were studied. Similar data were obtained in three independent experiments. * $p<0.05$, ** $p<0.01$.

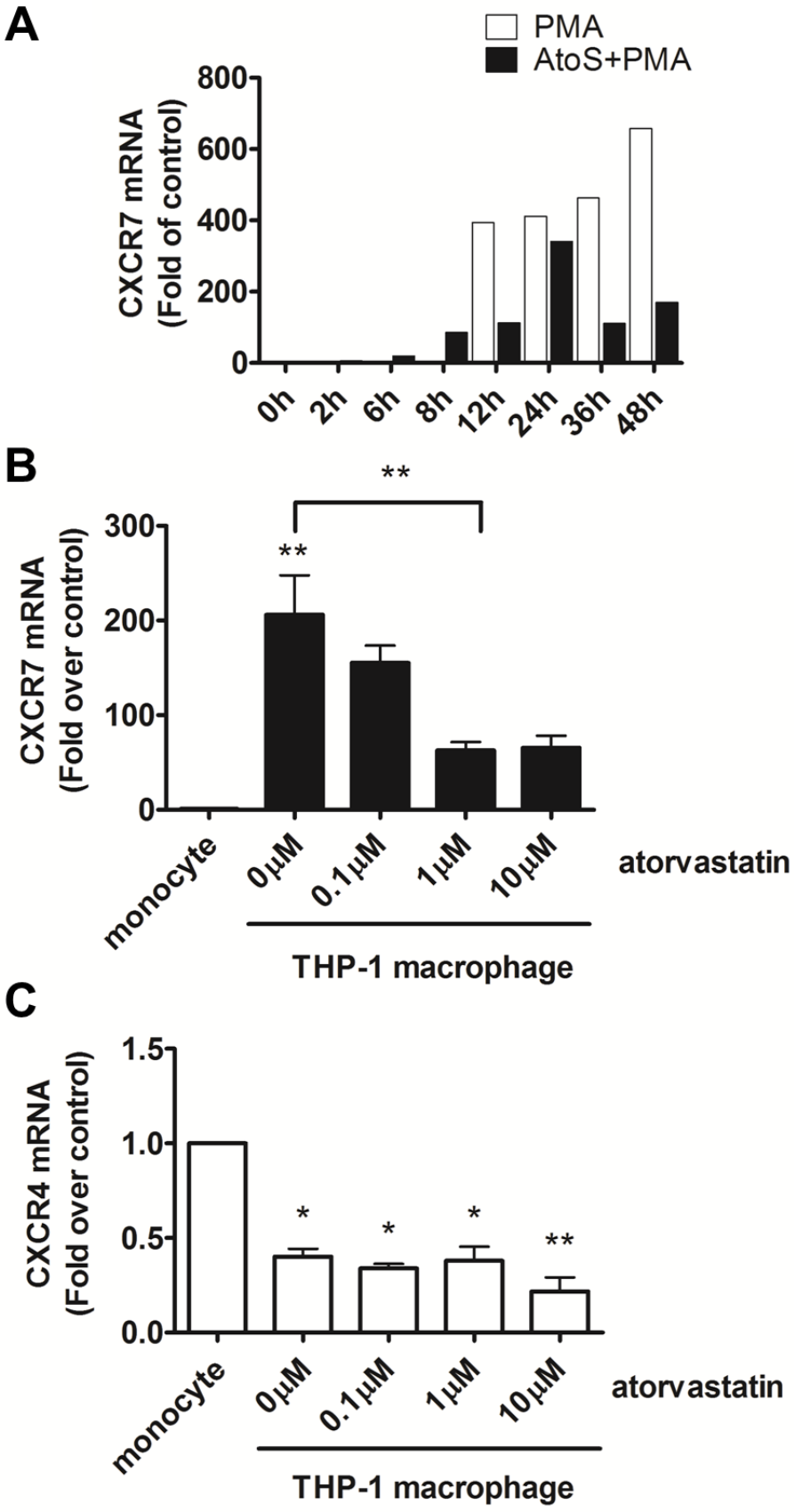
A
PMA
AtoS+PMA
CXCR7 mRNA
(Fold of control)
800
600
400
200
0
0h
2h
6h
8h
12h
24h
36h
48h
B
**
**
CXCR7 mRNA
(Fold over control)
300
200
100
0
monocyte
0μM
0.1μM
1μM
10μM
atorvastatin
THP-1 macrophage
C
CXCR4 mRNA
(Fold over control)
1.5
1.0
0.5
0.0
*
*
*
**
monocyte
0μM
0.1μM
1μM
10μM
atorvastatin
THP-1 macrophage

**Figure 5.25. Atorvastatin treatment inhibits CXCR7 protein expression in macrophages.**

(A) CXCR4 and CXCR7 protein levels were determined by Western blotting in total cell lysates isolated from vehicle-treated control monocytes, PMA-differentiated macrophages, and PMA-differentiated macrophages with of 1μM atorvastatin pre-treatment. MBA-MD-231 cell was used as a positive control. Similar data were obtained in three independent experiments.

(B) THP-1 monocytes, PMA-driven THP-1 macrophages with or without 1 μM atorvastatin pre-treatment were stained with CXCR4 or CXCR7 antibodies and the respective isotype-matched IgG controls before analyzed by flow cytometery. Flow cytometery plots are representative results from three independent experiments showing fluorescence intensity of isotype control antibodies (black line) compared to the CXCR4- or CXCR7-selective antibodies (red line).

(C) and (D) Summarized quantitative data for panel B. ** $p<0.01$. N.S. stands for statistic non-significance.

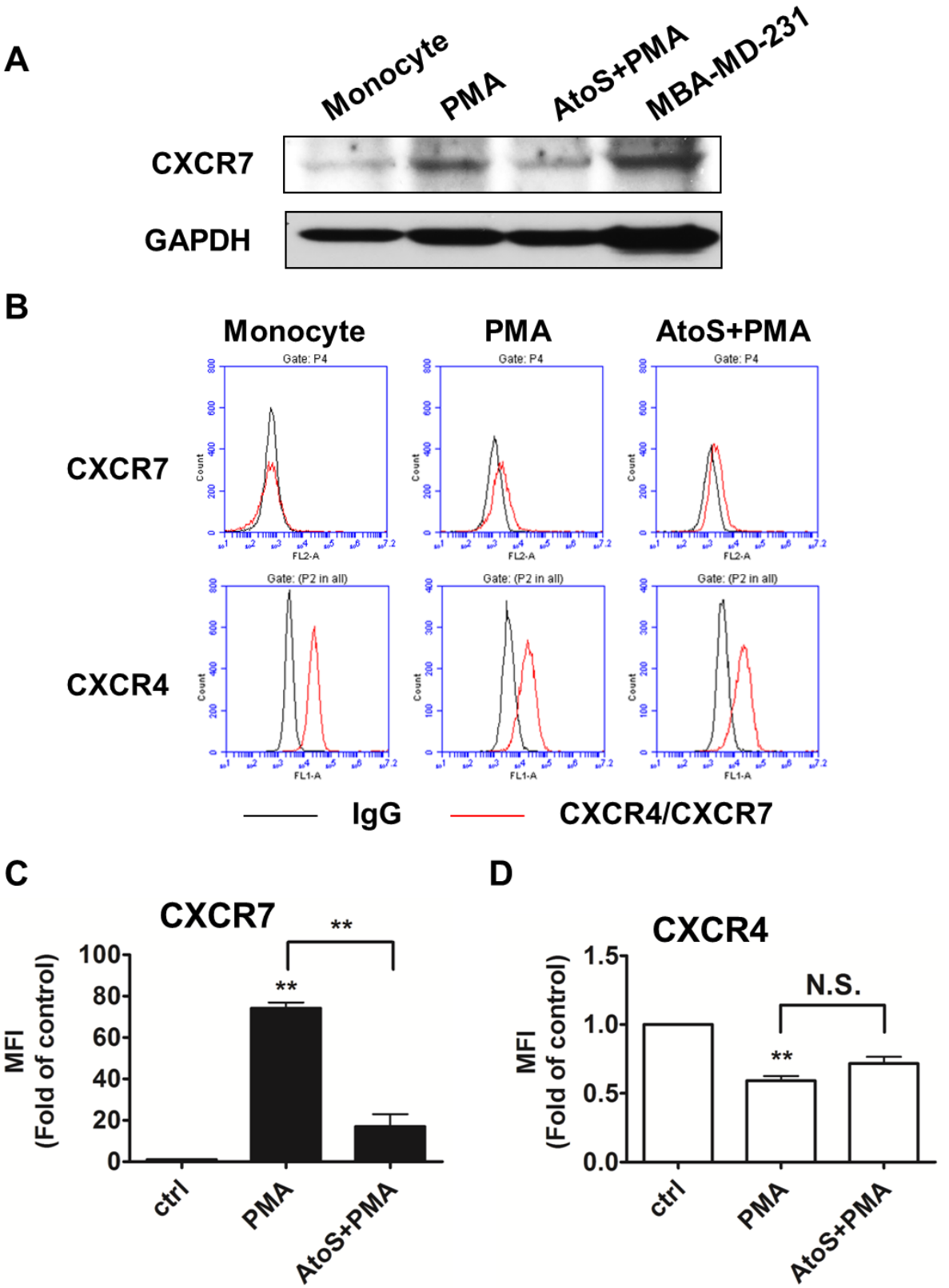
A
Monocyte
PMA
AtoS+PMA
MBA-MD-231
CXCR7
GAPDH
B
Monocyte
PMA
AtoS+PMA
CXCR7
CXCR4
Gate: P4
Gate: (P2 in all)
Count
FL2-A
FL1-A
IgG
CXCR4/CXCR7
C
CXCR7
MFI
(Fold of control)
**
ctrl
PMA
AtoS+PMA
D
CXCR4
N.S.
**

**Figure 5.26. Inhibition of CXCR7 protein expression by atorvastatin has no effect on macrophage differentiation.**

(A) THP-1 monocytes were seeded in 6 well plates and treated with atorvastatin in the indicated doses for 48 h. 4 h before the end of incubation, 100 µl resazurin was added to each well. The fluorescence intensity was read at 590 nm emission wavelengths with 570 nm excitation wavelengths. Results were expressed in mean fluorescence intensity. *$p < 0.05$. ($n = 3$)

(B) Morphology of macrophages induced from THP-1 monocytes by treating the cells with PMA (40 nM), or PMA plus 1 µM of atorvastatin pre-treatment was observed. Shown are the representative macrophage morphologies after 48 h differentiation. Magnification: 10 X. ($n = 3$)

(C) Effect of atorvastatin on expression of the macrophage surface markers CD36 and CD68 on THP-1 monocytes, PMA-driven THP-1 macrophages with or without 1 µM atorvastatin pre-treatment was analyzed by flow cytometry. Figures depict representative results from one independent experiment.

(D) Histographic presentation of quantitative data for panel C.

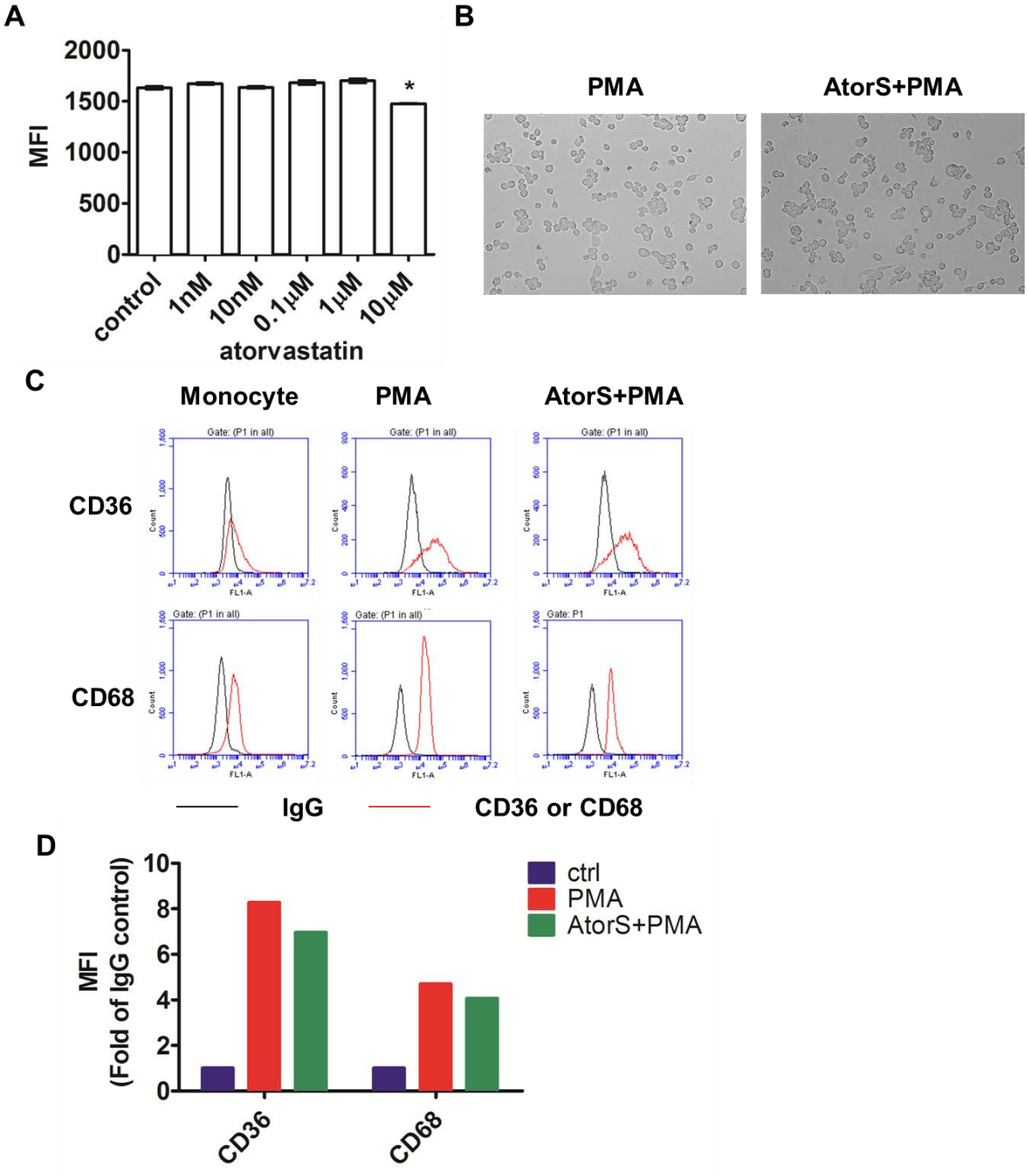
A
2000
1500
1000
500
0
MFI
*
control
1nM
10nM
0.1μM
1μM
10μM
atorvastatin
B
PMA
AtorS+PMA
C
Monocyte
PMA
AtorS+PMA
CD36
CD68
Gate: (P1 in all)
Gate: P1
Count
FL1-A
IgG
CD36 or CD68
D
MFI
(Fold of IgG control)
10
8
6
4
2
0
ctrl
PMA
AtorS+PMA
CD36
CD68

**Figure 5.27. Inhibition of CXCR7 protein expression by atorvastatin is reversed by mevalonate but not mimicked by protein geranylation inhibitors.**

(A) CXCR7 mRNA levels were determined by real-time PCR in vehicle-treated control monocytes; PMA-differentiated macrophages; PMA-differentiated macrophages with 1 μM atorvastatin pre-treatment in the presence or absence of mevalonate (Mev); and PMA-differentiated macrophages with 1 μM squalestatin (SquS) pre-treatment. The CXCR7 mRNA on monocytes treated with mevalonate, atorvastatin, and squalestatin were used as control. Similar data were obtained in three independent experiments. * $p<0.05$, ** $p<0.01$.

(B) CXCR7 mRNA levels were determined by real-time PCR in vehicle-treated control monocytes; PMA-differentiated macrophages; PMA-differentiated macrophages with 1 μM of atorvastatin, GGTI-286, FTI-276, or Y27632 pre-treatment. The CXCR7 mRNA on monocytes treated with GGTI-286, FTI-276, and Y27632 are used as control. Similar data were obtained in three independent experiments. ** $p<0.01$.

(C) CXCR4 mRNA levels were determined by real-time PCR in vehicle-treated control monocytes; PMA-differentiated macrophages; PMA-differentiated macrophages with 1 μM of atorvastatin, GGTI-286, FTI-276, or Y27632 pre-treatment. The CXCR7 mRNA on monocyte treated with GGTI-286, FTI-276, or Y-27632 were used as control. Similar data were obtained in three independent experiments. N.S. stands for statistic non-significance.

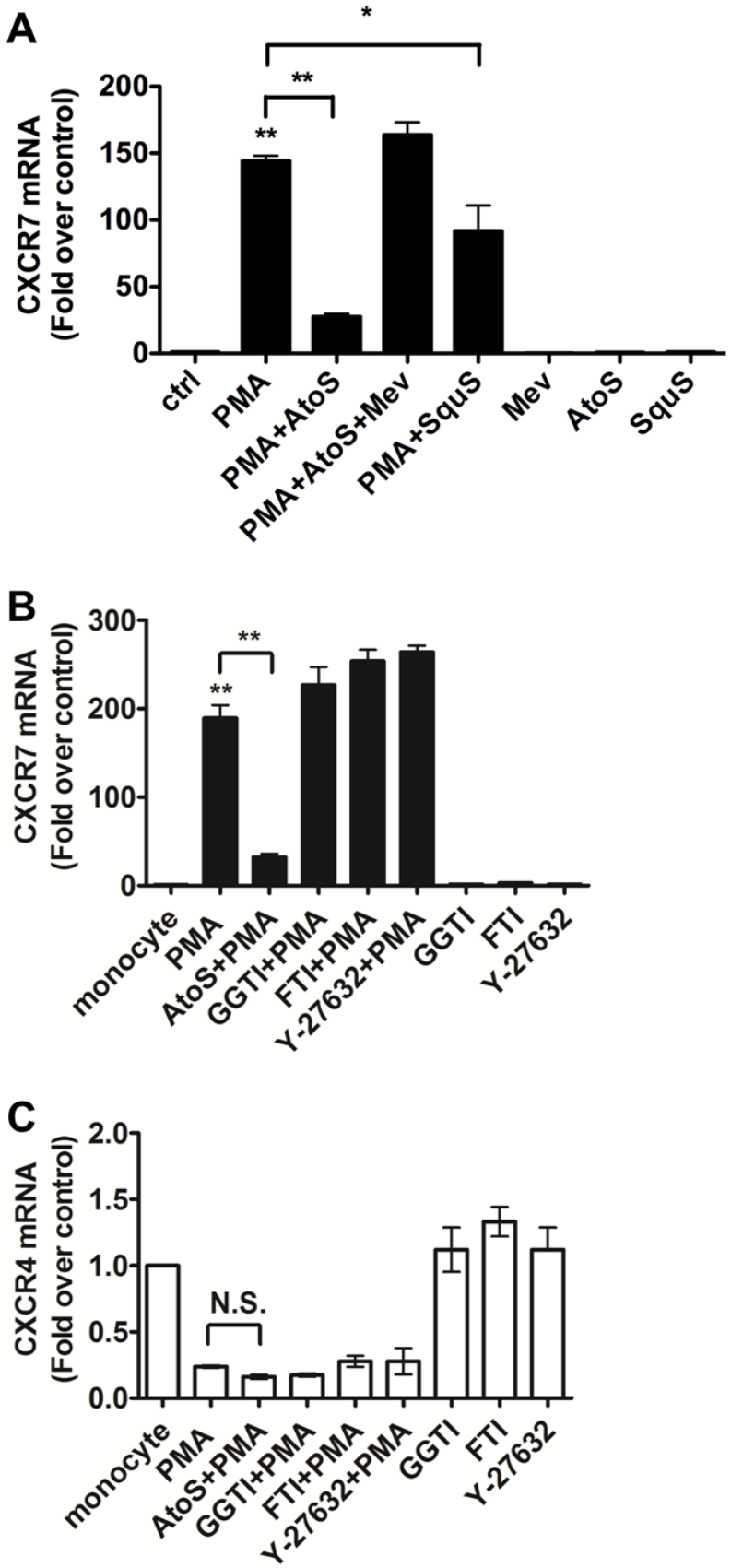
A
CXCR7 mRNA
(Fold over control)
200
150
100
50
0
*
**
**
ctrl
PMA
PMA+AtoS
PMA+AtoS+Mev
PMA+SquS
Mev
AtoS
SquS
B
CXCR7 mRNA
(Fold over control)
300
200
100
0
**
**
monocyte
PMA
AtoS+PMA
GGTI+PMA
FTI+PMA
Y-27632+PMA
GGTI
FTI
Y-27632
C
CXCR4 mRNA
(Fold over control)
2.0
1.5
1.0
0.5
0.0
N.S.
monocyte
PMA
AtoS+PMA
GGTI+PMA
FTI+PMA
Y-27632+PMA
GGTI
FTI
Y-27632

Reference

**Abi-Younes, S., Sauty, A., Mach, F., Sukhova, G.K., Libby, P., and Luster, A.D. (2000).** The stromal cell-derived factor-1 chemokine is a potent platelet agonist highly expressed in atherosclerotic plaques. Circ Res 86, 131-138.

**Aiuti, A., Webb, I.J., Bleul, C., Springer, T., and Gutierrez-Ramos, J.C. (1997).** The chemokine SDF-1 is a chemoattractant for human CD34+ hematopoietic progenitor cells and provides a new mechanism to explain the mobilization of CD34+ progenitors to peripheral blood. J Exp Med 185, 111-120.

**Akhtar, S., Gremse, F., Kiessling, F., Weber, C., and Schober, A. (2013).** CXCL12 Promotes the Stabilization of Atherosclerotic Lesions Mediated by Smooth Muscle Progenitor Cells in Apoe-Deficient Mice. Arterioscler Thromb Vasc Biol 33, 679-686.

**Ara, T., Tokoyoda, K., Okamoto, R., Koni, P.A., and Nagasawa, T. (2005).** The role of CXCL12 in the organ-specific process of artery formation. Blood 105, 3155-3161.

**Arnaud, C., Veillard, N.R., and Mach, F. (2005).** Cholesterol-independent effects of statins in inflammation, immunomodulation and atherosclerosis. Curr Drug Targets Cardiovasc Haematol Disord 5, 127-134.

**Balabanian, K., Lagane, B., Infantino, S., Chow, K.Y., Harriague, J., Moepps, B., Arenzana-Seisdedos, F., Thelen, M., and Bachelerie, F. (2005).** The chemokine SDF-1/CXCL12 binds to and signals through the orphan receptor RDC1 in T lymphocytes. J Biol Chem 280, 35760-35766.

**Becker, L., Gharib, S.A., Irwin, A.D., Wijsman, E., Vaisar, T., Oram, J.F., and Heinecke, J.W. (2010).** A Macrophage Sterol-Responsive Network Linked to Atherogenesis. Cell Metabolism 11, 125-135.

**Berahovich, R.D., Penfold, M.E., and Schall, T.J. (2010a).** Nonspecific CXCR7 antibodies. Immunol Lett 133, 112-114.

**Berahovich, R.D., Zabel, B.A., Penfold, M.E., Lewen, S., Wang, Y., Miao, Z., Gan, L., Pereda, J., Dias, J., Slukvin, II, et al. (2010b).** CXCR7 protein is not expressed on human or mouse leukocytes. J Immunol 185, 5130-5139.

**Bernhagen, J., Krohn, R., Lue, H., Gregory, J.L., Zernecke, A., Koenen, R.R., Dewor, M., Georgiev, I., Schober, A., Leng, L., et al. (2007).** MIF is a noncognate ligand of CXC chemokine receptors in inflammatory and atherogenic cell recruitment. Nat Med 13, 587-596.

**Bleul, C.C., Farzan, M., Choe, H., Parolin, C., Clark-Lewis, I., Sodroski, J., and Springer, T.A. (1996).** The lymphocyte chemoattractant SDF-1 is a ligand for LESTR/fusin and blocks HIV-1 entry. Nature 382, 829-833.

**Boldajipour, B., Mahabaleshwar, H., Kardash, E., Reichman-Fried, M., Blaser, H., Minina, S., Wilson, D., Xu, Q., and Raz, E. (2008)**. Control of chemokine-guided cell migration by ligand sequestration. Cell 132, 463-473.

**Braunersreuther, V., Mach, F., and Steffens, S. (2007).** The specific role of chemokines in atherosclerosis. Thromb Haemost 97, 714-721.

**Bruhl, H., Cohen, C.D., Linder, S., Kretzler, M., Schlondorff, D., and Mack, M. (2003).** Post-translational and cell type-specific regulation of CXCR4 expression by cytokines. Eur J Immunol 33, 3028-3037.

**Burns, J.M. (2006).** A novel chemokine receptor for SDF-1 and I-TAC involved in cell survival, cell adhesion, and tumor development. Journal of Experimental Medicine 203, 2201-2213.

**Canals, M., Scholten, D.J., de Munnik, S., Han, M.K., Smit, M.J., and Leurs, R. (2012).** Ubiquitination of CXCR7 controls receptor trafficking. PLoS One 7, e34192.

**Ceradini, D.J., Kulkarni, A.R., Callaghan, M.J., Tepper, O.M., Bastidas, N., Kleinman, M.E., Capla, J.M., Galiano, R.D., Levine, J.P., and Gurtner, G.C. (2004).** Progenitor cell trafficking is regulated by hypoxic gradients through HIF-1 induction of SDF-1. Nat Med 10, 858-864.

**Coffield, V.M., Jiang, Q., and Su, L. (2003).** A genetic approach to inactivating chemokine receptors using a modified viral protein. Nat Biotechnol 21, 1321-1327.

**Cole, A.G., Stroke, I.L., Brescia, M.R., Simhadri, S., Zhang, J.J., Hussain, Z., Snider, M., Haskell, C., Ribeiro, S., Appell, K.C., et al. (2006).** Identification and initial evaluation of 4-N-aryl-[1,4]diazepane ureas as potent CXCR3 antagonists. Bioorg Med Chem Lett 16, 200-203.

**Daigneault, M., Preston, J.A., Marriott, H.M., Whyte, M.K., and Dockrell, D.H. (2010).** The identification of markers of macrophage differentiation in PMA-stimulated THP-1 cells and monocyte-derived macrophages. PLoS One 5, e8668.

**Damas, J.K., Waehre, T., Yndestad, A., Ueland, T., Muller, F., Eiken, H.G., Holm, A.M., Halvorsen, B., Froland, S.S., Gullestad, L., et al. (2002).** Stromal cell-derived factor-1alpha in unstable angina: potential antiinflammatory and matrix-stabilizing effects. Circulation 106, 36-42.

**Dar, A., Schajnovitz, A., Lapid, K., Kalinkovich, A., Itkin, T., Ludin, A., Kao, W.M., Battista, M., Tesio, M., Kollet, O., et al. (2011).** Rapid mobilization of hematopoietic

progenitors by AMD3100 and catecholamines is mediated by CXCR4-dependent SDF-1 release from bone marrow stromal cells. Leukemia 25, 1286-1296.

**De La Luz Sierra, M., Yang, F., Narazaki, M., Salvucci, O., Davis, D., Yarchoan, R., Zhang, H.H., Fales, H., and Tosato, G. (2004).** Differential processing of stromal-derived factor-1alpha and stromal-derived factor-1beta explains functional diversity. Blood 103, 2452-2459.

**De Meyer, I., Martinet, W., and De Meyer, G.R.Y. (2012).** Therapeutic strategies to deplete macrophages in atherosclerotic plaques. British Journal of Clinical Pharmacology 74, 246-263.

**Debnath, B., Xu, S., Grande, F., Garofalo, A., and Neamati, N. (2013).** Small molecule inhibitors of CXCR4. Theranostics 3, 47-75.

**Decaillot, F.M., Kazmi, M.A., Lin, Y., Ray-Saha, S., Sakmar, T.P., and Sachdev, P. (2011).** CXCR7/CXCR4 heterodimer constitutively recruits beta-arrestin to enhance cell migration. J Biol Chem 286, 32188-32197.

**Ding, L., Ma, W., Littmann, T., Camp, R., and Shen, J. (2011).** The P2Y(2) nucleotide receptor mediates tissue factor expression in human coronary artery endothelial cells. J Biol Chem 286, 27027-27038.

**DiPersio, J.F., Micallef, I.N., Stiff, P.J., Bolwell, B.J., Maziarz, R.T., Jacobsen, E., Nademanee, A., McCarty, J., Bridger, G., and Calandra, G. (2009).** Phase III prospective randomized double-blind placebo-controlled trial of plerixafor plus granulocyte colony-stimulating factor compared with placebo plus granulocyte colony-stimulating factor for autologous stem-cell mobilization and transplantation for patients with non-Hodgkin's lymphoma. J Clin Oncol 27, 4767-4773.

**Dubeykovskaya, Z., Dubeykovskiy, A., Solal-Cohen, J., and Wang, T.C. (2009).** Secreted trefoil factor 2 activates the CXCR4 receptor in epithelial and lymphocytic cancer cell lines. J Biol Chem 284, 3650-3662.

**Esencay, M., Newcomb, E.W., and Zagzag, D. (2010).** HGF upregulates CXCR4 expression in gliomas via NF-kappaB: implications for glioma cell migration. J Neurooncol 99, 33-40.

**Fricker, S.P. (2008).** A novel CXCR4 antagonist for hematopoietic stem cell mobilization. Expert Opin Investig Drugs 17, 1749-1760.

**Göttle, P., Kremer, D., Jander, S., Ödemis, V., Engele, J., Hartung, H.-P., and Küry, P. (2010).** Activation of CXCR7 receptor promotes oligodendroglial cell maturation. Annals of Neurology 68, 915-924.

**Galkina, E., and Ley, K. (2007).** Vascular Adhesion Molecules in Atherosclerosis. Arteriosclerosis, Thrombosis, and Vascular Biology 27, 2292-2301.

**Gerrits, H., van Ingen Schenau, D.S., Bakker, N.E.C., van Disseldorp, A.J.M., Strik, A., Hermens, L.S., Koenen, T.B., Krajnc-Franken, M.A.M., and Gossen, J.A. (2008).** Early postnatal lethality and cardiovascular defects in CXCR7-deficient mice. genesis 46, 235-245.

**Glass, C.K., and Witztum, J.L. (2001).** Atherosclerosis. the road ahead. Cell 104, 503-516.

**Gleissner, C.A. (2012).** Macrophage Phenotype Modulation by CXCL4 in Atherosclerosis. Front Physiol 3, 1.

**Gordon, S., and Taylor, P.R. (2005).** Monocyte and macrophage heterogeneity. Nature Reviews Immunology 5, 953-964.

**Greenwood, J., Steinman, L., and Zamvil, S.S. (2006).** Statin therapy and autoimmune disease: from protein prenylation to immunomodulation. Nat Rev Immunol 6, 358-370.

**Grymula, K., Tarnowski, M., Wysoczynski, M., Drukala, J., Barr, F.G., Ratajczak, J., Kucia, M., and Ratajczak, M.Z. (2010).** Overlapping and distinct role of CXCR7-SDF-1/ITAC and CXCR4-SDF-1 axes in regulating metastatic behavior of human rhabdomyosarcomas. Int J Cancer 127, 2554-2568.

**Hansson, G.K. (2005).** Inflammation, atherosclerosis, and coronary artery disease. N Engl J Med 352, 1685-1695.

**Hansson, G.K., Robertson, A.K., and Soderberg-Naucler, C. (2006).** Inflammation and atherosclerosis. Annu Rev Pathol 1, 297-329.

**Hartmann, T.N., Grabovsky, V., Pasvolsky, R., Shulman, Z., Buss, E.C., Spiegel, A., Nagler, A., Lapidot, T., Thelen, M., and Alon, R. (2008).** A crosstalk between intracellular CXCR7 and CXCR4 involved in rapid CXCL12-triggered integrin activation but not in chemokine-triggered motility of human T lymphocytes and CD34+ cells. Journal of Leukocyte Biology 84, 1130-1140.

**Hatse, S., Princen, K., Bridger, G., De Clercq, E., and Schols, D. (2002).** Chemokine receptor inhibition by AMD3100 is strictly confined to CXCR4. FEBS Lett 527, 255-262.

**Hattermann, K., Held-Feindt, J., Lucius, R., Muerkoster, S.S., Penfold, M.E., Schall, T.J., and Mentlein, R. (2010).** The chemokine receptor CXCR7 is highly expressed in human glioma cells and mediates antiapoptotic effects. Cancer Res 70, 3299-3308.

**Heesen, M., Berman, M.A., Charest, A., Housman, D., Gerard, C., and Dorf, M.E. (1998).** Cloning and chromosomal mapping of an orphan chemokine receptor: mouse RDC1. Immunogenetics 47, 364-370.

**Hilgendorff, A., Muth, H., Parviz, B., Staubitz, A., Haberbosch, W., Tillmanns, H., and Holschermann, H. (2003).** Statins differ in their ability to block NF-kappaB activation in human blood monocytes. Int J Clin Pharmacol Ther 41, 397-401.

**Hong, X., Jiang, F., Kalkanis, S.N., Zhang, Z.G., Zhang, X.P., DeCarvalho, A.C., Katakowski, M., Bobbitt, K., Mikkelsen, T., and Chopp, M. (2006).** SDF-1 and CXCR4 are up-regulated by VEGF and contribute to glioma cell invasion. Cancer Lett 236, 39-45.

**Hou, K.L., Hao, M.G., Bo, J.J., and Wang, J.H. (2010).** CXCR7 in tumorigenesis and progression. Chin J Cancer 29, 456-459.

**Ii, M., and Losordo, D.W. (2007).** Statins and the endothelium. Vascular Pharmacology 46, 1-9.

**Infantino, S., Moepps, B., and Thelen, M. (2006).** Expression and regulation of the orphan receptor RDC1 and its putative ligand in human dendritic and B cells. J Immunol 176, 2197-2207.

**Kalatskaya, I., Berchiche, Y.A., Gravel, S., Limberg, B.J., Rosenbaum, J.S., and Heveker, N. (2009).** AMD3100 Is a CXCR7 Ligand with Allosteric Agonist Properties. Molecular Pharmacology 75, 1240-1247.

**Katschke, K.J., Jr., Rottman, J.B., Ruth, J.H., Qin, S., Wu, L., LaRosa, G., Ponath, P., Park, C.C., Pope, R.M., and Koch, A.E. (2001).** Differential expression of chemokine receptors on peripheral blood, synovial fluid, and synovial tissue monocytes/macrophages in rheumatoid arthritis. Arthritis Rheum 44, 1022-1032.

**Lapham, C.K., Romantseva, T., Petricoin, E., King, L.R., Manischewitz, J., Zaitseva, M.B., and Golding, H. (2002).** CXCR4 heterogeneity in primary cells: possible role of ubiquitination. J Leukoc Biol 72, 1206-1214.

**Leuschner, F., Dutta, P., Gorbatov, R., Novobrantseva, T.I., Donahoe, J.S., Courties, G., Lee, K.M., Kim, J.I., Markmann, J.F., Marinelli, B., et al. (2011).** Therapeutic siRNA silencing in inflammatory monocytes in mice. Nat Biotechnol 29, 1005-1010.

**Levoye, A., Balabanian, K., Baleux, F., Bachelerie, F., and Lagane, B. (2009).** CXCR7 heterodimerizes with CXCR4 and regulates CXCL12-mediated G protein signaling. Blood 113, 6085-6093.

**Ley, K., Miller, Y.I., and Hedrick, C.C. (2011).** Monocyte and macrophage dynamics during atherogenesis. Arterioscler Thromb Vasc Biol 31, 1506-1516.

**Li, A.C., and Glass, C.K. (2002).** The macrophage foam cell as a target for therapeutic intervention. Nat Med 8, 1235-1242.

**Liao, J.K., and Laufs, U. (2005).** Pleiotropic Effects of Statins. Annual Review of Pharmacology and Toxicology 45, 89-118.

**Libby, P. (2001).** What have we learned about the biology of atherosclerosis? The role of inflammation. Am J Cardiol 88, 3J-6J.

**Libby, P. (2002).** Inflammation in atherosclerosis. Nature 420, 868-874.

**Libby, P., and Aikawa, M. (2003).** Effects of statins in reducing thrombotic risk and modulating plaque vulnerability. Clin Cardiol 26, I11-14.

**Lu, D.Y., Tang, C.H., Yeh, W.L., Wong, K.L., Lin, C.P., Chen, Y.H., Lai, C.H., Chen, Y.F., Leung, Y.M., and Fu, W.M. (2009).** SDF-1alpha up-regulates interleukin-6 through CXCR4, PI3K/Akt, ERK, and NF-kappaB-dependent pathway in microglia. Eur J Pharmacol 613, 146-154.

**Luker, K.E., Steele, J.M., Mihalko, L.A., Ray, P., and Luker, G.D. (2010).** Constitutive and chemokine-dependent internalization and recycling of CXCR7 in breast cancer cells to degrade chemokine ligands. Oncogene 29, 4599-4610.

**Lusis, A.J. (2000).** Atherosclerosis. Nature 407, 233-241.

**Ma, Q., Jones, D., Borghesani, P.R., Segal, R.A., Nagasawa, T., Kishimoto, T., Bronson, R.T., and Springer, T.A. (1998).** Impaired B-lymphopoiesis, myelopoiesis, and derailed cerebellar neuron migration in CXCR4- and SDF-1-deficient mice. Proc Natl Acad Sci U S A 95, 9448-9453.

**Ma, W., Liu, Y., Ellison, N., and Shen, J. (2013).** Induction of C-X-C Chemokine Receptor Type 7 (CXCR7) Switches Stromal Cell-Derived Factor-1 (SDF-1) Signaling and Phagocytic Activity in Macrophages Linked to Atherosclerosis. J Biol Chem.

**Massy, Z.A., and Guijarro, C. (2001).** Statins: effects beyond cholesterol lowering. Nephrol Dial Transplant 16, 1738-1741.

**Moore, Kathryn J., and Tabas, I. (2011).** Macrophages in the Pathogenesis of Atherosclerosis. Cell 145, 341-355.

**Nagasawa, T., Kikutani, H., and Kishimoto, T. (1994).** Molecular cloning and structure of a pre-B-cell growth-stimulating factor. Proc Natl Acad Sci U S A 91, 2305-2309.

**Naumann, U., Cameroni, E., Pruenster, M., Mahabaleshwar, H., Raz, E., Zerwes, H.G., Rot, A., and Thelen, M. (2010).** CXCR7 functions as a scavenger for CXCL12 and CXCL11. PLoS One 5, e9175.

**Nieto, J.C., Canto, E., Zamora, C., Ortiz, M.A., Juarez, C., and Vidal, S. (2012).** Selective loss of chemokine receptor expression on leukocytes after cell isolation. PLoS One 7, e31297.

**Odemis, V., Boosmann, K., Heinen, A., Kury, P., and Engele, J. (2010).** CXCR7 is an active component of SDF-1 signalling in astrocytes and Schwann cells. Journal of Cell Science 123, 1081-1088.

**Odemis, V., Lipfert, J., Kraft, R., Hajek, P., Abraham, G., Hattermann, K., Mentlein, R., and Engele, J. (2011).** The presumed atypical chemokine receptor CXCR7 signals through G(i/o) proteins in primary rodent astrocytes and human glioma cells. Glia.

**Oh, J.W., Drabik, K., Kutsch, O., Choi, C., Tousson, A., and Benveniste, E.N. (2001).** CXC chemokine receptor 4 expression and function in human astroglioma cells. J Immunol 166, 2695-2704.

**Oh, Y.S., Kim, H.Y., Song, I.C., Yun, H.J., Jo, D.Y., Kim, S., and Lee, H.J. (2012).** Hypoxia induces CXCR4 expression and biological activity in gastric cancer cells through activation of hypoxia-inducible factor-1alpha. Oncol Rep 28, 2239-2246.

**Patrussi, L., and Baldari, C.T. (2011).** The CXCL12/CXCR4 axis as a therapeutic target in cancer and HIV-1 infection. Curr Med Chem 18, 497-512.

**Puato, M., Faggin, E., Rattazzi, M., Zambon, A., Cipollone, F., Grego, F., Ganassin, L., Plebani, M., Mezzetti, A., and Pauletto, P. (2010).** Atorvastatin Reduces Macrophage Accumulation in Atherosclerotic Plaques: A Comparison of a Nonstatin-Based Regimen in Patients Undergoing Carotid Endarterectomy. Stroke 41, 1163-1168.

**Rajagopal, S., Kim, J., Ahn, S., Craig, S., Lam, C.M., Gerard, N.P., Gerard, C., and Lefkowitz, R.J. (2010).** Beta-arrestin- but not G protein-mediated signaling by the "decoy" receptor CXCR7. Proc Natl Acad Sci U S A 107, 628-632.

**Ramos, E.A., Grochoski, M., Braun-Prado, K., Seniski, G.G., Cavalli, I.J., Ribeiro, E.M., Camargo, A.A., Costa, F.F., and Klassen, G. (2011).** Epigenetic changes of CXCR4 and its ligand CXCL12 as prognostic factors for sporadic breast cancer. PLoS One 6, e29461.

**Ray, P., Lewin, S.A., Mihalko, L.A., Lesher-Perez, S.C., Takayama, S., Luker, K.E., and Luker, G.D. (2012a).** Secreted CXCL12 (SDF-1) forms dimers under physiological conditions. Biochem J 442, 433-442.

**Ray, P., Mihalko, L.A., Coggins, N.L., Moudgil, P., Ehrlich, A., Luker, K.E., and Luker, G.D. (2012b).** Carboxy-terminus of CXCR7 regulates receptor localization and function. Int J Biochem Cell Biol 44, 669-678.

**Ross, R. (1999).** Atherosclerosis--an inflammatory disease. N Engl J Med 340, 115-126.

**Saha, P., Modarai, B., Humphries, J., Mattock, K., Waltham, M., Burnand, K.G., and Smith, A. (2009).** The monocyte/macrophage as a therapeutic target in atherosclerosis. Curr Opin Pharmacol 9, 109-118.

**Saini, V., Marchese, A., and Majetschak, M. (2010).** CXC chemokine receptor 4 is a cell surface receptor for extracellular ubiquitin. J Biol Chem 285, 15566-15576.

**Sanchez-Martin, L., Estecha, A., Samaniego, R., Sanchez-Ramon, S., Vega, M.A., and Sanchez-Mateos, P. (2011).** The chemokine CXCL12 regulates monocyte-macrophage differentiation and RUNX3 expression. Blood 117, 88-97.

**Sato, N., Matsubayashi, H., Fukushima, N., and Goggins, M. (2005).** The chemokine receptor CXCR4 is regulated by DNA methylation in pancreatic cancer. Cancer Biol Ther 4, 70-76.

**Schnoor, M., Buers, I., Sietmann, A., Brodde, M.F., Hofnagel, O., Robenek, H., and Lorkowski, S. (2009).** Efficient non-viral transfection of THP-1 cells. J Immunol Methods 344, 109-115.

**Schober, A., Knarren, S., Lietz, M., Lin, E.A., and Weber, C. (2003).** Crucial role of stromal cell-derived factor-1alpha in neointima formation after vascular injury in apolipoprotein E-deficient mice. Circulation 108, 2491-2497.

**Seeger, F.H., Tonn, T., Krzossok, N., Zeiher, A.M., and Dimmeler, S. (2007).** Cell isolation procedures matter: a comparison of different isolation protocols of bone marrow mononuclear cells used for cell therapy in patients with acute myocardial infarction. Eur Heart J 28, 766-772.

**Senokuchi, T., Matsumura, T., Sakai, M., Yano, M., Taguchi, T., Matsuo, T., Sonoda, K., Kukidome, D., Imoto, K., Nishikawa, T., et al. (2005).** Statins suppress oxidized low density lipoprotein-induced macrophage proliferation by inactivation of the small G protein-p38 MAPK pathway. J Biol Chem 280, 6627-6633.

**Sever, P.S., Dahlof, B., Poulter, N.R., Wedel, H., Beevers, G., Caulfield, M., Collins, R., Kjeldsen, S.E., Kristinsson, A., McInnes, G.T., et al. (2003).** Prevention of coronary and stroke events with atorvastatin in hypertensive patients who have average or lower-than-average cholesterol concentrations, in the Anglo-Scandinavian Cardiac Outcomes Trial--Lipid Lowering Arm (ASCOT-LLA): a multicentre randomised controlled trial. Lancet 361, 1149-1158.

**Shen, J., Chandrasekharan, U.M., Ashraf, M.Z., Long, E., Morton, R.E., Liu, Y., Smith, J.D., and DiCorleto, P.E. (2010).** Lack of mitogen-activated protein kinase phosphatase-1 protects ApoE-null mice against atherosclerosis. Circ Res 106, 902-910.

**Shioda, T., Kato, H., Ohnishi, Y., Tashiro, K., Ikegawa, M., Nakayama, E.E., Hu, H., Kato, A., Sakai, Y., Liu, H., et al. (1998).** Anti-HIV-1 and chemotactic activities of human stromal cell-derived factor 1alpha (SDF-1alpha) and SDF-1beta are abolished by CD26/dipeptidyl peptidase IV-mediated cleavage. Proc Natl Acad Sci U S A 95, 6331-6336.

**Sierro, F., Biben, C., Martinez-Munoz, L., Mellado, M., Ransohoff, R.M., Li, M., Woehl, B., Leung, H., Groom, J., Batten, M., et al. (2007).** Disrupted cardiac development but normal hematopoiesis in mice deficient in the second CXCL12/SDF-1 receptor, CXCR7. Proc Natl Acad Sci U S A 104, 14759-14764.

**Singh, A.K., Arya, R.K., Trivedi, A.K., Sanyal, S., Baral, R., Dormond, O., Briscoe, D.M., and Datta, D. (2012).** Chemokine receptor trio: CXCR3, CXCR4 and CXCR7 crosstalk via CXCL11 and CXCL12. Cytokine & Growth Factor Reviews.

**Sivapalaratnam, S., Motazacker, M.M., Maiwald, S., Hovingh, G.K., Kastelein, J.J., Levi, M., Trip, M.D., and Dallinga-Thie, G.M. (2011).** Genome-wide association studies in atherosclerosis. Curr Atheroscler Rep 13, 225-232.

**Sun, X., Cheng, G., Hao, M., Zheng, J., Zhou, X., Zhang, J., Taichman, R.S., Pienta, K.J., and Wang, J. (2010).** CXCL12 / CXCR4 / CXCR7 chemokine axis and cancer progression. Cancer and Metastasis Reviews 29, 709-722.

**Swirski, F.K., Libby, P., Aikawa, E., Alcaide, P., Luscinskas, F.W., Weissleder, R., and Pittet, M.J. (2007).** Ly-6Chi monocytes dominate hypercholesterolemia-associated monocytosis and give rise to macrophages in atheromata. Journal of Clinical Investigation 117, 195-205.

**Swirski, F.K., and Nahrendorf, M. (2013).** Leukocyte behavior in atherosclerosis, myocardial infarction, and heart failure. Science 339, 161-166.

**Tachibana, K., Hirota, S., Iizasa, H., Yoshida, H., Kawabata, K., Kataoka, Y., Kitamura, Y., Matsushima, K., Yoshida, N., Nishikawa, S., et al. (1998).** The chemokine receptor CXCR4 is essential for vascularization of the gastrointestinal tract. Nature 393, 591-594.

**Tarnowski, M., Grymula, K., Reca, R., Jankowski, K., Maksym, R., Tarnowska, J., Przybylski, G., Barr, F.G., Kucia, M., and Ratajczak, M.Z. (2010a).** Regulation of expression of stromal-derived factor-1 receptors: CXCR4 and CXCR7 in human rhabdomyosarcomas. Mol Cancer Res 8, 1-14.

**Tarnowski, M., Liu, R., Wysoczynski, M., Ratajczak, J., Kucia, M., and Ratajczak, M.Z. (2010b).** CXCR7: a new SDF-1-binding receptor in contrast to normal CD34+ progenitors is functional and is expressed at higher level in human malignant hematopoietic cells. European Journal of Haematology 85, 472-483.

**Tashiro, K., Tada, H., Heilker, R., Shirozu, M., Nakano, T., and Honjo, T. (1993).** Signal sequence trap: a cloning strategy for secreted proteins and type I membrane proteins. Science 261, 600-603.

**Thelen, M., and Thelen, S. (2008).** CXCR7, CXCR4 and CXCL12: An eccentric trio? Journal of Neuroimmunology 198, 9-13.

**Tiwari, R.L., Singh, V., and Barthwal, M.K. (2008).** Macrophages: an elusive yet emerging therapeutic target of atherosclerosis. Med Res Rev 28, 483-544.

**Tsuchiya, A., Nagotani, S., Hayashi, T., Deguchi, K., Sehara, Y., Yamashita, T., Zhang, H., Lukic, V., Kamiya, T., and Abe, K. (2007).** Macrophage infiltration, lectin-like oxidized-LDL receptor-1, and monocyte chemoattractant protein-1 are reduced by chronic HMG-CoA reductase inhibition. Curr Neurovasc Res 4, 268-273.

**Tsuchiya, S., Kobayashi, Y., Goto, Y., Okumura, H., Nakae, S., Konno, T., and Tada, K. (1982).** Induction of maturation in cultured human monocytic leukemia cells by a phorbol diester. Cancer Res 42, 1530-1536.

**Tsuchiya, S., Yamabe, M., Yamaguchi, Y., Kobayashi, Y., Konno, T., and Tada, K. (1980).** Establishment and characterization of a human acute monocytic leukemia cell line (THP-1). Int J Cancer 26, 171-176.

**Tuomisto, T.T. (2003).** Gene Expression in Macrophage-Rich Inflammatory Cell Infiltrates in Human Atherosclerotic Lesions as Studied by Laser Microdissection and DNA Array: Overexpression of HMG-CoA Reductase, Colony Stimulating Factor Receptors, CD11A/CD18 Integrins, and Interleukin Receptors. Arteriosclerosis, Thrombosis, and Vascular Biology 23, 2235-2240.

**Uchimura, K., Morimoto-Tomita, M., Bistrup, A., Li, J., Lyon, M., Gallagher, J., Werb, Z., and Rosen, S.D. (2006).** HSulf-2, an extracellular endoglucosamine-6-sulfatase, selectively mobilizes heparin-bound growth factors and chemokines: effects on VEGF, FGF-1, and SDF-1. BMC Biochem 7, 2.

**Veldkamp, C.T., Peterson, F.C., Pelzek, A.J., and Volkman, B.F. (2005).** The monomer-dimer equilibrium of stromal cell-derived factor-1 (CXCL 12) is altered by pH, phosphate, sulfate, and heparin. Protein Sci 14, 1071-1081.

**Virmani, R., Burke, A.P., Kolodgie, F.D., and Farb, A. (2002).** Vulnerable plaque: the pathology of unstable coronary lesions. J Interv Cardiol 15, 439-446.

**Wang, H., Beaty, N., Chen, S., Qi, C.F., Masiuk, M., Shin, D.M., and Morse, H.C., 3rd (2012).** The CXCR7 chemokine receptor promotes B-cell retention in the splenic marginal zone and serves as a sink for CXCL12. Blood 119, 465-468.

**Wang, J., Shiozawa, Y., Wang, J., Wang, Y., Jung, Y., Pienta, K.J., Mehra, R., Loberg, R., and Taichman, R.S. (2008).** The role of CXCR7/RDC1 as a chemokine receptor for CXCL12/SDF-1 in prostate cancer. J Biol Chem 283, 4283-4294.

**Wang, Y., Li, G., Stanco, A., Long, J.E., Crawford, D., Potter, G.B., Pleasure, S.J., Behrens, T., and Rubenstein, J.L. (2011).** CXCR4 and CXCR7 have distinct functions in regulating interneuron migration. Neuron 69, 61-76.

**Weber, C., and Noels, H. (2011).** Atherosclerosis: current pathogenesis and therapeutic options. Nature Medicine 17, 1410-1422.

**Woollard, K.J., and Geissmann, F. (2010).** Monocytes in atherosclerosis: subsets and functions. Nature Reviews Cardiology 7, 77-86.

**Xu, Q., Wang, J., He, J., Zhou, M., Adi, J., Webster, K.A., and Yu, H. (2011).** Impaired CXCR4 expression and cell engraftment of bone marrow-derived cells from aged atherogenic mice. Atherosclerosis 219, 92-99.

**Yan, X., Cai, S., Xiong, X., Sun, W., Dai, X., Chen, S., Ye, Q., Song, Z., Jiang, Q., and Xu, Z. (2012).** Chemokine receptor CXCR7 mediates human endothelial progenitor cells survival, angiogenesis, but not proliferation. J Cell Biochem 113, 1437-1446.

**Yu, L., Cecil, J., Peng, S.B., Schrementi, J., Kovacevic, S., Paul, D., Su, E.W., and Wang, J. (2006).** Identification and expression of novel isoforms of human stromal cell-derived factor 1. Gene 374, 174-179.

**Zabel, B.A., Wang, Y., Lewen, S., Berahovich, R.D., Penfold, M.E.T., Zhang, P., Powers, J., Summers, B.C., Miao, Z., Zhao, B., et al. (2009).** Elucidation of CXCR7-Mediated Signaling Events and Inhibition of CXCR4-Mediated Tumor Cell Transendothelial Migration by CXCR7 Ligands. The Journal of Immunology 183, 3204-3211.

**Zagzag, D., Lukyanov, Y., Lan, L., Ali, M.A., Esencay, M., Mendez, O., Yee, H., Voura, E.B., and Newcomb, E.W. (2006).** Hypoxia-inducible factor 1 and VEGF upregulate CXCR4 in glioblastoma: implications for angiogenesis and glioma cell invasion. Lab Invest 86, 1221-1232.

**Zeller, T., Blankenberg, S., and Diemert, P. (2012).** Genomewide association studies in cardiovascular disease--an update 2011. Clin Chem 58, 92-103.

**Zernecke, A., Bot, I., Djalali-Talab, Y., Shagdarsuren, E., Bidzhekov, K., Meiler, S., Krohn, R., Schober, A., Sperandio, M., Soehnlein, O., et al. (2008).** Protective role of CXC receptor 4/CXC ligand 12 unveils the importance of neutrophils in atherosclerosis. Circ Res 102, 209-217.

**Zernecke, A., Schober, A., Bot, I., von Hundelshausen, P., Liehn, E.A., Mopps, B., Mericskay, M., Gierschik, P., Biessen, E.A., and Weber, C. (2005).** SDF-1alpha/CXCR4 axis is instrumental in neointimal hyperplasia and recruitment of smooth muscle progenitor cells. Circ Res 96, 784-791.

**Zhou, Q., and Liao, J.K. (2009).** Statins and cardiovascular diseases: from cholesterol lowering to pleiotropy. Curr Pharm Des 15, 467-478.

**Zhu, Y., Yu, T., Zhang, X.C., Nagasawa, T., Wu, J.Y., and Rao, Y. (2002).** Role of the chemokine SDF-1 as the meningeal attractant for embryonic cerebellar neurons. Nat Neurosci 5, 719-720.

Appendix

**Table 6.1. Atherosclerosis-related gene expression profiles in SDF-1-treated THP-1 macrophages**

PCR array catalog number: PAHS-038

| | | PMA-driven Macrophages | | | |
|---|---|---|---|---|---|
| Position | Genes | Ct in Control Cells | Ct in SDF-1 Treated Cells | ΔCt | Fold Change |
| A01 | ABCA1 | 23.62 | 24.47 | -0.85 | 0.8011 |
| A02 | ACE | 26.65 | 27.62 | -0.97 | 0.7371 |
| A03 | PLIN2 | 19.31 | 19.98 | -0.67 | 0.9075 |
| A04 | APOA1 | 29.88 | 30.58 | -0.7 | 0.8888 |
| A05 | APOB | 35 | 35 | 0 | 1.4439 |
| A06 | APOE | 23.07 | 23.8 | -0.73 | 0.8706 |
| A07 | BAX | 22.14 | 23.08 | -0.94 | 0.7526 |
| A08 | BCL2 | 24.7 | 25.59 | -0.89 | 0.7792 |
| A09 | BCL2A1 | 22.8 | 23.33 | -0.53 | 1 |
| A10 | BCL2L1 | 24.22 | 25.16 | -0.94 | 0.7526 |
| A11 | BID | 22.73 | 23.22 | -0.49 | 1.0281 |
| A12 | BIRC3 | 27.79 | 28.69 | -0.9 | 0.7738 |
| B01 | CCL2 | 26.6 | 27.06 | -0.46 | 1.0497 |
| B02 | CCL5 | 20.47 | 21.18 | -0.71 | 0.8827 |
| B03 | CCR1 | 22.02 | 22.58 | -0.56 | 0.9794 |
| B04 | CCR2 | 26.46 | 27.72 | -1.26 | 0.6029 |
| B05 | CD44 | 20.04 | 20.83 | -0.79 | 0.8351 |
| B06 | CDH5 | 26.93 | 28.1 | -1.17 | 0.6417 |
| B07 | CFLAR | 23.68 | 24.4 | -0.72 | 0.8766 |
| B08 | COL3A1 | 35 | 35 | 0 | 1.4439 |

| | | | | | |
|---|---|---|---|---|---|
| B09 | CSF1 | 26.25 | 26.82 | -0.57 | 0.9727 |
| B10 | CSF2 | 33.14 | 34.06 | -0.92 | 0.7631 |
| B11 | CTGF | 27.78 | 28.64 | -0.86 | 0.7955 |
| B12 | EGR1 | 24.62 | 25.84 | -1.22 | 0.6199 |
| C01 | ELN | 31.6 | 35 | -3.4 | 0.1368 |
| C02 | ENG | 20.01 | 20.8 | -0.79 | 0.8351 |
| C03 | FABP3 | 27.9 | 29.01 | -1.11 | 0.669 |
| C04 | FAS | 26.86 | 27.72 | -0.86 | 0.7955 |
| C05 | FGA | 35 | 35 | 0 | 1.4439 |
| C06 | FGF2 | 21.91 | 22.89 | -0.98 | 0.732 |
| C07 | FN1 | 24.58 | 25.28 | -0.7 | 0.8888 |
| C08 | HBEGF | 21.75 | 22.33 | -0.58 | 0.9659 |
| C09 | ICAM1 | 20.81 | 21.4 | -0.59 | 0.9593 |
| C10 | IFNAR2 | 21.82 | 22.84 | -1.02 | 0.712 |
| C11 | IFNG | 35 | 35 | 0 | 1.4439 |
| C12 | IL1A | 27.77 | 28.41 | -0.64 | 0.9266 |
| D01 | IL1R1 | 24.66 | 25.5 | -0.84 | 0.8066 |
| D02 | IL1R2 | 29.45 | 30.45 | -1 | 0.722 |
| D03 | IL2 | 33.75 | 34.5 | -0.75 | 0.8586 |
| D04 | IL3 | 33.33 | 35 | -1.67 | 0.4538 |
| D05 | IL4 | 14.01 | 35 | -20.99 | 0 |
| D06 | IL5 | 29.81 | 30.79 | -0.98 | 0.732 |
| D07 | ITGA2 | 25.99 | 27 | -1.01 | 0.717 |
| D08 | ITGA5 | 19.79 | 20.52 | -0.73 | 0.8706 |
| D09 | ITGAX | 22.16 | 23.2 | -1.04 | 0.7022 |
| D10 | ITGB2 | 15.9 | 16.57 | -0.67 | 0.9075 |
| D11 | KDR | 31 | 32.05 | -1.05 | 0.6974 |
| D12 | KLF2 | 25.34 | 25.91 | -0.57 | 0.9727 |
| E01 | LAMA1 | 35 | 35 | 0 | 1.4439 |
| E02 | LDLR | 23.72 | 24.65 | -0.93 | 0.7579 |
| E03 | LIF | 35 | 32.37 | 2.63 | 8.9383 |
| E04 | LPA | 35 | 35 | 0 | 1.4439 |
| E05 | LPL | 21.05 | 22.1 | -1.05 | 0.6974 |
| E06 | MMP1 | 20.57 | 21.53 | -0.96 | 0.7423 |
| E07 | MMP3 | 28.92 | 30.41 | -1.49 | 0.5141 |
| E08 | MSR1 | 20.8 | 21.79 | -0.99 | 0.727 |
| E09 | NFKB1 | 22.08 | 22.79 | -0.71 | 0.8827 |
| E10 | NOS3 | 26.06 | 28.42 | -2.36 | 0.2813 |
| E11 | NPY | 23.27 | 24.03 | -0.76 | 0.8526 |
| E12 | NR1H3 | 28.57 | 30.31 | -1.74 | 0.4323 |

| | | | | | |
|---|---|---|---|---|---|
| F01 | PDGFA | 20.95 | 21.92 | -0.97 | 0.7371 |
| F02 | PDGFB | 29.13 | 29.69 | -0.56 | 0.9794 |
| F03 | PDGFRB | 28.06 | 28.75 | -0.69 | 0.895 |
| F04 | PPARA | 25.21 | 26.32 | -1.11 | 0.669 |
| F05 | PPARD | 21.81 | 22.76 | -0.95 | 0.7474 |
| F06 | PPARG | 22.14 | 22.87 | -0.73 | 0.8706 |
| F07 | PTGS1 | 22.41 | 22.97 | -0.56 | 0.9794 |
| F08 | RXRA | 21.55 | 22.14 | -0.59 | 0.9593 |
| F09 | SELE | 35 | 35 | 0 | 1.4439 |
| F10 | SELL | 28.97 | 29.96 | -0.99 | 0.727 |
| F11 | SELPLG | 25.87 | 27.06 | -1.19 | 0.6329 |
| F12 | SERPINB2 | 29.49 | 30.85 | -1.36 | 0.5625 |
| G01 | SERPINE1 | 26.17 | 26.83 | -0.66 | 0.9138 |
| G02 | SOD1 | 20.91 | 21.71 | -0.8 | 0.8293 |
| G03 | SPP1 | 15.16 | 15.83 | -0.67 | 0.9075 |
| G04 | TGFB1 | 18.6 | 19.31 | -0.71 | 0.8827 |
| G05 | TGFB2 | 23.19 | 23.77 | -0.58 | 0.9659 |
| G06 | THBS4 | 27.63 | 28.61 | -0.98 | 0.732 |
| G07 | TNC | 29.72 | 30.33 | -0.61 | 0.9461 |
| G08 | TNF | 22.04 | 22.59 | -0.55 | 0.9862 |
| G09 | TNFAIP3 | 22.86 | 23.24 | -0.38 | 1.1096 |
| G10 | VCAM1 | 29.59 | 31.53 | -1.94 | 0.3763 |
| G11 | VEGFA | 22.89 | 23.92 | -1.03 | 0.7071 |
| G12 | VWF | 26 | 26.81 | -0.81 | 0.8236 |
| H01 | B2M | 17.94 | 19.22 | -1.28 | 0.5946 |
| H02 | HPRT1 | 23.05 | 23.89 | -0.84 | 0.8066 |
| H03 | RPL13A | 19.74 | 20.36 | -0.62 | 0.9395 |
| H04 | GAPDH | 17.51 | 18.04 | -0.53 | 1 |
| H05 | ACTB | 14.2 | 15.09 | -0.89 | 0.7792 |
| H06 | HGDC | 35 | 34.93 | 0.07 | 1.5157 |
| H07 | RTC | 22.41 | 22.71 | -0.3 | 1.1728 |
| H08 | RTC | 22.72 | 22.76 | -0.04 | 1.4044 |
| H09 | RTC | 21.92 | 22.53 | -0.61 | 0.9461 |
| H10 | PPC | 17.78 | 18.47 | -0.69 | 0.895 |
| H11 | PPC | 17.5 | 18.16 | -0.66 | 0.9138 |
| H12 | PPC | 17.61 | 17.84 | -0.23 | 1.2311 |

**Table 6.2. Inflammation-related gene expression profiles in SDF-1-treated THP-1 macrophages**

PCR array catalog number: PAHS-077

| | PMA-driven Macrophages | | | | |
|---|---|---|---|---|---|
| Position | Genes | Ct in Control Cells | Ct in SDF-1 Treated Cells | ΔCt | Fold Change |
| A01 | BCL6 | 5.325461 | 4.991871 | 0.33359 | 1.2601 |
| A02 | C3 | 7.975461 | 7.271871 | 0.70359 | 1.6286 |
| A03 | C3AR1 | 9.345461 | 8.741871 | 0.60359 | 1.5195 |
| A04 | C4A | 11.43546 | 11.18187 | 0.25359 | 1.1922 |
| A05 | CCL11 | 13.88546 | 18.32187 | -4.43641 | 0.0462 |
| A06 | CCL13 | 16.41546 | 18.32187 | -1.90641 | 0.2668 |
| A07 | CCL16 | 14.57546 | 17.01187 | -2.43641 | 0.1847 |
| A08 | CCL17 | 16.12546 | 18.32187 | -2.19641 | 0.2182 |
| A09 | CCL19 | 13.85546 | 14.78187 | -0.92641 | 0.5262 |
| A10 | CCL2 | 10.29546 | 9.511871 | 0.78359 | 1.7214 |
| A11 | CCL21 | 8.035461 | 7.191871 | 0.84359 | 1.7945 |
| A12 | CCL22 | 10.79546 | 10.79187 | 0.00359 | 1.0025 |
| B01 | CCL23 | 8.055461 | 7.571871 | 0.48359 | 1.3982 |
| B02 | CCL24 | 11.02546 | 10.71187 | 0.31359 | 1.2428 |
| B03 | CCL3 | 6.915461 | 6.061871 | 0.85359 | 1.807 |
| B04 | CCL4 | 10.21546 | 9.141871 | 1.07359 | 2.1047 |
| B05 | CCL5 | 4.175461 | 3.561871 | 0.61359 | 1.5301 |
| B06 | CCL7 | 14.96546 | 15.19187 | -0.22641 | 0.8548 |
| B07 | CCL8 | 14.02546 | 13.96187 | 0.06359 | 1.0451 |
| B08 | CCR1 | 6.165461 | 5.721871 | 0.44359 | 1.36 |
| B09 | CCR2 | 11.43546 | 10.89187 | 0.54359 | 1.4576 |
| B10 | CCR3 | 13.99546 | 14.77187 | -0.77641 | 0.5838 |
| B11 | CCR4 | 15.19546 | 18.32187 | -3.12641 | 0.1145 |
| B12 | CCR7 | 14.86546 | 15.57187 | -0.70641 | 0.6128 |
| C01 | CD40 | 9.035461 | 8.481871 | 0.55359 | 1.4677 |
| C02 | CD40LG | 14.36546 | 14.03187 | 0.33359 | 1.2601 |
| C03 | CEBPB | 7.605461 | 6.891871 | 0.71359 | 1.6399 |
| C04 | CRP | 13.84546 | 18.32187 | -4.47641 | 0.0449 |
| C05 | CSF1 | 9.995461 | 9.221871 | 0.77359 | 1.7095 |

| | | | | | |
|---|---|---|---|---|---|
| C06 | CXCL1 | 10.24546 | 9.291871 | 0.95359 | 1.9367 |
| C07 | CXCL10 | 12.48546 | 13.00187 | -0.51641 | 0.6991 |
| C08 | CXCL2 | 12.35546 | 11.88187 | 0.47359 | 1.3886 |
| C09 | CXCL3 | 10.18546 | 9.591871 | 0.59359 | 1.509 |
| C10 | CXCL5 | 14.92546 | 15.07187 | -0.14641 | 0.9035 |
| C11 | CXCL6 | 13.33546 | 13.19187 | 0.14359 | 1.1047 |
| C12 | CXCL9 | 15.09546 | 15.11187 | -0.01641 | 0.9887 |
| D01 | CXCR4 | 8.865461 | 8.381871 | 0.48359 | 1.3982 |
| D02 | FASLG | 14.21546 | 15.60187 | -1.38641 | 0.3825 |
| D03 | FLT3LG | 10.28546 | 9.891871 | 0.39359 | 1.3137 |
| D04 | FOS | 6.035461 | 5.321871 | 0.71359 | 1.6399 |
| D05 | HDAC4 | 7.995461 | 7.271871 | 0.72359 | 1.6513 |
| D06 | IFNG | 14.08546 | 18.32187 | -4.23641 | 0.0531 |
| D07 | IL10 | 12.86546 | 12.73187 | 0.13359 | 1.097 |
| D08 | IL10RB | 4.435461 | 4.051871 | 0.38359 | 1.3046 |
| D09 | IL18 | 9.675461 | 8.911871 | 0.76359 | 1.6977 |
| D10 | IL18RAP | 13.31546 | 16.79187 | -3.47641 | 0.0898 |
| D11 | IL1A | 11.55546 | 10.67187 | 0.88359 | 1.845 |
| D12 | IL1B | 2.155461 | 1.711871 | 0.44359 | 1.36 |
| E01 | IL1F10 | 16.65546 | 18.32187 | -1.66641 | 0.315 |
| E02 | IL1R1 | 9.105461 | 8.911871 | 0.19359 | 1.1436 |
| E03 | IL1RAP | 8.975461 | 8.361871 | 0.61359 | 1.5301 |
| E04 | IL1RN | 3.955461 | 3.531871 | 0.42359 | 1.3413 |
| E05 | IL22 | 15.03546 | 18.32187 | -3.28641 | 0.1025 |
| E06 | IL22RA2 | 15.16546 | 18.32187 | -3.15641 | 0.1122 |
| E07 | IL23A | 11.18546 | 10.82187 | 0.36359 | 1.2866 |
| E08 | IL23R | 15.19546 | 18.23187 | -3.03641 | 0.1219 |
| E09 | IL6 | 14.28546 | 15.58187 | -1.29641 | 0.4071 |
| E10 | IL6R | 4.095461 | 3.531871 | 0.56359 | 1.4779 |
| E11 | IL8 | 4.255461 | 3.901871 | 0.35359 | 1.2777 |
| E12 | CXCR1 | 15.38546 | 18.32187 | -2.93641 | 0.1306 |
| F01 | CXCR2 | 11.97546 | 11.77187 | 0.20359 | 1.1516 |
| F02 | IL9 | 15.83546 | 18.32187 | -2.48641 | 0.1784 |
| F03 | ITGB2 | 0.105461 | 0.031871 | 0.07359 | 1.0523 |
| F04 | KNG1 | 13.89546 | 15.84187 | -1.94641 | 0.2595 |
| F05 | LTA | 12.08546 | 12.31187 | -0.22641 | 0.8548 |
| F06 | LTB | 10.61546 | 10.43187 | 0.18359 | 1.1357 |
| F07 | LY96 | 6.205461 | 6.071871 | 0.13359 | 1.097 |
| F08 | MYD88 | 7.405461 | 7.141871 | 0.26359 | 1.2005 |
| F09 | NFATC3 | 5.655461 | 5.091871 | 0.56359 | 1.4779 |

| | | | | | |
|---|---|---|---|---|---|
| F10 | NFKB1 | 5.595461 | 5.171871 | 0.42359 | 1.3413 |
| F11 | NOS2 | 8.345461 | 8.271871 | 0.07359 | 1.0523 |
| F12 | NR3C1 | 5.225461 | 4.921871 | 0.30359 | 1.2342 |
| G01 | RIPK2 | 8.175461 | 8.191871 | -0.01641 | 0.9887 |
| G02 | TIRAP | 9.575461 | 9.351871 | 0.22359 | 1.1676 |
| G03 | TLR1 | 8.375461 | 8.021871 | 0.35359 | 1.2777 |
| G04 | TLR2 | 5.985461 | 5.681871 | 0.30359 | 1.2342 |
| G05 | TLR3 | 12.23546 | 12.44187 | -0.20641 | 0.8667 |
| G06 | TLR4 | 7.135461 | 6.891871 | 0.24359 | 1.1839 |
| G07 | TLR5 | 13.65546 | 14.14187 | -0.48641 | 0.7138 |
| G08 | TLR6 | 8.175461 | 8.101871 | 0.07359 | 1.0523 |
| G09 | TLR7 | 9.635461 | 9.121871 | 0.51359 | 1.4276 |
| G10 | TNF | 5.755461 | 5.401871 | 0.35359 | 1.2777 |
| G11 | TNFSF14 | 8.355461 | 8.041871 | 0.31359 | 1.2428 |
| G12 | TOLLIP | 7.445461 | 7.041871 | 0.40359 | 1.3228 |
| H01 | B2M | 1.585461 | 1.561871 | 0.02359 | 1.0165 |
| H02 | HPRT1 | 7.125461 | 6.961871 | 0.16359 | 1.1201 |
| H03 | RPL13A | 3.695461 | 3.601871 | 0.09359 | 1.067 |
| H04 | GAPDH | 1.045461 | 0.961871 | 0.08359 | 1.0597 |
| H05 | ACTB | -1.45454 | -1.42813 | -0.02641 | 0.9819 |
| H06 | HGDC | 13.79546 | 18.32187 | -4.52641 | 0.0434 |
| H07 | RTC | 6.035461 | 5.541871 | 0.49359 | 1.4079 |
| H08 | RTC | 6.005461 | 5.711871 | 0.29359 | 1.2257 |
| H09 | RTC | 5.815461 | 5.331871 | 0.48359 | 1.3982 |
| H10 | PPC | 1.245461 | 1.341871 | -0.09641 | 0.9354 |
| H11 | PPC | 1.065461 | 1.101871 | -0.03641 | 0.9751 |
| H12 | PPC | 1.005461 | 1.071871 | -0.06641 | 0.955 |